Utilization of Accelerator Based Real Time Methods in Investigation of Materials with High Technological Importance

IAEA
International Atomic Energy Agency

IAEA RADIATION TECHNOLOGY SERIES PUBLICATIONS

One of the main objectives of the IAEA Radioisotope Production and Radiation Technology programme is to enhance the expertise and capability of IAEA Member States in utilizing the methodologies for radiation processing, compositional analysis and industrial applications of radioisotope techniques in order to meet national needs as well as to assimilate new developments for improving industrial process efficiency and safety, development and characterization of value-added products, and treatment of pollutants/hazardous materials.

Publications in the IAEA Radiation Technology Series provide information in the areas of: radiation processing and characterization of materials using ionizing radiation, and industrial applications of radiotracers, sealed sources and non-destructive testing. The publications have a broad readership and are aimed at meeting the needs of scientists, engineers, researchers, teachers and students, laboratory professionals, and instructors. International experts assist the IAEA Secretariat in drafting and reviewing these publications. Some of the publications in this series may also be endorsed or co-sponsored by international organizations and professional societies active in the relevant fields.

There are two categories of publications: the **IAEA Radiation Technology Series and the IAEA Radiation Technology Reports**.

IAEA RADIATION TECHNOLOGY SERIES

Publications in this category present guidance information or methodologies and analyses of long term validity, for example protocols, guidelines, codes, standards, quality assurance manuals, best practices and high level technological and educational material.

IAEA RADIATION TECHNOLOGY REPORTS

In this category, publications complement information published in the IAEA Radiation Technology Series in the areas of: radiation processing of materials using ionizing radiation, and industrial applications of radiotracers, sealed sources and NDT. These publications include reports on current issues and activities such as technical meetings, the results of IAEA coordinated research projects, interim reports on IAEA projects, and educational material compiled for IAEA training courses dealing with radioisotope and radiopharmaceutical related subjects. In some cases, these reports may provide supporting material relating to publications issued in the IAEA Radiation Technology Series.

All of these publications can be downloaded cost free from the IAEA web site:

http://www.iaea.org/Publications/index.html

Further information is available from:

Marketing and Sales Unit
International Atomic Energy Agency
Vienna International Centre
PO Box 100
1400 Vienna, Austria

Readers are invited to provide feedback to the IAEA on these publications. Information may be provided through the IAEA web site, by mail at the address given above, or by email to:

Official.Mail@iaea.org

UTILIZATION OF ACCELERATOR BASED
REAL TIME METHODS IN INVESTIGATION
OF MATERIALS WITH
HIGH TECHNOLOGICAL IMPORTANCE

The following States are Members of the International Atomic Energy Agency:

AFGHANISTAN
ALBANIA
ALGERIA
ANGOLA
ARGENTINA
ARMENIA
AUSTRALIA
AUSTRIA
AZERBAIJAN
BAHAMAS
BAHRAIN
BANGLADESH
BELARUS
BELGIUM
BELIZE
BENIN
BOLIVIA
BOSNIA AND HERZEGOVINA
BOTSWANA
BRAZIL
BRUNEI DARUSSALAM
BULGARIA
BURKINA FASO
BURUNDI
CAMBODIA
CAMEROON
CANADA
CENTRAL AFRICAN
  REPUBLIC
CHAD
CHILE
CHINA
COLOMBIA
CONGO
COSTA RICA
CÔTE D'IVOIRE
CROATIA
CUBA
CYPRUS
CZECH REPUBLIC
DEMOCRATIC REPUBLIC
  OF THE CONGO
DENMARK
DOMINICA
DOMINICAN REPUBLIC
ECUADOR
EGYPT
EL SALVADOR
ERITREA
ESTONIA
ETHIOPIA
FIJI
FINLAND
FRANCE
GABON
GEORGIA
GERMANY
GHANA

GREECE
GUATEMALA
GUYANA
HAITI
HOLY SEE
HONDURAS
HUNGARY
ICELAND
INDIA
INDONESIA
IRAN, ISLAMIC REPUBLIC OF
IRAQ
IRELAND
ISRAEL
ITALY
JAMAICA
JAPAN
JORDAN
KAZAKHSTAN
KENYA
KOREA, REPUBLIC OF
KUWAIT
KYRGYZSTAN
LAO PEOPLE'S DEMOCRATIC
  REPUBLIC
LATVIA
LEBANON
LESOTHO
LIBERIA
LIBYA
LIECHTENSTEIN
LITHUANIA
LUXEMBOURG
MADAGASCAR
MALAWI
MALAYSIA
MALI
MALTA
MARSHALL ISLANDS
MAURITANIA, ISLAMIC
  REPUBLIC OF
MAURITIUS
MEXICO
MONACO
MONGOLIA
MONTENEGRO
MOROCCO
MOZAMBIQUE
MYANMAR
NAMIBIA
NEPAL
NETHERLANDS
NEW ZEALAND
NICARAGUA
NIGER
NIGERIA
NORWAY
OMAN

PAKISTAN
PALAU
PANAMA
PAPUA NEW GUINEA
PARAGUAY
PERU
PHILIPPINES
POLAND
PORTUGAL
QATAR
REPUBLIC OF MOLDOVA
ROMANIA
RUSSIAN FEDERATION
RWANDA
SAN MARINO
SAUDI ARABIA
SENEGAL
SERBIA
SEYCHELLES
SIERRA LEONE
SINGAPORE
SLOVAKIA
SLOVENIA
SOUTH AFRICA
SPAIN
SRI LANKA
SUDAN
SWAZILAND
SWEDEN
SWITZERLAND
SYRIAN ARAB REPUBLIC
TAJIKISTAN
THAILAND
THE FORMER YUGOSLAV
  REPUBLIC OF MACEDONIA
TOGO
TRINIDAD AND TOBAGO
TUNISIA
TURKEY
UGANDA
UKRAINE
UNITED ARAB EMIRATES
UNITED KINGDOM OF
  GREAT BRITAIN AND
  NORTHERN IRELAND
UNITED REPUBLIC
  OF TANZANIA
UNITED STATES OF AMERICA
URUGUAY
UZBEKISTAN
VENEZUELA, BOLIVARIAN
  REPUBLIC OF
VIET NAM
YEMEN
ZAMBIA
ZIMBABWE

The Agency's Statute was approved on 23 October 1956 by the Conference on the Statute of the IAEA held at United Nations Headquarters, New York; it entered into force on 29 July 1957. The Headquarters of the Agency are situated in Vienna. Its principal objective is "to accelerate and enlarge the contribution of atomic energy to peace, health and prosperity throughout the world''.

IAEA RADIATION TECHNOLOGY REPORTS No. 4

UTILIZATION OF ACCELERATOR BASED REAL TIME METHODS IN INVESTIGATION OF MATERIALS WITH HIGH TECHNOLOGICAL IMPORTANCE

PROCEEDINGS OF AN IAEA TECHNICAL MEETING

INTERNATIONAL ATOMIC ENERGY AGENCY
VIENNA, 2015

COPYRIGHT NOTICE

FOREWORD

Particle and electron accelerators have played an important role in the development and application of nuclear science and technology for more than 60 years. Over the decades, many different types of radiation produced by accelerators have been harnessed, developed and optimized to support the research and development needs of industry and academia. New accelerator based research tools utilizing high intensity X ray and neutron sources are increasingly becoming available to researchers for studying dynamic processes as they occur in real time, for example, for following and recording the evolution and change of a material's structure in real time as it undergoes physical or chemical changes. The information revealed and knowledge gained from real time studies is leading to energy savings, pollution reduction and productivity increases through better design and engineering of more robust materials and efficient processes.

The most widely used advanced accelerator based radiation source is synchrotron radiation, and there are more than 50 such research facilities operational worldwide. The unique properties of synchrotron radiation, with its high intensity X rays make it a very versatile tool which is in high demand for the exploration of processes in real time in a wide range of matter. Complementary to synchrotron radiation are accelerator based high intensity neutron beams from spallation neutron sources, ions from particle accelerators and electron beams from electron accelerators, all of which are increasingly being utilized for real time studies in a wide and diverse range of applications, such as human health, sustainable energy systems and the protection of the environment.

The IAEA held a Technical Meeting on the utilization of accelerator based real time methods in the investigation of materials with high technological importance, with the objective of presenting the state of the art of the development and application of various accelerator based real time techniques, to identify research trends and scientific challenges and to highlight the need for and benefits of increased interdisciplinary and international collaboration. The meeting discussed specific techniques and research areas that can benefit from real time material characterizations using synchrotron radiation; neutron, ion and electron beams; and simultaneous combinations of different techniques. A recurrent theme emerging from the presentations is a need to develop more robust materials with longer working lives for energy related applications, through a better understanding of the processes that degrade a material's performance with use or age. Such materials are essential for the development and successful deployment of next generation energy sources. This publication summarizes the available accelerator technologies and recommendations for further developments in real time and in situ methods.

The IAEA wishes to thank all meeting participants and contributors, and to express its gratitude to the Argonne National Laboratory (United States of America) for hosting this Technical Meeting. Finally, the IAEA wishes to thank W. Bras (Netherlands) and N. Dytlewski, R. van Silfhout and L. Soderholm (United States of America) for their help in the preparation of this report. The IAEA officer responsible for this publication was A. Zeman of the Division of Physical and Chemical Sciences.

CONTENTS

SUMMARY

INTRODUCTION

Accelerators are playing an ever increasing role in research directed towards the development and advancement of materials for energy applications. Research on materials for energy applications covers a broad spectrum of chemistry and physics topics, such as synthesis of new materials, structural and mechanistic characterization, optimization, utilization and performance degradation. Accelerator based techniques provide X ray, neutron or electron beams for interrogating materials and their properties and ion beams for inducing damage, which is particularly relevant to the development of batteries, fuel cells, solar and nuclear energy.

The variable energy photon, electron, neutron or ion beams produced by modern accelerators are directed into specialized instruments that probe and detect the interaction of radiations with matter, providing information on structure–property relationships, material defects, chemical composition, atomic speciation, and electronic and magnetic behaviour. The high intensity beams that can be generated by modern accelerators enable time resolved measurements of processes that occur as fast as a few milliseconds and to follow and characterize the behaviour of materials as a function of time. The pulsed structure of many accelerator based beams provides an added opportunity to extend the accessible time domain to the nanosecond scale.

The wide range of techniques developed to probe and analyse materials can generally be divided into three major categories: spectroscopy, scattering and imaging. Spectroscopic techniques provide information from matter after it absorbs energy from the beam, which can be used to further the understanding of how a material's composition influences a targeted behaviour, or how energy is stored or distributed within a sample. Synchrotron and neutron techniques provide the bulk of experimental probes in this area. Scattering techniques are ubiquitous, and these include the use of X rays, neutrons and electrons to probe atomic correlations and structures that span length scales from the atomic through to the macroscopic. Imaging techniques, primarily found at neutron facilities, provide information on material defects and mid-size structural organization. Such techniques have recently been applied in areas involving operational large scale machines and mechanical device such as motors and turbines.

Recently, a rich landscape of accelerator based methods for real time materials studies has emerged. These methods are categorized in two main types: time resolved studies and in situ probes. Rapid developments in both radiation sources and experimental set-ups are increasingly combining these experimental modalities, providing researchers with detailed information about the processes influencing and driving complex structural, chemical and morphological changes in materials. Further developments in these techniques will provide more and better information to critically analyse future energy directions and choices and help determine the best ways forward in materials research.

METHODS

Accelerator based methods can be subdivided into three main areas based on the type of radiation used to probe the material under investigation: X rays, neutrons or ions/electrons.

X ray beam methods

Synchrotron radiation X rays, with their unique properties such as a continuous energy spectrum, spatial coherence, temporal structure, high brightness and changeable polarization, are an indispensable tool in the investigation of matter in advanced science and technology. The experimental techniques that use synchrotron radiation as probes are classified here into three broad categories: spectroscopy, scattering and diffraction, and imaging.

X ray spectroscopy

The most commonly used technique is X ray absorption spectroscopy, which uses photons in the energy range of 300 eV to 60 keV. The methods of X ray absorption near edge structure (XANES), extended X ray absorption fine

structure (EXAFS) and resonant inelastic X ray scattering provide single atom chemical speciation and structural information over a wide range of concentrations in solid, liquid and gaseous samples. X ray fluorescence (XRF) is used to probe chemical compositions as low as a few ppm, providing information of trace elements critical to energy applications. X ray fluorescence is also used to probe the electronic structure of various kinds of matter and provide two dimensional spatial maps of elemental distributions in materials. Low energy photons are used in both the photon in / electron out and photon in / photon out approaches and applications include photoelectron spectroscopy (PES) with all its variants of angle resolved photoelectron spectroscopy (ARPES) and infrared spectroscopy. These techniques can be used to make both in situ and real time measurements.

X ray diffraction and scattering

X ray diffraction techniques provide information about long range correlations and the atomic structures of materials. The use of anomalous diffraction, enabled by the tunability of the synchrotron X ray energy, is a growing field of research. Intense X ray beams provide opportunities to probe much smaller samples than before and enhanced beam collimation allows increased resolution for powder diffraction techniques, permitting phase identification in complex, multicomponent samples. Traditional diffraction techniques, which are carried out in a non-time resolved mode with desktop X ray sources, have now been extended to the time resolved domain. Time resolutions down to the millisecond level can now be obtained.

Low ordered materials can be studied by applying X ray scattering techniques in which the experimental methodology closely parallels those of the diffraction techniques. Newly emerging data handling techniques developed for these methods are being applied to enhance the capabilities that were already available with conventional X ray sources. The Fourier transformation of data, collected over a wide momentum space using high energy X rays, provides real space pair distribution functions that offer a wealth of structural information on amorphous and solution samples. Time resolution is possible in the millisecond time domain, allowing access to real time studies of polymeric materials, catalysts, stress failure mechanisms and chemical transformations.

Small angle X ray scattering (SAXS) provides information on larger scale structures up to 200 nm and is particularly suitable to be combined with wider angle diffraction and scattering techniques for time resolved studies dealing with structure growth or crystallization. By using grazing incidence geometry, it is possible to prevent the X rays from penetrating the bulk of the material and obtain information solely on the atomic structure of the surface layers.

X ray microscopy and imaging

Imaging techniques have greatly benefitted from the latest generation of synchrotron radiation sources. The abundance of hard X rays and much improved X ray optics provides the bright and well-focused beams required for high resolution X ray microscopy and tomography. Data handling issues are considered the main bottleneck in the implementation process. In the lower energy range, infrared microspectroscopy, infrared imaging and infrared microprobe techniques are becoming an important source of chemical and materials information.

The most common techniques are photoelectron emission microscopy (PEEM), scanning transmission X ray microscopy (STXM), full field X ray microscopy (TXM), scanning photoemission microscopy (SPEM), X ray tomography, radiography, phase contrast imaging and diffraction enhanced imaging. Most of these techniques can operate in both the soft and hard X ray regime. Typical experiments addressed by soft X ray imaging techniques include the spatial characterization of chemical, electronic, magnetic and physical behaviours. Some of the above mentioned techniques (STXM, TXM, SPEM) have made important advances in their capabilities to perform in situ real time experiments on, for example, materials in their natural ambient environment or while undergoing chemical reactions.

Hard X ray imaging is routinely used to map magnetic domains in two dimensions and composite materials in three dimensions, structural properties of individual grains in polycrystalline materials, strains in near perfect crystals and to produce time resolved imaging of sprays. Infrared microspectroscopy, infrared imaging and infrared microprobe techniques are being used to address problems in the identification of the molecular configuration and electronic properties of novel materials.

By using a synchrotron light source that has a high degree of transverse coherence, coherent X ray imaging can image single sub-micrometre particles at nanometre resolutions. A conventional X ray detector is used to record

the diffraction pattern and when the sample is rotated about an axis perpendicular to the beam, a three dimensional image can be reconstructed. Transverse coherence can be attained with either synchrotrons or X ray free electron lasers (FEL), which are inherently transversely coherent. An X ray FEL allows two dimensional imaging of single particles at high resolution with short pulse durations, thus limiting radiation damage to the sample during the measurement.

NEUTRON BEAM METHODS

The de Broglie wavelength of thermal or cold neutrons is similar to that of X rays, as both are of the order of interatomic distances and molecular dimensions, which makes them useful to probe the structure of materials. The main analytical properties of neutrons are: (a) they interact primarily with the atomic nuclei; consequently, their scattering cross-sections are angularly independent; (b) they display a relatively irregular Z dependence, which can differ markedly for different isotopes of the same element; (c) they carry a magnetic moment, allowing them to interact with unpaired electron spins; (d) they can scatter inelastically, losing (or gaining) enough momentum to allow the measurement of collective atomic motions and vibrations, as well as electronic transitions; and (e) they penetrate deep into matter, thus enabling measurements of large and bulky materials. To some degree, there is an overlap between the results that can be obtained with neutrons and those obtained with X ray techniques. The difference, and often the complementarity, lies in the different contrast mechanisms due to X rays being scattered by the electron clouds and the neutrons by atomic nuclei.

Neutrons are complementary to X ray sources, providing indispensable tools for spectroscopy, diffraction and imaging for structural and dynamic investigations in condensed matter research. Examples of research areas suitable for neutron based techniques include materials science, industrial applications and the broad but rapidly growing field of soft matter research, such as polymer science, dispersions and emulsions, rheology on solutions of micelles, and membrane lipids. The above mentioned analytical properties of neutrons make their use well suited for the investigation and development of energy applications such as fuel cells, batteries and automotive particulate filters, in addition to the well-established fields of magnetism, high temperature superconductivity and soft matter applications.

The transparency of certain materials to neutrons (notably vanadium) provides the possibility of engineering sample containers mimicking extreme environmental conditions. These controlled and transparent environments allow many industrially and technologically important dynamic processes to be followed in real time.

The applications of neutron beams are very similar to X ray/synchrotron techniques and can be grouped into three main categories.

Neutron scattering and diffraction

Elastic neutron diffraction is suitable for structural analysis with atomic or nanoscale resolution. Atomic resolution is achieved by wide angle or time of flight diffraction, using the Laue method, powder or single crystal techniques and nanoscale resolution by small angle scattering and neutron reflectometry.

The large scattering difference between hydrogen and deuterium is of special relevance in soft condensed matter systems such as phase separation or self-assembly studies in block co-polymers. Whereas X ray scattering or diffraction lack the electron density contrast, neutron scattering can benefit from the deuteration of one of the components to create contrast without altering the system chemistry.

Neutron spectroscopy

Neutron spectroscopy is mainly used for the investigation of inelastic scattering events such as lattice vibrations (phonons and magnons) and molecular vibrations and rotations, but also from magnetic/electronic excitations and relaxations. The latter finds applications of particular importance in the field of highly correlated electron systems and high temperature superconductors.

Neutron imaging and tomography

Neutron imaging methods include tomography, phase contrast imaging, stroboscopic imaging and the use of polarized neutrons. The selection of neutron energy for neutron imaging is important to effectively delineate the direct visualization of textures, the determination of stress and quantitative neutron tomography. Neutron imaging and tomography are sufficiently mature techniques to allow in situ experiments. Technical developments have progressed to a point that it is feasible to examine model devices on-line and under real operating conditions. Recent realization of these capabilities is demonstrated by work on diesel sprays in combustion chambers (imaging) and the structural modifications that take place in lithium batteries as the lithium is incorporated in the cathode and electrolyte materials. These experiments provide information complementary to similar and ongoing X ray studies.

ION AND ELECTRON BEAM METHODS

Beams of low, medium and highly energetic ions and electrons are extensively used to elucidate the structure, morphology and chemical composition of materials. Some of the main analytical techniques used are described below. Most of these methods are difficult to combine with in situ sample processing as the analysis requires both the material and measurement detectors to be placed and operated in a vacuum.

Ion beams

Ion beams impacting on the surface of a material generate a variety of radiations such as the emission of visible light, electrons, characteristic X rays and the ejection of material atoms and the backscattering of the incident ions, all of which can be used for analytical purposes.

The emission of light (ionoluminescence) is a technique used in studies of radiation damage accumulation and correlated structural changes in insulators. It provides information on the nature and behaviour of impurities in materials and intrinsic and radiation induced defects. Emission of electrons (Auger spectroscopy) gives important information about the electron temperature in the material, thus providing basic input data for elaboration of atomistic models of latent track formation. The emission of characteristic X rays (particle induced X ray emission, or PIXE) enables a material's composition to be determined in the near surface region to concentrations down to a few ppm. PIXE, when used with a nuclear microprobe, generates two dimensional maps of the elemental composition and distribution across the surface of a material surface with spatial resolution on the micrometre level. This information is used to study the stoicheiometry of individual grains in polycrystalline materials and to examine areas close to and across grain boundaries. Such information is of high importance in radiation damage studies of materials.

Ion beam induced charge imaging is a valuable tool used for the electrical characterization of microelectronic devices and circuitry. It is a fast and non-destructive way to assess possible manufacturing defects in microelectronic devices and to help improve the design of such devices. It is used to aid the design and radiation hardness testing of robust electronic devices for use in outer space applications such as satellites for telecommunications and global environmental monitoring.

Rutherford backscattering spectroscopy (RBS) is a non-destructive technique that can determine the elemental composition and its depth profile in the surface and near surface region of materials by measuring the energy distribution of the backscattered ion beam. A complement to RBS is elastic recoil detection analysis (ERDA), which detects ions ejected from a material and enables quantitative concentration and depth profiles of light elements, which are not normally accessible using other analytical techniques.

Electron beams

Electron beams are the most widely used tool to study the surfaces of solid materials. Electron beams provide a capability to visualize surfaces at the atomic level using scanning electron microscopy (SEM) or transmission electron microscopy (TEM). TEM, combined with in situ ion irradiation, permits the real time observation of defect formation and evolution in materials under well controlled irradiation conditions. It is a powerful tool to reveal the underlying kinetics of radiation damage processes and to benchmark computer models of radiation damage.

Other electron beam techniques commonly used include low energy electron diffraction (LEED) and reflection high energy electron diffraction, which are used to study the atomic arrangements in outer surface layers, and electron beam induced X ray spectroscopy (EDX), which is used to detect the chemical composition of atoms on material surfaces. Many of these electron beam techniques are commonly available with commercial scanning or transmission electron microscopes.

ENABLING TECHNOLOGY DEVELOPMENTS

To expand the possibilities of time resolved and in situ experiments, further development of key instrumental components such as detectors, beam conditioning optics and sample environment cells is required.

Development of enabling technologies is important to broaden research vistas by opening up new time domains, increasing count rate limitations, increasing scattering vector ranges and improving energy resolution. It is considered necessary to develop these new technologies, as existing technologies are becoming hard to maintain owing to components or materials becoming difficult to procure and not having easy to find replacements.

DETECTORS

For experiments in which the required time resolution is of the order of seconds or longer, position sensitive gas detectors using ^{3}He gas are widely used. However, there is a worldwide shortage of ^{3}He, so it is less available to fill new detectors or replenish existing ones. New technology must be developed in order to replace the presently used ^{3}He gas detectors.

For the very fast time domain, which becomes accessible with free electron laser (FEL) X ray based sources, the situation is at present far from satisfactory. In order to benefit from the very short but high intensity X ray pulses that FEL accelerators can deliver, new detectors are required to have performance parameters above what is presently available, namely, the peak flux of photons to be detected is several orders of magnitude higher than what is possible at present. It does not yet appear likely that current technology can be scaled up to make this feasible.

Technological developments of X ray detectors have historically been derived mainly from modified versions of consumer electronics, or have grown out of spin offs from high energy physics laboratories. Thus, a major part of the required budget to develop the technology base was supplied by the private sector. The developments for the rather specialist and low sales volume detectors that are required for FELs operating in the X ray regime will be very expensive and difficult to realize by individual laboratories. The lack of detectors that can capture the full range of the potential benefits that the FEL can produce should not, however, be seen as the most important rate limiting step towards obtaining results with FEL facilities. Historically, detector developments lag behind photon producing technology by at least a decade. Researchers have always found ingenious and novel ways to adapt existing technologies and devise measurement strategies that can, to a large extent, circumvent deficiencies in existing measurement technologies until a better and more permanent solution is found.

BEAM CONDITIONING OPTICS

Developments in optical systems are required in order to satisfy the demand of microfocus applications. With charged particle beams, the use of electrostatic or magnetic lenses is well established. The situation for neutron and photon probes is less so. There are no fundamental problems with X ray optics, however, practical issues such as thermal load management, radiation damage and focusing conditions have moved from the realm of technological development to engineering issues. The situation for neutrons is far from satisfactory.

SAMPLE ENVIRONMENTS

Recent developments in creating specialized sample environments now enable researchers to study in situ chemical and physical transformations while controlling environmental conditions such as atmosphere,

temperature, pressure or magnetic fields. Sample cells with specialized geometries to permit flowing solutions or gases have been developed to study surface phenomenons associated with corrosion or catalysis, and to mimic various industrial (processing) conditions and equipment, such as film blowers and reaction injection moulders. Such sample cells are being used to study the crystallization and phase separation behaviour during solidification as a function of external strain fields.

Other cell designs permit the encapsulation and study of air sensitive or radioactive samples. Among recent improvements in the development of synchrotron based capabilities is the ability to perform experiments over wide pressure ranges, enabling the in situ study of material failure and phase changes. Recent results obtained by performing soft X ray fluorescent spectroscopy (and microscopy) have demonstrated the possibility of performing deeper analysis of low Z elements in surfaces and thin films.

Sample cells can not only be used to mimic static conditions but also to initiate structural evolution in the sample. This capability is exemplified by experiments that use thermal or pressure jumps. For such experiments, the time resolution achievable will be a convolution of X ray beam intensity and the speed with which the sample can be perturbed homogeneously. The reduction of thermal gradients in this situation is easiest when the sample size is small, and therefore there is a tendency to miniaturize such containment cells.

RESEARCH DOMAINS

Materials research

Materials research that can benefit from the information provided by accelerator based technologies is wide ranging. The technology provides the opportunity to study materials and phenomenons occurring over a wide range of temperatures, times, pressures and length scales. Large research efforts are being directed towards the development and characterization of new materials that are relevant in energy production and utilization efficiency, such as low cost and efficient polymer solar cells, and renewed interest in the catalytic processes which generate combustible synthetic fuels. Real time characterization methods are indispensable for further developments in this area.

Research on materials for energy production is directed at improving materials properties to better withstand extremes of pressure, temperature or magnetic, electric or radiation fields. This research is highly applicable to materials for the production or life extension of nuclear reactors. The very harsh radiation environments found in parts of these reactors require thorough studies of the radiation induced ageing and degradation of materials properties. To simulate such behaviour, synchrotron X rays, neutrons and charged particle accelerators are being utilized to investigate the structural changes of materials in real time. Spin off studies of this type of research are slowly being adapted and applied to materials applications in other harsh environments such as outer space, large scale chemical reaction vessels and blast furnaces.

Radiation damage and the structural integrity of materials

The development of new reactor cladding materials that can endure a prolonged bombardment with neutrons and high energy photons and electrons is important when designing fusion and advanced fission reactors. The use of charged particle accelerators can render highly relevant ageing data in timescales much shorter than the expected lifetime of the reactors. This, in combination with improved computer modelling software, and combined with on-line X ray and neutron experiments, is of vital importance for the accelerated development and testing of new materials.

The stability of solar cells to prolonged exposure to sunlight is especially relevant for the long life performance of organic solar cells. Material lifetime issues have so far been a major barrier for their large scale introduction, and performance degradation is difficult to predict purely on thermodynamic principles. On-line testing with different radiation probes is required, where the damage due to photoelectrons can be simulated by electron accelerators.

One of the recurring themes in the research of energy related materials is the requirement to study the structural degradation suffered by working devices during their operational cycle (e.g. batteries, hydrogen storage materials). This damage might have multiple causes and be spread out over multiple length scales. A multidisciplinary approach, using several accelerator based techniques and theoretical modelling, might in some circumstances be

the best way to obtain a comprehensive research path. In the first instance, a model 'damaged' material can be created by exposure to heavy ions, electrons or neutrons. The structural damage and damage creating mechanisms can subsequently be studied by synchrotron, neutron or electron beams.

Materials development

Synchrotron and neutron based techniques provide information over and above conventional laboratory X ray tools used in materials analysis and characterization. The accelerator driven high intensity facilities are essential when studying transient processes. The existing portfolio of synchrotron and neutron radiation based techniques is largely adequate with respect to the variety of available techniques, but may not be adequate with respect to the available volume of beamtime demanded by researchers.

The requirements for time resolved or real time experiments come from the fact that not only the basic material properties are relevant but also that the processing pathways may have influence on the structure of the materials. For instance, the temperature quench rate and shearing treatment of semi-crystalline polymers will influence the degree of crystallinity and orientation of the crystallites, and thus influence the macroscopic material properties. The same is true for catalytic materials, where it would be desirable to develop 'one pot' methods in which a single heat treatment will suffice for the self-assembly and structure formation of the catalyst carrier, as well as the appropriate positioning of the catalytically active particles in the carrier material.

In order to be able to study such processes, quite often, an array of characterization techniques is required. To perform these experiments independently and merge the derived information at a later stage is not always the best option. Ideally, one would like to derive the information from a single sample that is simultaneously studied with different techniques in order to eliminate the systematic experimental errors intrinsic to the combination of independent experiments. The intrinsic systematic errors have a variety of causes, most notably thermal gradients, different thermal histories and sample inhomogeneities. Although some efforts have already been expended to construct experimental facilities that enable combinations of techniques, it is still difficult to implement owing to the extra expense that is required for the construction of the required multipurpose facilities and to have researchers capable of simultaneously operating complex and specialized instruments and analysing and integrating the data outputs.

Interface studies

It has long been recognized that studies characterizing the interface between two different materials, be they solid–gas, solid–liquid or solid–solid, are important for the understanding of many phenomenons such as corrosion, absorption, catalysis and separations. Also, the increased importance of chemically and physically functionalized surfaces, useful for sensor development relevant to process control, makes a detailed understanding of the interfacial structure at the molecular level an important area for energy research.

Interfacial studies are technically challenging. The main difficulty originates from the intrinsically limited amount of material probed by the beam, since by design, the interfacial region inherently consists only of a small number of atomic or molecular layers. For solid–liquid and liquid–liquid interfaces, this situation is complicated further by beam attenuation resulting from the experimental geometry, which requires the incident beam and often the scattered beam, to travel at grazing angle incidence to the surface. In general, demanding geometry requirements impose their own experimental challenges when dealing with liquid interfaces. In most cases, the experimental configuration is restricted by the requirement to optimize the fraction of surface material contributing to the signal, while minimizing the signal from underlying material that contributes to the background. Further complications arise from beam induced damage when using electrons or X rays as probes.

Such demanding experimental conditions complicate the situation with respect to time resolved studies. The new generation of synchrotron radiation sources allows better control over beam dimensions and stability, which in combination with more sensitive low noise detectors, are enabling some time resolved experiments. The introduction of two dimensional detectors capable of high dynamic range measurements has been of particular benefit to the speed by which comprehensive structural information from surfaces and interfaces is obtained. The method of grazing angle incidence small angle diffraction is an example of this new capability, where processes at surfaces and interfaces can be studied in a time resolved way.

Spectroscopic methods that probe changes in the chemical state of surface atoms can be carried out in some cases. The use of energy dispersive methods in the case of solid or gas surface studies in a time resolved fashion are feasible and carry promise for the fundamental understanding of catalytic, absorption and corrosion processes. Techniques that render more structural information, such as interfacial scattering, are more difficult to bring into the time resolved domain but, by utilizing faster data collection methods, it is feasible to utilize 'freeze frame' techniques in which the process is temporarily halted and the diffraction data collected before allowing the process to continue again. These methods assume that structural changes during data collection are small enough to be ignored.

Device characterization

At present, there is a growing realization of the need to implement in situ studies of model devices on instrument beamlines. This realization arises from many examples in which the results from ex situ experiments, when extrapolated to in situ operation, produced erroneous conclusions.

The proper characterization of working devices often requires a step in the pre-measurement set-up process in which the device has to be imaged in order to know where to properly place the neutron or synchrotron beam to perform the local characterization. For the imaging of whole devices, one requires the high penetration power of either neutrons or high energy X rays, depending on which absorption contrast renders the best results, such as the fuel distribution inside the cylinder of an internal combustion engine.

Time domains

The time domains that need to be addressed in materials research can be quite wide ranging. For example, in the high energy consuming processes regarding the production of building materials such as concrete and brick, where energy savings will have large benefits on a global scale, long time resolutions (minutes) are required to study the processes involved. At the other end of the timescale, nanosecond time resolutions are required for real time studies of catalytic or corrosion reactions. For most materials science studies, the required timing rate should be compatible with process conditions, i.e. from 0.1 sec/time frame, and longer.

CONCLUSIONS

The summary of the IAEA Technical Meeting on the Utilization of Accelerator Based Real Time Methods in the Investigation of Materials with High Technological Importance underlined that accelerators can be effectively used for the in situ real time preparation and characterization of materials for energy production and storage. It was pointed out that there is a very diverse range of accelerator technologies, grouped around synchrotron, neutron and particle beams. From this point of view, the great value of this publication is the inside view it offers of the experimental details of accelerator based technologies applied for real time investigation, which also includes practical applications of in situ methods. Within this context, it has been agreed that the definition of 'real time' is on the scale of seconds to hours, corresponding to the events that induce changes in the sample properties.

Nowadays, the main emphasis is placed on the simultaneous utilization of different techniques for studies involving materials processes. This approach can render a fully comprehensive picture of structure development and catalytic activity. In addition, real time experiments can help to address and understand some complicated phenomena such as stress accumulation or radiation damage formation, and have the capability of evaluating crucial material characteristics. A brief review on spallation neutron sources and other accelerator driven neutron sources with lower intensity is also given, since this is a very promising trend for research and development in the area of nuclear science and technology.

The individual papers report on various different approaches to experimental set-ups and equipment design. A short overview of the presented papers is given in following text.

The paper presented by J. Becker entitled Peering into the Black Box: In Situ X ray SAXS/WAXS/PDF Studies of the Formation and Growth of Inorganic Nanoparticles During Near or Supercritical Synthesis reports on the development of self-built equipment designed for in situ studies of nanoparticle growth in sub- and supercritical

fluids. The fact that the same reactors are used for different experiment types, including WAXS, SAXS and PDF, at a handful of different beamlines worldwide demonstrates their flexibility.

The second paper was presented by W. Bras under the title "Time resolved X ray scattering and spectroscopy in materials science". The paper reviews the application of beamlines at synchrotron radiation sources where materials can routinely be studied under relevant processing conditions with an array of techniques that render a fully comprehensive picture of structure development and catalytic activity. These types of experiments can be performed in most synchrotron radiation laboratories, but in general, this is done in an improvized fashion.

The third paper, presented by V.A. Skuratov, is entitled "Real time studies of materials at FLNR JINR cyclotrons" and summarizes real time experiments, focussing on the study of electron stopping power and the threshold of radiation damage formation via electronic excitations. The authors claim that ion track region overlapping may stimulate the stress relaxation processes.

The fourth paper was presented by L. Gregoratti under the title "Chemical imaging of materials with scanning photoemission spectromicroscopy". It reviews some of the recent achievements in the investigation of the chemical and electronic properties of nanostructured materials and the identification of local surface processes related to chemical interactions or mass transport.

The fifth paper, presented by D.K. Avasthi, discussed the "Development of facilities for the in situ characterization of materials in the materials science beamline at the IUAC Pelletron accelerator". The paper provides a brief description of the in situ facilities at the beamlines of the 15 MV Pelletron accelerators. A few examples of experiments are quoted and some results obtained using these in situ characterization tools in the beamlines are given.

The sixth paper, presented by Y. Kiyanagi and entitled "Imaging of texture, crystallite size and strain in materials using accelerator based pulsed neutron sources", introduces imaging of the crystallographic structure over a wide area, in which the image was obtained at one measurement without scanning. Therefore, it is suggested that this method may be unique in that it can measure information on the actual material at the same period as the real time measurement.

The seventh paper presented by E.H. Lehmann with the title "Spallation neutrons used for imaging in the time and energy domain" reports that spallation neutron sources and other accelerator driven neutron sources with lower intensity will be the future of neutron generation for research purposes. New time of flight techniques are also of high importance for neutron imaging applications where the energy selection has to be made for the highest performance and flexibility.

The eighth paper, presented by T. Kamwanna, described the "Establishment of an ASEAN ion beam analysis centre for material characterizations at Chiang Mai University". It reviews the accelerator based ion beam facilities composed of a high energy tandem accelerator and a medium energy pulsed beam accelerator which have been developed to form a comprehensive ion beam analysis centre. The IBA centre has developed and applied key ion beam analysis techniques such as RBS, RBS/channelling, EBS, PIXE, ionoluminescence (IL), low/medium energy time of flight (ToF) RBS and microbeam reading/writing for applications in various fields.

The ninth paper was presented by Meimei Li under the title "In situ characterization of nuclear energy materials by synchrotron radiation and electron microscopy" and presents the applications which of transmission electron microscopy combined with in situ ion irradiation and high energy X ray diffraction with simultaneous thermal-mechanical loading in the study of nuclear energy materials. Examples are given, including a novel experiment of TEM with in situ ion irradiation of Mo thin films designed to improve and validate a rate theory based cluster dynamic model.

The last paper was presented by L. Soderholm under the title "The advanced photon source: using synchrotron radiation to study actinide containing samples relevant to nuclear energy systems" and reports on the application of synchrotron radiation, which currently holds untapped potential to contribute to state of the art research and development in the area of nuclear energy. Very few developments, both on the part of the synchrotron and user communities, are required to begin to realize this potential.

In general, this publication provides an overview of research themes for which accelerator based techniques are effectively used for real time studies of materials relevant to energy production and conservation. This is particularly important since new scientific and technical challenges are posed by current trends and the emergence of new directions in energy related research and development programmes. In general, particle accelerators can be utilized to mimic damage processes, while the techniques available at large scale user facilities are employed to study damage mechanisms. A recurrent theme in energy research is the damage sustained by working devices during

their operational cycle or as a result of ageing effects. The increased level of complexity in modern materials often requires real time experiments to be undertaken, whilst applying several experimental techniques simultaneously. It would be a real advantage if the design and methodology for this more complex instrumentation could be more widely disseminated between the central facilities and their user communities. Specifically, the design of sample environments that enable in situ and real time studies of devices or materials processing cycles under realistic conditions remains an area where major improvements can be made and significant practical benefits realized.

At the time of writing, it is clearly recognized that synergy exists with respect to the pivotal issues identified, which are pertinent to the function of ongoing international research programmes, namely: (a) the combination of experimental techniques to enable data correlation on multiple scales in spatial and temporal domains; (b) material containment and manipulation of the sample environment; (c) the types of radiation damage/formation expected upon exposure to extreme environments; (d) the evolution of structures of both bulk systems and thin films.

Finally, the meeting also helped to summarize the pertinent techniques available at different institutions for materials research, which has value for newcomers, interested end users and potential research partners.

PAPERS PRESENTED AT THE TECHNICAL MEETING

PEERING INTO THE BLACK BOX: IN SITU X RAY SAXS/WAXS/PDF STUDIES OF THE FORMATION AND GROWTH OF INORGANIC NANOPARTICLES DURING NEAR OR SUPERCRITICAL SYNTHESIS

J. BECKER, N. LOCK, M. BREMHOLM, C. TYRSTED, B. PAUW, K.M.Ø. JENSEN,
J. ELTZHOLTZ, M. CHRISTENSEN, B.B. IVERSEN
Center for Energy Materials and Center for Materials Crystallography,
Aarhus University,
Aarhus, Denmark
Email: bo@chem.au.dk

Abstract

In recent years, the applications of inorganic nanomaterials within the field of energy production and storage have grown. This is spurring a need for synthesis methods that allow a specific tailoring of material properties, e.g. size and size distribution, crystallinity or morphology. One promising candidate to resolve this is wet chemical synthesis at elevated temperatures and pressures, also known as hydrothermal or solvothermal synthesis. Unfortunately, the fundamental chemical processes taking place under these conditions are to a large extent unknown, since they are confined inside a closed reactor/container commonly made of steel. Here, the design, construction and application of two experimental set-ups are presented, both of which allow in situ studies of the chemical reactions going on 'inside the pressure cooker' by means of synchrotron X ray radiation. Effectively, they act as video cameras designed for capturing 'movies' of the birth, growth and development of nanoparticles inside a reaction environment which has a temperature of 100–600°C and a pressure of several megapascal. The main characterization techniques which make this possible are wide angle X ray scattering (WAXS), Small angle X ray scattering (SAXS), pair distribution function measurements (PDF) and X ray absorption spectroscopy (XAS), applied either separately or simultaneously, e.g. as SAXS/WAXS or WAXS/PDF. Since time resolutions (the 'frame rates') are usually <10 seconds, this allows a complete survey of the entire course of a synthesis reaction, right from before the onset of the material formation until the final product is obtained.

1. INTRODUCTION

One of the most common synthesis techniques within inorganic chemistry is that of solvothermal synthesis, i.e. a wet chemical approach where dissolved or suspended precursors, usually metal salts, are subjected to high temperatures and high pressures (T ~ 70–600°C, P ~ 100 000–50 000 000 bar), which trigger a chemical reaction. The products are particles, usually with sizes in the nanometre range, with properties which depend on the specific route of synthesis and the parameters involved. Two such routes are commonly employed: solvostatic/hydrostatic autoclave (batch) synthesis (Fig. 1) and continuous flow synthesis in a tubular reactor (Fig. 2) [1, 2].

The common advantage is that the reaction environment may be considerably manipulated through the synthesis parameters. Naturally, fundamental choices of solvent, precursor and pH value have a huge impact on any wet chemical synthesis, but in solvothermal syntheses the additional parameters of temperature and pressure offer yet another way of manipulating solvent properties such as redox potentials, solvent power, density, diffusivity, etc. Indeed, a solvent may achieve highly unusual properties when its critical point is approached (near critical regime) or exceeded (supercritical regime).

Some of the most common characterization methods for inorganic nanomaterials are powder X ray diffraction (PXRD, also known as WAXS), electron microscopy (TEM or SEM), surface area measurements (BET), SAXS and occasionally dynamic light scattering. Each offers certain advantages to the characterization at hand, but several of the techniques are usually employed to exploit their complementarity.

Another way of attacking the issue of characterization has been developed [3, 4]. The techniques in question are all X ray based, notably WAXS, SAXS, PDF and XAS. Where possible, SAXS and WAXS have been applied simultaneously to obtain complementary information on amorphous and crystalline sample contents.

The purpose is to elucidate the chemical reactions and materials transformations occurring inside a flow reactor throughout a near or supercritical synthesis. With such insight, the kinetic and thermodynamic effects of external parameters can be scrutinized and reaction intermediates identified, which would be invaluable knowledge in any subsequent attempt to design a real flow synthesis (in the home lab) of the material in question [5].

FIG. 1. 20 mL batch autoclaves (common design).
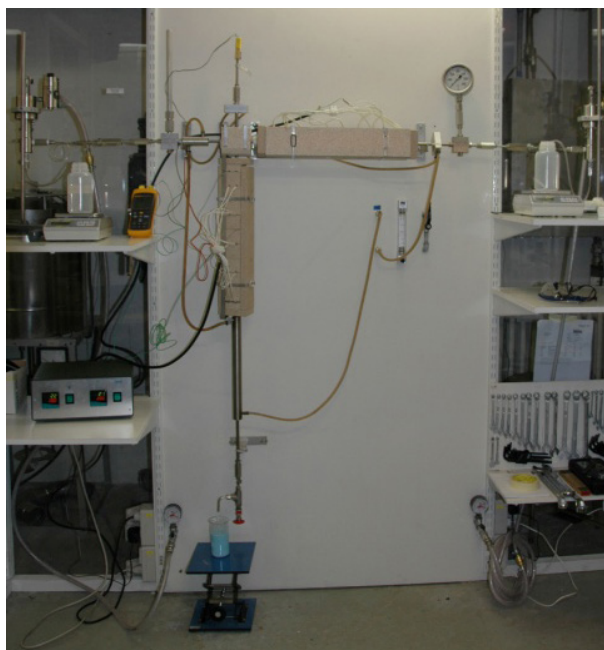
FIG. 2. Example of a reactor for continuous flow synthesis.

2. EXPERIMENTAL CHALLENGES

The relatively slow heating rates of regular autoclave vessels (whether used for in situ or ex situ experiments) renders them unsuitable for studying reactions or transition phenomenons occurring on short timescales. Various reactions may be initiated within different temperature intervals during heating which will likely result in a poorly defined overall composition of the reaction medium. This situation persists until the point where (a) some intermediate with long term stability is formed or (b) all chemical reactions have ceased. This is exemplified by the broad size distribution of TiO_2 particles resulting from synthesis in an autoclave in comparison with those synthesized in a supercritical flow reactor [6].

Generally, the timescale on which the kinetics of the studied reaction evolves defines the required heating rate. Obviously, the slower the reaction, the more time there will be to reach the set point temperature without affecting the outcome of the experiment. Consequently, if one wishes to study the rapid reaction kinetics dominating at high temperature in a meaningful way, heating must be extraordinarily swift and the set point usually reached within seconds of the initiation of the experiment. This is a significant concern with in situ PXRD studies of solvothermal reactions in near or supercritical media, since high temperatures are required to reach these states (Tc(water) = 374°C) and reactions are usually complete within minutes or even seconds at these conditions.

Apart from the issue of heating rate, which concerns the chemistry being studied, certain general requirements must also be addressed for an in situ PXRD experiment to work. The most important are:

— The X ray transmission through the high pressure vessel should be as high as possible.
— The flux of the applied X ray beam should be as high as possible.
— The sample must be thin relative to the detector distance in order to obtain a good line profile (instrumental peak broadening) of the set-up.
— The readout time of the detector should be short.

All of these issues arise from two basic experimental concerns: data quality and time resolution. For instance, low incident flux or high absorption of the beam will both result in poor data quality unless the exposure time is increased, which in turn will mean a loss of time resolution and a 'smear' of synthesis phenomenons which occur on short timescales. The same situation occurs if the detector readout time is too slow. Generally, each dataset must be collected in a matter of seconds to give an appreciable time resolution even at high synthesis temperatures.

Optimization may be achieved in three ways.

— Choosing a vessel made of an X ray transparent material, i.e. made predominantly of light elements;
— Reducing the wall thickness of the vessel, which of course requires the chosen material to be strong and possess a high thermal stability in order to handle the elevated temperatures and pressures of the synthesis inside;
— Using a higher X ray energy to lower the absorption.

The latter option seems attractive as it also reduces air scattering of the scattered beam. Unfortunately for WAXS and SAXS applications, a higher X ray energy also means that scattering angles will be reduced, which means that a longer sample to detector distance is required to optimise the resolution (which again increases air scattering). Another complication at very high energies may be the photon capture efficiency of the detector, which is gradually lost with increasing photon energy, meaning that a careful choice of detector is needed. Finally, the scattering intensity varies with λ^2, which results in an overall loss of diffraction intensity as the X ray energy is increased.

Necessary conditions may be met by using a small vessel [7, 8]. Such a reactor will be more pressure resistant than a large container owing to the reduced internal surface area, and the wall thickness can thus be minimized. Unfortunately, a thin sample will also mean that the X rays have less material to scatter from, which places a lower limit on the precursor concentrations used in the experiments, particularly when studying materials consisting of light elements. A longer detector distance allows a thicker sample without sacrificing the line profile, but at the expense of a reduced pressure rating of the vessel or thicker walls, meaning a loss of transmission.

As it appears, a completely optimal solution to the requirements of an in situ PXRD experiment on a near or supercritical synthesis is seldom achievable. Certain trade-offs must be made in order to preserve data quality while minimizing the time required for collecting each dataset. Both concerns are closely connected to the capabilities of the X ray source. The lower the flux and/or available X ray energy, the more extra ingenuity regarding the whole experimental set-up will be required for the in situ experiment to work.

3.   SET-UP INTRODUCTION

The in situ X ray scattering studies of solvothermal nanomaterials syntheses carried out by the Aarhus group have relied on two experimental set-ups. One is used for SAXS/WAXS/PDF studies at moderate conditions up to

450–500°C and 25 MPa, [4] the other is used for high temperature SAXS/WAXS studies, up to 650°C and 350 bar [3, 9]. The two experimental set-ups are described in the following subsections.

3.1. Set-up 1 — sapphire capillary reactor

Some of the basic design concepts for this set-up were inspired by Clausen et al. [7] and Norby et al. [8], who both employed the microreactor concept by using thin capillaries for the reaction vessels. Generally, the reduced bulk of a microreactor compared with an autoclave is highly advantageous with regard to obtainable heating rates. At the same time, the low internal surface area gives high pressure tolerance and the relatively thin container walls enhance X ray transmission, thus addressing all the experimental challenges outlined above. With autoclaves used for in situ studies, high X ray energy must be used to achieve a similar transmission or the set-up must be equipped with X ray windows [9], which are hard to manage experimentally because of the high pressures inside.

Figure 3 below shows one of the recent versions of the microreactor developed at Aarhus University [4]. The reactor itself is a sapphire ($\alpha\,Al_2O_3$) capillary, giving acceptable transmission even at relatively high wavelengths (~1.0 Å). Figure 4 shows the design of the reactor mount. The capillary has been proven to withstand pressures of up to >300 bars, which is more than enough for the use of supercritical water in the syntheses being studied (Pcrit of water being only 22.1 MPa). This is an important feature as hydrothermal syntheses are of great technological interest owing to the environmental advantage of using water rather than other (organic) solvents. The pressure is delivered externally by means of an HPLC pump and adjusted to the desired value with a proportional relief valve (PRV).
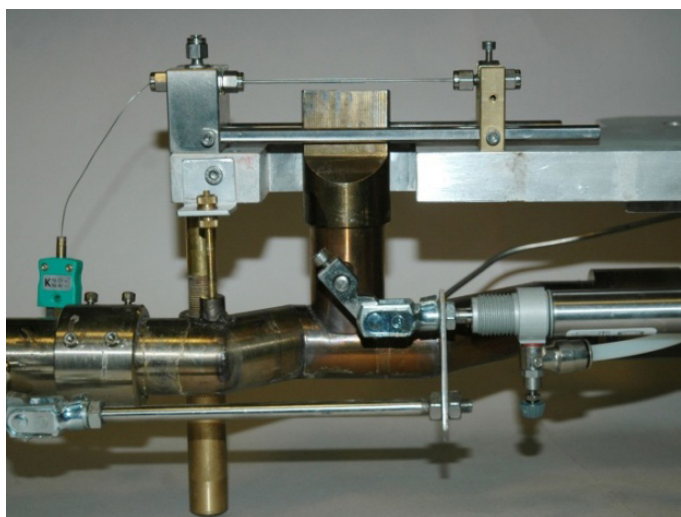

FIG. 3. One of the reactor designs developed at Aarhus University for in situ studies of solvothermal/hydrothermal materials syntheses. A thermocouple inside the capillary allows an accurate monitoring of temperature.
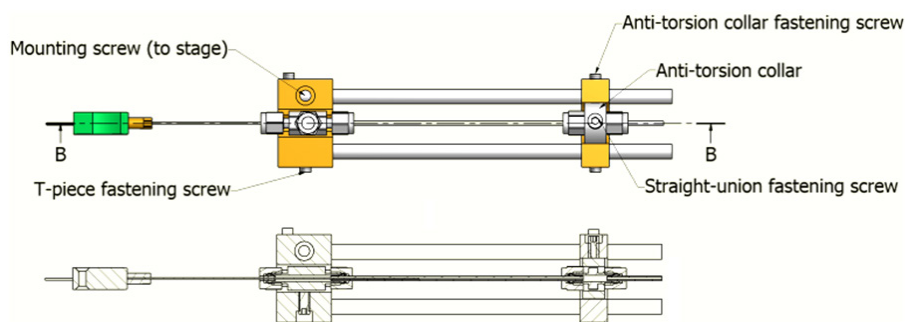

FIG. 4. Design of the capillary reactor mounting system.

The heating of the reactor is provided by a jet of hot air delivered from a commercial heater (Leister LHS 20 L), allowing an effective temperature range up to approx. 450°C, which is also enough for the use of supercritical water, as Tcrit for water is 374°C. The temperature is measured internally in the capillary, which allows an accurate adjustment of the actual synthesis temperature.

A swift heating to the set point temperature is provided by a pneumatic shutter system, which allows the airstream to be preheated while blowing into an exhaust tube. When beginning the experiment, the shutters are switched and the already hot air is directed onto the capillary, which gives a very steep heating profile (Fig. 5) compared to a 'cold started' heating system, as exemplified in Fig. 6 by means of an ordinary heat gun. Further upgrades to this system have recently led to a heating profile which reaches set point temperature within 10 s of initiation of the experiment (data not shown).

3.2. Set-up 2 — steel tube reactor

This set-up was initially developed as a miniature version of a flow synthesis reactor, complete with preheating, mixing tee and a reactor tube (SS316, 1/8 in. O.D.) surrounded by two electrically heated metal blocks. Gaps between the blocks allow an incident X ray beam to reach the reactor tube and the diffracted beams to exit on the other side (Fig. 7) [3].

As with Set-up 1, the pressure is controlled by means of high pressure pumps and a PRV. Initially, HPLC pumps were also used for Set-up 2 to directly pump precursor solution into the preheated reactor tube. Unfortunately, this approach turned out to damage the pumps and a simple injector reservoir was therefore added to the set-up, consisting of an adjacent 3/8 in. tube filled with precursor solution. By feeding pressurized solvent to one end of this tube, the solution could be forced into the preheated reactor tube without being diluted too much. The concept worked relatively well, except that precipitation inside the reactor tube forced the improvized use of a socket head screw placed inside it (supported by the bottom end fitting (Fig. 8), onto which the as-formed nanoparticles could settle while still remaining inside the heated zone. The X ray was aimed right above the head of the screw and the internal thermocouple placed immediately underneath it.
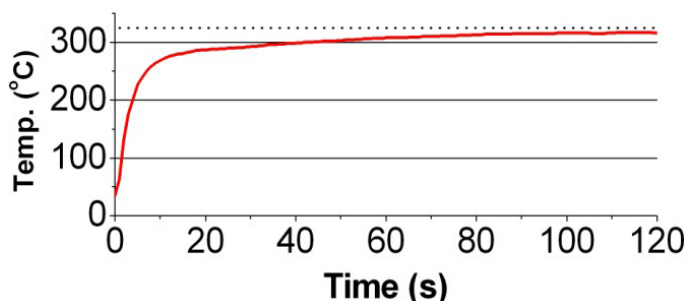

FIG. 5. Temperature profile during heating for second version of Set-up 1 (Leister heater + air shutter system). T_{set} = 325°C (dotted line). T_{120s} = 316°C.
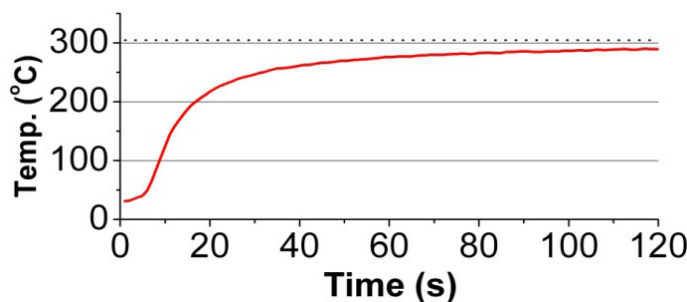
FIG. 6. Temperature profile during heating for first version of Set-up 1 (heat gun, no air shutters). T_{set} = 305°C (dotted line). T_{120s} = 290°C.
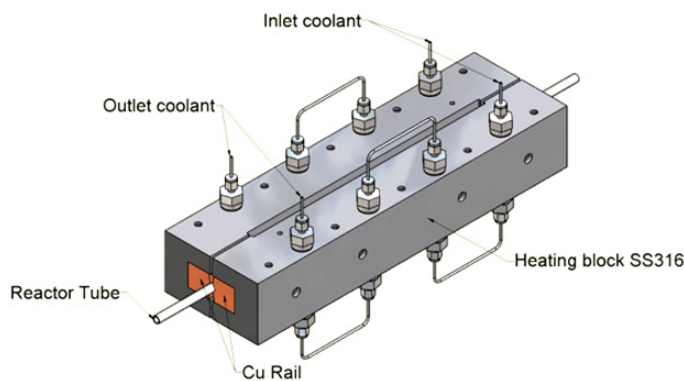
FIG. 7. Schematic drawing of the reactor body of Set-up 2. The inlaid cooling system is used between experiments, to avoid wasting time on passive cooling to lower set point temperatures.
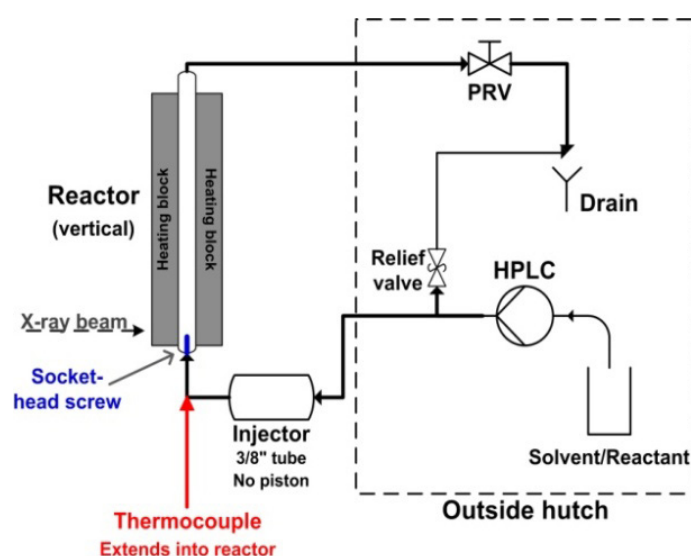
FIG. 8. Representation of the original use of Set-up 1 in an autoclave like mode with pressurization by HPLC pump.

With this concept, some interesting studies could be made. Thanks to the sturdy steel tube, appreciable temperatures could be reached without worrying about the pressure integrity of the set-up. Early on, the basic limitation was indeed the heater blocks; at the time these were made of aluminium, which melts at a temperature of 660°C. As such, temperatures above 500–550°C were avoided, and were in any case difficult to reach. Consequently, more recent versions of the set-up use steel blocks with inserted copper rails to improve heat transmission, assisted by enhanced electric heating, thus increasing the accessible temperature range up to 600–650°C.

One experimental series which benefitted from the early version of Set-up 2 was the synthesis of boehmite, AlOOH [10]. However, the relatively slow injection caused a non-negligible temperature loss inside the tube upon precursor injection. A similar experiment could have been conducted using the updated version of Set-up 1 presented above, which is simpler to work with and does not require such high X ray energies. Consequently, the basic use of Set-up 2 has been changed and technically updated to suit experiments which were outside the reach of Set-up 1. The tube diameter was reduced to 1/8 in. and the HPLC pumps replaced with pneumatic high pressure pumps. Since one pump stroke is generally enough to fill the reaction tube, the cooling of the tube is minimal, which allows a very well defined beginning of the experiment and the set point temperature is consequently reached in <3 seconds, even with syntheses operating in the excess of 500°C.

4. EXPERIMENTS AND SELECTED RESULTS

WAXS, SAXS, PDF theory and XAS are techniques that provide complementary structural information. Such information is used to elucidate the mechanisms for nanoparticle growth in sub- and supercritical fluids. Our main technique is WAXS, which is applied either alone or in combination with one or more of the techniques described below. Furthermore, the in situ results are often combined with ex situ electron microscopy, thermal analysis and surface area determination. The mechanisms behind the growth of various functional materials have been studied. This section describes the types of in situ experiments we perform with the main focus on WAXS, and selected results are briefly described.

4.1. WAXS and SAXS

WAXS, as mentioned above, is typically referred to PXRD. Powder diffraction is Bragg diffraction from a large number of randomly oriented single crystals, e.g. nanoparticles [11]. A powder diffraction pattern represents scattering from all possible crystal planes and can therefore be used for the simple phase analysis of a sample. Alternatively, a model can be refined to the data. Profile fitting, also known as Le Bail fitting [12], is a method to extract the unit cell and profile parameters from powder diffraction data with very high accuracy. It requires the space group to be known, but no structural parameters are included in the Le Bail model. Refinable parameters include the unit cell and Gaussian and Lorentzian profile parameters to describe the peak shape profile. In a structural refinement, the Rietveld refinement, a model is fitted to the observed data to extract information on the structure of the sampled material. Variables in the Rietveld algorithm include: the unit cell parameters, atomic positions, site occupation fractions and thermal parameters, as well as the instrumental parameters included in the Le Bail model.

Powder diffraction data collected on a sample consisting of large grains of ideal crystals produce extremely narrow Bragg peaks. However, a nanocrystalline sample gives rise to broad peaks in a powder diagram. An estimate of a particle size can be determined using the Scherrer equation [13], where $B(2\theta)$ is the full width at half maximum (FWHM) intensity of a diffraction peak. The dimensions of non-cubic nanocrystalline materials are determined by looking at different reflections hkl. L is the length of the crystal in the direction normal to the corresponding reflecting hkl planes and K is a constant attaining a value of 0.9.

$$L = \frac{K\lambda}{B(2\theta)\cos\theta} \tag{1}$$

Owing to the $1/\cos\theta$ relation between B and θ, the size broadening is most pronounced at large diffraction angles. Using the software FullProf [14], it is possible to describe the morphology of non-spherical particles by fitting profiles with spherical harmonic functions. Thereby not only the evolution in size but also in morphology can be followed as a function of time. As an example of this, Fig. 1 (left) displays the morphology of AlOOH nanoparticles formed in subcritical water in the sapphire reactor. The corresponding diffraction data are shown in Fig. 9 (right).

It is important to note that only the size of the crystalline nanoparticle is determined from WAXS. If the particles consist of e.g. a crystalline core and an amorphous shell, the actual particle size may differ from that determined by WAXS. Furthermore, WAXS does not provide any information on the nucleation state until a crystalline particle is formed. SAXS, which is elastic scattering of X rays by a sample at very low angles, can provide information on the total size and shape of particles and their size distribution. As opposed to high resolution WAXS, which provides structural information on the atomic scale, SAXS provides information on nanosized structures, e.g. nanoparticles, colloids and polymers [13]. The radius of gyration, R_g, is a structural parameter which can be extracted from the intensity profile of SAXS data. (R_g is defined as the mean square distance from the centre of mass). However, obtaining a detailed structural description of the sample, including a size distribution, requires a reasonable structural starting model and sometimes supplementing information obtained by other techniques (e.g. knowledge on particle morphology from electron microscopy). In terms of in situ studies of nanoparticle growth, SAXS gives information on the total particle size, regardless of the crystallinity of the particles.
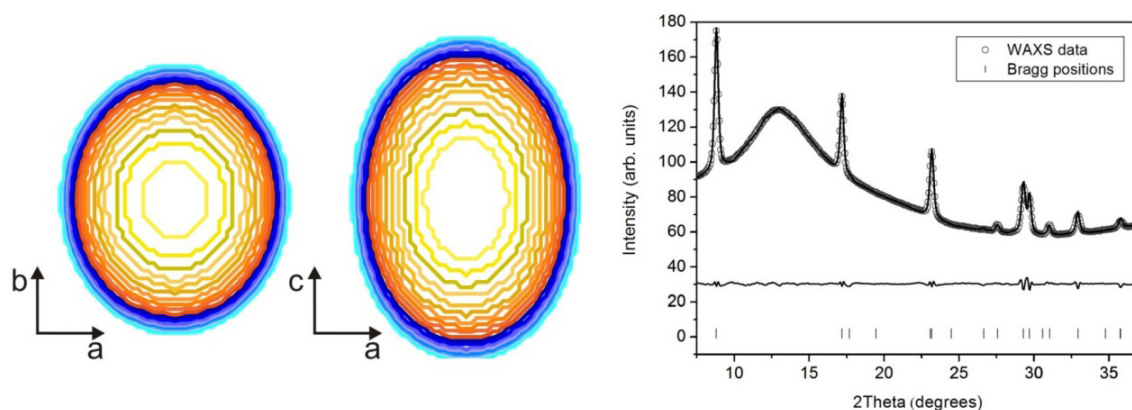
FIG. 9. (left) Projections of average AlOOH nanoparticles determined from WAXS data (right) collected at 12.4 keV at the I711 beamline, MAX II synchrotron (MAX lab, Sweden). The data (y_{obs}) are shown as open grey circles, the model (y_{calc}) as a bold line, y_{obs}–y_{calc} as a narrow line and the Bragg positions as vertical lines.

The synthesis of magnetite, Fe_3O_4, in sub- and supercritical water has been studied in the steel reactor using in situ SAXS and WAXS by Bremholm et al. [5]. WAXS demonstrates that phase pure magnetite forms without the formation of any crystalline intermediates. In contrast, SAXS demonstrates the formation of an amorphous intermediate. Furthermore, the study shows a textbook example of how the particle growth rate increases with increasing reaction temperature. Through detailed data analyses, not just the time dependent size, but also the size distributions as a function of time were extracted from SAXS. The data show that the particles become more polydisperse with increasing reaction time.

Reaction kinetic models can be applied on growth curves (particle size as a function of time) from WAXS or SAXS data. Tyrsted et al. [15] report how the growth kinetics of $Ce_xZr_{1-x}O_2$ varies with the sample stoicheiometry. The growth of samples with high cerium content is initially limited by surface reaction kinetics and is later limited by the diffusion of monomers towards the particle surface. The trend is the opposite for samples with low cerium content.

Another interesting aspect of detailed WAXS data analysis is the change in unit cell parameters as functions of the particle size, which have been observed for several chemical systems. The magnetite system shows that the cubic unit cell decreases with increasing particle size [5]. Such behaviour is known from the literature and is explained by the fact that going towards smaller crystals corresponds to applying a negative pressure resulting in an expansion of the unit cell [16]. We also observed a complex unit cell evolution with particle size for the battery material $LiCoO_2$ [17].

4.2. PDF and XAS

PDF and XAS are complementary to WAXS and SAXS, which mainly focus on the overall particle phase, size and shape. PDF and XAS provide information on the local structure of the nanoparticles and/or intermediate crystalline or amorphous phases formed during particle nucleation/growth. The interatomic distances obtained from these studies are the actual atomic pair correlations which are not time and space averaged similarly to Bragg diffraction data (i.e. WAXS data).

PDF data, in fact, are Fourier transforms of powder diffraction data collected to very high Q values (>20 Å^{-1}). In order to reach these, the experiments require X ray energies significantly higher than those necessary for SAXS or WAXS experiments, usually 70–80 keV. PDF analysis uses the diffuse scattering data contained in powder diffraction data in addition to the Bragg peaks as a source of structural information [18]. By Fourier transforming the reciprocal lattice data, a real space pair distribution function (intensity as a function of r(Å)) is obtained. It has peaks corresponding to characteristic interatomic distances in the crystalline or amorphous material. Such data can confirm the crystal structure of the expected crystal phase of the nanoparticles and the actual non-averaged interatomic distances can be determined by refining a model against the data. As the PDF contains correlations between atoms spaced by distances out to several nanometres (>10 nm), the total particle size for small particles can be extracted directly from the PDF as the maximum distance at which correlations are observed.

XAS data are collected by scanning a sample with monochromatic X rays with energies from approximately 150 eV below to 700–1000 eV above the absorption edge of the absorber atom [19]. Information on the local structure around the absorber atom is contained in XAS data. The data are typically divided into X ray absorption near edge structure (XANES) and extended X ray absorption fine structure (EXAFS) data. Information on the absorber atom oxidation state can be determined from the XANES data. EXAFS data can be refined against a structural model; the refinable parameters include non-Bragg averaged interatomic distances, coordination numbers and vibrational parameters. EXAFS and PDF are complementary techniques. The main difference between applying the techniques is that only one type of atoms is probed with EXAFS, whereas correlations between all atoms are contained in the PDF. This makes EXAFS a strong tool for studying the coordination environment around e.g. dopant atoms.

5.   CONCLUDING REMARKS

In summary, this paper presents two pieces of self-built equipment designed for in situ studies of nanoparticle growth in sub- and supercritical fluids. The fact that the same reactors are used for different experiment types including WAXS, SAXS and PDF at a handful of different beamlines worldwide demonstrates their flexibility. In the last section of the paper, we have focused on describing the experiments. This gives the reader an overview of the information obtainable from synchrotron based time resolved studies with respect to particle formation and growth. The reader who is interested in learning more about specific techniques or materials is referred to the cited references.

ACKNOWLEDGEMENTS

REFERENCES

[1]   REVERCHON, E., ADAMI, R., Nanomaterials and supercritical fluids, J. Supercrit. Fluids **37** (2006) 1–22.

[2]   AYMONIER, C., et al., Review of supercritical fluids in inorganic materials science, J. Supercrit. Fluids **38** (2006) 242–251.

[3]   BREMHOLM, M., et al., Reactor design for in situ X-ray scattering studies of nanoparticles formation in supercritical water syntheses, J. Supercrit. Fluids **44** (2008) 385–390.

[4]   BECKER, J., et al., Experimental setup for in situ X ray SAXS/WAXS/PDF studies of the formation and growth of nanoparticles in near- and supercritical fluids, J. Appl. Cryst. **43** (2010) 729–736.

[5]   BREMHOLM, M., et al., Time-resolved in situ synchrotron X-ray study and large-scale production of magnetite nanoparticles in supercritical water, Angew. Chem. Int. Ed. **48** (2009) 4788–4791.

[6]   HALD, P., et al., Supercritical propanol–water synthesis and comprehensive size characterisation of highly crystalline anatase TiO$_2$ nanoparticles, J. Solid State Chem. **179** (2006) 2674–2680.

[7]   CLAUSEN, B.S., et al., In situ cell for combined XRD and on-line catalysis tests: studies of Cu-based water gas shift and methanol catalysis, J. Catal. **132** (1991) 524–535.

[8]   NORBY, P., et al., Hydrothermal conversion of zeolites: An in situ synchrotron X ray powder diffraction study, J. Am. Chem. Soc. **119** (1997) 5215–5221.

[9]   JENSEN, H., et al., In situ high-energy synchrotron radiation study of sol–gel nanoparticle formation in supercritical fluids, Angew. Chem. Int. Ed. **46** (2007) 1113–1116.

[10] LOCK, N., et al., In situ high energy synchrotron radiation study of boehmite formation: growth and phase transition to alumina in sub- and supercritical water, Chem. Eur. J **15** (2009) 13381–13390.

[11] BARUCHEL, J., et al., Neutron and Synchrotron Radiation for Condensed Matter Studies, Springer, Berlin (1993).

[12] DINNEBIER, R.E., BILLINGE, S. (Eds), Powder Diffraction, Theory and Practice, RSC Publishing, Cambridge (2009).

[13] WARREN, B.E., X ray Diffraction, Dover Publications, New York (1990).

[14] RODRIGUEZ-CARVAJAL, J., Recent advances in magnetic structure determination by neutron powder diffraction, Physica B **192** (1993) 55–69.

[15] TYRSTED, C., et al., In situ synchrotron radiation study of formation and growth of crystalline $Ce_xZr_{1-x}O_2$ nanoparticles synthesized in supercritical water, Chem. Mater. **22** (2010) 1814–1820.

[16] AYYUB, P., et al., Effect of crystal size-reduction on lattice symmetry and cooperative properties, Phys. Rev. B. **51** (1995) 6135.

[17] JENSEN, K.M.Ø., et al., Structure, size and morphology control of nanocrystalline lithium cobalt oxide, Cryst. Growth Des. **11** (2011) 753–758.

[18] EGAMI, T., BILLINGE, S., Underneath the Bragg Peaks, Pergamon, Oxford (2003).

[19] HIPPERT, F., et al., Neutron and X ray spectroscopy, Springer, Berlin (2006).

TIME RESOLVED X RAY SCATTERING AND SPECTROSCOPY IN MATERIALS SCIENCE

W. BRAS
Netherlands Organization for Scientific Research (NWO),
Grenoble, France
Email: wim.bras@esrf.eu

Abstract

The study of materials relevant for energy applications covers a large array of experimental techniques, time domains and types of materials. In this paper, we will discuss some of the issues that we have encountered and describe some experiments and which combinations of techniques were used. The paper mainly presents results based on synchrotron radiation X ray techniques but also shows how important it is to complement their results with those obtained through non X ray techniques in order to obtain a comprehensive picture of the time evolution of the materials under study.

1. DEFINING THE TIME AND PHOTON ENERGY REGIME

Since the first accelerators dedicated to the production of synchrotron radiation were constructed in the early 1980s, several experimental techniques have been developed for real time studies relevant to materials science. In this context, one should first define which timescale is addressed when one uses the phrase 'real time'. The time regime where one studies fast processes relevant to the understanding of detailed functioning for electronics or catalysis at the atomic level is in general very fast (nanosecond level) and quite far removed from the regime where one studies structure formation in materials. For example, in many industrially relevant processes, a 0.1–1 second per time frame would usually suffice.

For real time processes to be studied with synchrotron radiation, an optimal illumination of the sample is essential. The high absorption of air for soft X rays places a lower limit on the energy of the photons that can be used. Also, the requirement for high pressures and/or temperatures demands the use of windows to gain access to the sample that is usually placed inside an environmental cell. Typical experiments are limited to synchrotron energies above 5 keV.

There are industrial processes that require faster timescales, for instance, fast temperature quenches or other types of perturbations. However, if the intention is to not only perform experiments in real time but also to interpret the data, then great care has to be taken when thermal or chemical gradients are present in the sample volume probed by the X ray beam. If such gradients exist, the data analysis will be rather complicated since one cannot apply a single simple model but instead one must usually use a continuous set of states. The gradients are rather dependent on the magnitude of the perturbation and materials constants such as thermal conductivity, mixing speed and homogeneity. The size of the X ray beam and the severity of the gradients will play a significant role in determining the severity of the problem and with what time resolution a process can still be usefully followed.

For microfocus beamlines, the gradient problems will be less severe since the sample volume probed by the X ray beam is much smaller. However, another danger for time resolved experiments is the increased risk of radiation damage. In order to obtain a statistically relevant diffraction pattern/spectroscopy curve etc., one requires a minimum number of photons, N, to interact with the sample. If the sample volume in which these interactions take place is reduced, then the probability increases that, in the same volume, damaging interactions are taking place.

For the different techniques, it is difficult to derive the highest achievable time resolution. In our opinion, it is not necessarily an appropriate strategy to chase the highest possible time resolution. One should aim for a time resolution that provides the answers to the scientific questions of interest. Very fast experiments require a high time resolution of the experimental technique. The readout time of the detector system in use is a key parameter, just as the available beam intensity and the beam attenuation due to experimental factors such as absorption in windows will play a role. The experimental contrast, for instance, the electron density contrast in X ray scattering experiments, or the maximum count rate that a detector can handle, should also be taken into account. It is possible to define some symbolic relations which can be used to assess the feasibility of success before one starts to design

an experiment [1]. Combining most of these parameters, one arrives at relation 1. Three further parameters are present; however, these play more or less the role of δ functions. For instance 'memory' is the rate at which data can be stored. With the large amounts of digital memory that are now available, one would think this a non-issue. However, data transfer rates from the physical detector to the storage medium are not infinitely high. Especially now that detectors are increasing in size, and at the same time, pixel sizes are becoming smaller. If one cannot achieve the required transfer rates, the experiment becomes impossible. The same is true if the radiation damage is too severe before the end of the experiment or when the required statistical quality of the data cannot be obtained within the time framing required by the experiment.

$$\text{time resolution} \propto \frac{\text{read-out} \times \text{attenuation}}{\text{beam intensity} \times \text{detector efficiency} \times \text{countrate} \times \text{contrast}} \times ... $$
$$... \times |\text{memory}| \times |\text{radiation damage}| \times |\text{statistical quality}| \tag{1}$$

The amount of radiation damage that is inflicted on the sample is heavily dependent on what kind of materials one investigates. For samples consisting of soft condensed matter or biological materials, the damage threshold is lower than that of ceramic or metallic materials. However, with the increasing popularity of micro focus beamlines, one should keep in mind that the technological possibilities to create smaller and still intense focuses is not always compatible with the time resolutions, and the amount of time the sample has to be followed in time, which are required for a large group of time resolved experiments. This is also true for experiments where one exposes the sample to white or pink beams [2]. These radiation issues lead to Eq. (2).

$$\text{radiation damage} \propto \frac{\text{beam intensity}}{\text{beam size}} \tag{2}$$

The statistical quality of the data depends on several objective and, unfortunately, several rather less objective parameters. Higher beam intensity, a longer timescale and a very efficient detector will obviously lead to better statistics and can be fairly well objectively characterized. Theoretically, this is also the case for the final data interpretation. In many cases, when the data is noisy, some researchers rely more on 'gut feeling' than others. See Eq. (3).

$$\text{statistical quality} \propto \frac{\text{beam intensity} \times \text{time frame length} \times \text{detector efficiency}}{\text{detector noise}} \tag{3}$$

The chemical or temperature gradients due to the perturbation that are present in the sample have not been added to the main equation. It is up to the individual researcher to determine what kind of gradients he/she thinks are acceptable for a particular experiment. However, it will be clear that the larger the perturbation and the larger the sample volume probed by the X ray beam, the more severe this problem will be. See Eq. (4).

$$\text{sample gradient} \propto \text{perturbation} \times \text{beam size} \tag{4}$$

The above equations are intended as symbolic relations. It is possible to find exceptions to these 'rules' by, for example, finding a smart way to reduce radiation damage. For example, one can use flow cells or defocus the beam so that a larger sample volume is exposed. The role of these relations, however, is to show that by, for instance, combatting radiation damage it is beneficial to use as large a beam size as is feasible. That the consequence of increasing the beam size is that it is counterproductive in the reduction of perturbation gradients over the sample is something that also should be taken into consideration. In the end, it is the researcher designing the experiment who must decide where to make the experimental compromises.

2. TECHNIQUES

Hard X ray scattering, diffraction and spectroscopy are techniques that are not only suitable for the static characterization of materials, but also to follow their structural evolution in materials at different length scales. Therefore, they are indispensable for research into modern materials in relation to energy research. While extended and near edge spectroscopy, EXAFS and XANES, can shed light on the local electronic environment around probe atoms, diffraction techniques (WAXS, powder diffraction) can answer questions regarding the larger scale crystalline structure. Small angle scattering (SAXS) provides information on an even longer length scale.

The minimum time frame that one can utilize in a certain technique depends on what kind of information one would like to gather from the data. Assuming that one performs X ray spectroscopy with a scanning monochromator, then it is possible, depending on the concentration of the probe atoms, to reach down to around 30–40 seconds/frame if one is satisfied with only observing the XANES energy region. The larger the scanning range and the lower the concentration, the longer the required scanning time [3]. Faster experiments are feasible with energy dispersive techniques, but this is at the expense of a higher radiation dose on the sample. For X ray diffraction (XRD) experiments on a poor crystalline sample, where the crystalline peaks are barely above the background, 0.1 frame/second could be the lower limit. For SAXS data, the time frame limit can even be lower if one only looks at the occurrence of larger scale structures [4]. However, if one would like to study the more detailed morphology, this time frame becomes longer again. The time domain versus length scale for these techniques is given in Fig. 1.

The above approximations are based upon the assumption that the experiments are being carried out in a single shot and not by combining different data obtained in a stroboscopic way. By utilizing such experimental tricks, one can reduce the minimum frame length to very low values at the expense of a more complicated experimental protocol and a reliance on the reproducibility of the experiment. This approach often has repercussions for data quality. The latter is acceptable as long as the parameters that one wants to derive from the experiments are still statistically relevant.

One of the innovative developments that has become popular in the last decade is the combination of on-line techniques. The higher quality of the X ray beams generated by more recently constructed beamlines on second and third generation synchrotron sources make this a lot easier than it was for the pioneers in this field in the years 1960–1975. The advantage of combining different techniques is that one can study different aspects of the sample. This can be done with X ray based techniques but Raman spectroscopy, Fourier transform infrared (FTIR), differential scanning calorimetry / differential thermal analysis (DSC/DTA), UV and visible light techniques have also been combined with X ray techniques in recent years [5, 6].

The driving force behind many of these technical developments was the realization that the information derived from using only a single technique in a time resolved process was rarely sufficient to provide significant insights. For example, the temperature dependent structure development of more complex materials, such as well-defined block co-polymers [7, 8], where both lengths scale at the molecular level as well as at the longer range, up to 100 nm, are important. But even in less complicated materials, such as isotactic polypropylene, it is relevant not only to study the structural evolution but also to know exactly where in the thermodynamic state a material resides [9, 10]. Quite often, it is not only relevant to know what the morphology is at different length scales but also in which order the structure develops. For the final product, this will rarely be relevant, but it can be of prime importance to influence the production process in such a way that a more favourable morphology will be created.

3. ENERGY RELATED MATERIALS

Materials important in energy related research constitute a large segment of the spectrum of the field. Studies range from alloys required for the construction of nuclear fission or fusion reactors [11, 12] to complicated conjugated block co-polymers under development for solar cell production [13, 14]. Lithium ion battery materials [15] and metal–organic frameworks (MOFs) for hydrogen storage belong in this category [16–17]. Other examples include fuel cell components [18, 19] or research into quality improvements in oil production [20]. No specialized experimental techniques on synchrotron radiation sources have to be invented to research these materials; the main challenge is to provide sufficient access to the required resources. Effectively, this means that
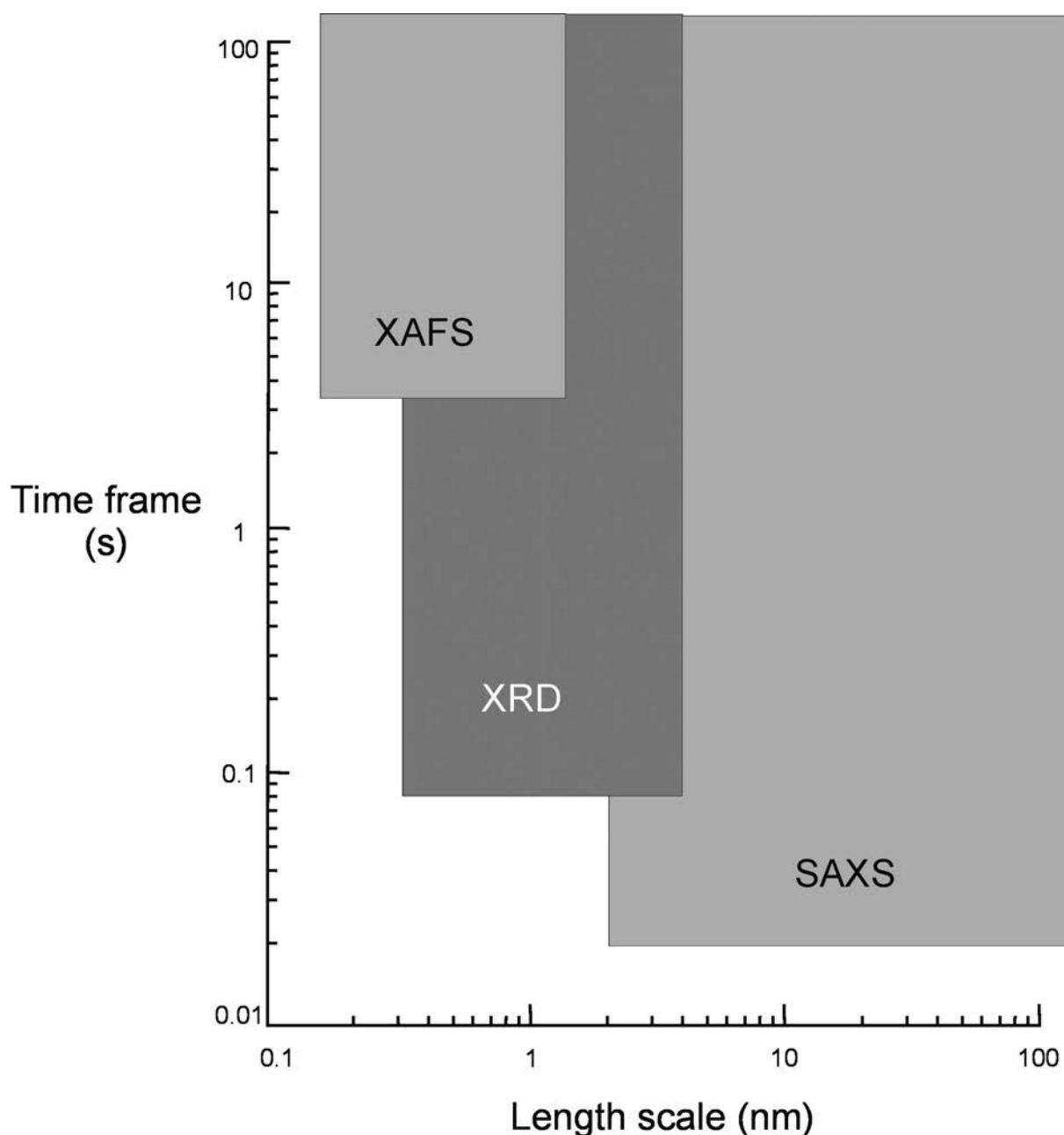
FIG. 1. Time versus length scale domain for different synchrotron radiation based X ray techniques. This diagram indicates which time resolution is achievable using moderate intensity monochromatic synchrotron beamlines. With more specialized equipment, these domains can be extended but this is often only realized at the expense of data quality.

there should be a reasonable number of beamlines providing the appropriate techniques and that the available beamtime should be used efficiently.

There are two areas which have important impact on energy related research and applications. First, it is possible to improve the experimental conditions used to study the on-line formation of materials relevant for energy research. In this case, improvements in the data quality of individual experimental set-ups are not necessary. If a beamline renders data of insufficient quality, the problem should be addressed by the directors of the experimental facility, but not necessarily as a fundamental research issue. However, the combinations of different techniques as well as the improvement in sample handling facilities are issues relevant to individual research groups and can be so driven. This should obviously be done in close collaboration with the personnel involved in beamline operations.

The second issue which has been addressed to a limited extent is the on-line study of working (model) devices. For instance, the imaging of fuel sprays inside the combustion chamber of an engine or the formation of soot during

the same combustion process [21, 22]. Another example is the on-line operation of fuel cells or batteries where information is sought on the stability of the different components [23]. The major challenge in these experiments is to not only make the device X ray transparent but to also make sure that the relevant information is obtained from the device components of interest. In this case, neutron based techniques quite often have an advantage when it comes to penetration power but there is still the issue that neutron beams and interaction cross-sections are lower in intensity and efficiency than X rays. This means that it is very desirable to develop X ray based techniques, alongside the already existing neutron based techniques, to shed light on the operation of real devices.

4. EXAMPLES

It is well known throughout the automotive industry that an increasing emphasis on environmental issues requires that engines become more economical and environmentally friendly through the use of sustainable fuels. Electric cars are looked upon by some as a valid alternative to the combustion engines currently used, although this ignores the fact that the required electric power must be generated and transported to the place where it is consumed. In heavily polluted regions, such as the inner cities of large metropolitan areas, it might be an advantage if the polluting energy generation process is displaced to areas that are less polluted so that the environmental impact is more evenly distributed. However, this does not remove the requirement to make modern combustion engines more energy efficient and less polluting, since this technology will not easily be replaced in the near future.

One of the factors influencing the environmental impact of diesel engines is the production of soot. To reduce soot production, manufacturers are obliged to install filters in the exhaust system. However, in the long run, poorly designed and mechanically vulnerable filters are incompatible with requirements for low fuel consumption. Therefore, new materials are required that are mechanically stable at high temperatures, have a large resistance to mechanical shock and allow a constant gas throughput over the whole temperature range in which they operate. The latter condition implies that the thermal expansion coefficient of the filter material is small.

One material used for such filters is the glass ceramic cordierite ($Mg_2Al_4Si_5O_{18}$), which is also used as a carrier for catalytic materials. Cordierite glass ceramics consist of a glassy matrix in which small crystallites are embedded. This material fulfils the requirements of low thermal expansion and shock resistance even at higher temperatures. Even though the manufacturing technology of this material is empirically well known, there are still uncertainties in some manufacturing processes that are based upon the thermally induced conversion of cordierite composition glass into a real glass ceramic. This process consists of a shaping process and subsequent heat treatments to induce the appropriate morphology. In order to influence the degree of crystallinity, a small amount of crystallization enhancer, in the form of a metal oxide, such as one based on Cr, is added to the glass melt. In order to obtain a comprehensive insight into structure development during heat treatment and to eliminate some interpretation ambiguities that resulted when utilizing a single technique, SAXS, WAXS, SANS, TEM and STM were all employed, with SAXS and WAXS experiments carried out simultaneously.

SAXS experiments provide data from which the evolution of particle size can be derived (Figs 2 and 3). At the same time, the intensity in the WAXS peaks is directly related to the degree of crystallinity. (For data not shown see Refs [24, 25]). With off-line characterization and suitable standards, one can also determine the crystallite size and the degree of crystallinity. However, there are some parameters that are more difficult to interpret with only off-line data. In Fig. 2, the squared particle radius, R^2, and the unit cell axis length of the cubic spinels that are growing in the glassy matrix are co-plotted.

The squared particle radius initially grows linearly with time, which indicates diffusion limited growth. This is confirmed by an Avrami analysis [26]. Once the entire nucleating agent, an oxide of Cr, is depleted, the growth slows down and the cubic spinel unit cell length stops shrinking and instead begins to elongate. Coincident with this change, the final slope of the SAXS curves starts to fall off as $I(q) = Cq^{-4}$, becoming steeper. This behaviour means that the interface between the crystallites and the matrix smoothens out. This can be understood in terms of fast growing crystallites with a surrounding amorphous zone. Once the rate of growth starts to slow down, there is sufficient time to allow the atoms to 'jump' into their crystalline lattice positions, and the surface defects anneal out, thus reducing the apparent unit cell size. This model does not explain the intriguing fact that this behaviour is followed by a long period in which the unit cell size increases again. This riddle can be explained by assuming that the specific volume of the glass matrix is larger than the specific volume of the newly formed crystallites. This creates a tension within the crystal that slowly anneals out.
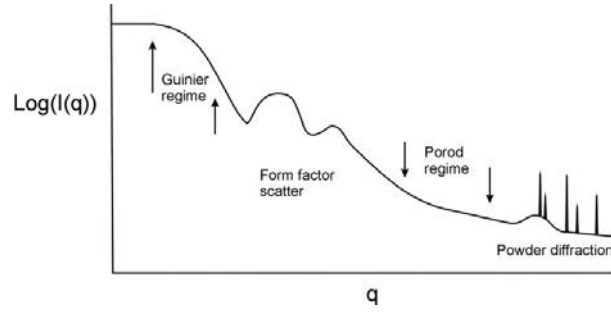
FIG. 2. *The structural information that can be derived from a combined SAXS/WAXS X ray scattering experiment.($q=4\pi sin\theta/\lambda$). The SAXS regimes start at q= 0. The Guinier regime ($q \approx 5 \times 10^{-2}$ nm^{-1}) contains information on the particle size, or any other specific long range electron density variations. The particle shape information can be found at intermediate scattering angles and the Porod regime ($q \approx 1$ nm^{-1}) renders information on the interface between the scattering entities. The powder diffraction range supplies information at the crystalline level.*
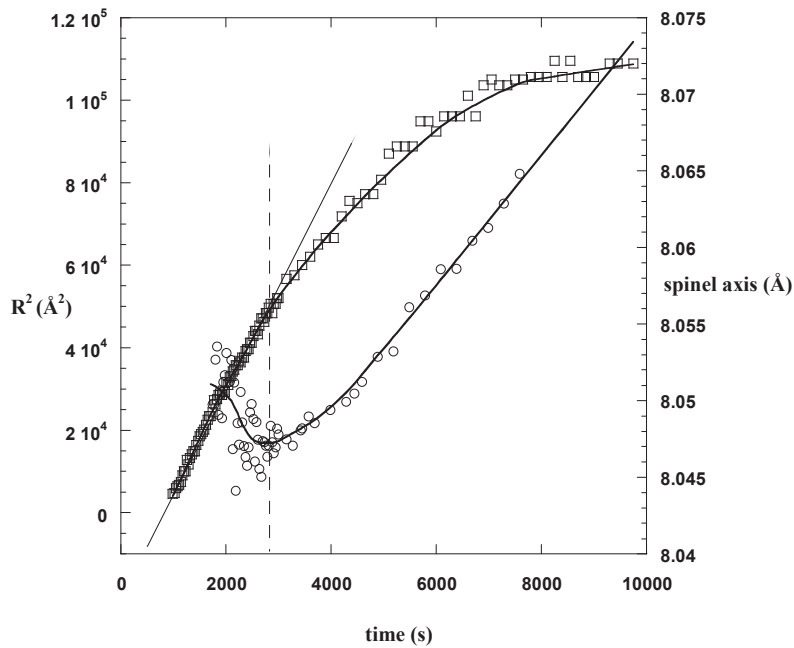
FIG. 3. *Squared particle radius (square symbols and left hand scale) and crystalline unit cell size (circle symbols and right hand scale) development, in an isothermal crystallization experiment on cordierite glass, as function of time. For further explanation see text.*

Employing the observed changes in the unit cell, one can calculate the pressure between the particles and the glass matrix. The magnitude of the 'pulling' pressure exerted on the spinel spheres, estimated using a second order Birch-Murnaghan equation of state [27], is 9.5 GPa, rising to ~10 GPa before monotonically dropping to ~8.5 GPa. The final morphology is depicted in the TEM graph shown in Fig. 4.

Whereas TEM data was required to elucidate the final morphology, it did not provide any information on the actual growth process. However, owing to the low degree of crystallinity, the SAXS data could be fitted with both a cuboidal as well as a slightly polydisperse spherical form factor, *F(q)*; see Ref. [28]. Distinguishing between these two options requires real space imaging.

The little crystallites have different expansion coefficients compared with the matrix and it is the combination of this pseudo-composite material that gives it its unique properties, with the crystallites acting as stress concentrators. The technological importance of this methodology is that it is now possible to understand the macroscopic material properties while also understanding the potential effects of ageing from prolonged exposure to hot exhaust gases. These exhaust gases mimic a temperature annealing which could cause a macroscopic volume change. It is crucial that the extent of this change is limited.

FIG. 4. Transmission electron micrograph of a heat treated cordierite glass. The cuboidal spinel particles are clearly visible (≈ 4% volume fraction) within the uncrystallized glass. The size bar is 20 nm.

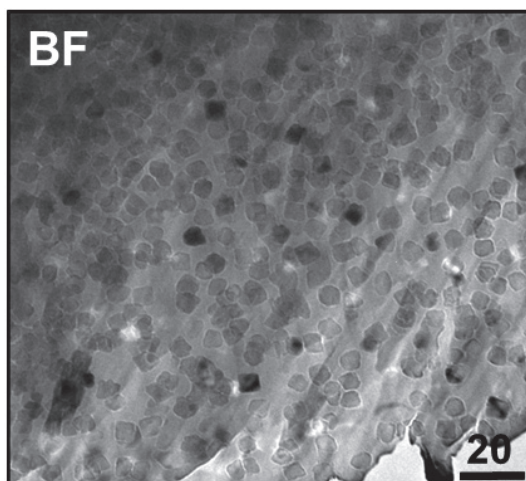Another set of experimental techniques that can be combined are X ray scattering and X ray spectroscopy as described in Ref. [3]. With this system, it is possible to perform the scattering and spectroscopy (XANES/EXAFS) quasi-simultaneously. The monochromator scan required for the spectroscopy is temporarily halted at the start and in between each EXAFS scan to collect the scattering data. An EXAFS scan requires somewhere between 30–120 seconds.

Although technical constraints limit this system to slower time resolved experiments, there remain a wealth of interesting experiments that can be undertaken in the area of catalysis and the development of the catalytic materials and carriers on-line [29–31].

This kind of system requires a 'one pot' catalysis from start to finish. In the initial sludge, i.e. the starting material, one can follow the electronic environment of template directing metallic additives. The crystalline structure that subsequently forms can be studied with WAXS. This is feasible from a crystalline volume fraction of approximately 0.5 Vol%, for low electron contrast polymer crystallization experiments, to 0.005 Vol% when strongly scattering metals are incorporated into one of the phases [4]. At a later stage, when the particle sizes are 1 nm or larger, it is possible to detect this by SAXS.

In order to obtain information relevant to real catalysis, one has to maintain the sample material under realistic conditions. This means that the temperature, pressure and flow rate of the catalysed gas has to be identical to industrially relevant conditions. For temperatures up to 500°C, pressures of 30–40 bars have to be exerted whilst the gas flow has to be monitored by mass flow controllers. For materials relevant to hydrogen storage, the pressures have to be even higher. Only for catalytic processes related to combustion engines can one lower the pressure, but the temperature and gas flow control become relevant again.

5.   CONCLUSIONS

At present, there still is a severe shortage of beamlines at synchrotron radiation sources at which materials can routinely be studied under relevant processing conditions with an array of techniques that renders a fully comprehensive picture of structure development and catalytic activity. In most synchrotron radiation laboratories, these types of experiments are carried out, but in general, this is done in an improvized fashion.

Materials science and energy related research would benefit greatly if more experimental stations were to become available. In addition to providing access to the required techniques, they would also need to supply the required experimental infrastructure with respect to sample control.
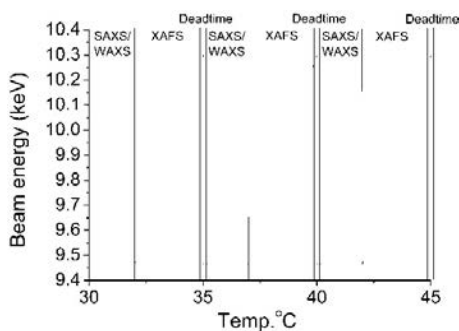
FIG. 5. Schematic diagram of the data collection strategy in a quasi-simultaneous SAXS/WAXS/XANES experiment. The horizontal axis units can be time, pressure, temperature etc. The vertical axis is determined by the absorption edge of the metallic element that serves as the probe.
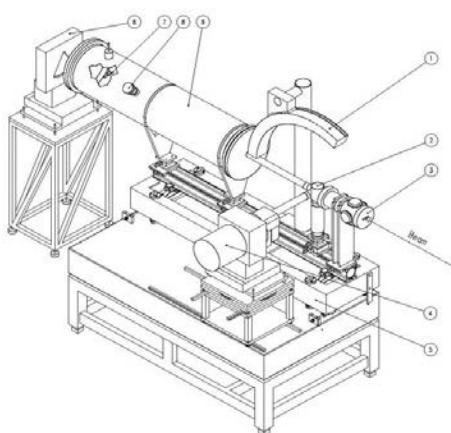
FIG. 6. Schematic diagram of a combined SAXS/WAXS/Spectroscopy beamline. (1) WAXS detector, (2) sample stage, (3), (4) and (7) spectroscopy detectors, (6) SAXS detector and (9) vacuum chamber for SAXS.

REFERENCES

[1]   BRAS, W., "Time-resolved SAXS/WAXS experiments", Scattering in Polymeric and Colloidal systems, (BROWN, W., MORTENSEN, K., Eds), Gordon and Breach, Boca Raton, FL (2000) 457–494.

[2]   MESU, J.G., et al., Probing the influence of X rays on aqueous copper solutions using time-resolved in situ combined video/X ray absorption near-edge/ultraviolet-visible spectroscopy, J. Phys. Chem. B, **110** (2006) 17671–17677.

[3]   NIKITENKO, S., et al., Implementation of a combined SAXS/WAXS/QEXAFS set-up for time-resolved in situ experiments, J. Synch. Rad. **15** (2008) 632–640.

[4]   BRAS, W., et al., Recent experiments on a combined small-angle/wide-angle X ray scattering beam line at the ESRF, J. .Appl. Cryst. **36** (2003) 791–794.

[5]   BRAS, W., RYAN, A.J., Sample environments and techniques combined with Small Angle X ray Scattering, Adv. Coll. Inter. Sc. **75** (1998) 1–43.

[6]   NEWTON, M.A., VAN BEEK, W., Combining synchrotron-based X ray techniques with vibrational spectroscopies for the in situ study of heterogeneous catalysts: a view from a bridge, Chem. Soc. Rev. **39** (2010) 4845–4863.

[7]   KHANDPUR, A.K., et al., Polyisoprene-polystyrene diblock copolymer phase diagram near the order-disorder transition, Macromol. **28** (1995) 8796–8806.

[8]   RYAN, A.J., et al., Structure development in semicrystalline diblock copolymers crystallizing from the ordered melt, Macromol. **28** (1995) 3860–3868.

[9]   BRAS, W., et al., The combination of thermal-analysis and time-resolved X ray techniques — a powerful method for materials characterization, J. App. Cryst. **28** (1995) 26–32.

[10] TERRILL, N.J., et al., Density fluctuations: the nucleation event in isotactic polypropylene crystallization, Polymer **39** (1998) 2381–2385.

[11] DEGUELDRE, G., et al., Nuclear material investigations by advanced analytical techniques, Nucl. Instr. Meth. Phys. Res. **268** (2010) 3364–3370.

[12] LINDIG, S., et al., Characterisation of plasma-sprayed boron carbide and tungsten layers for fusion applications, J. High Temp. Mat. Proc. **9** (2005) 127–139.

[13] PARK, M.J., BALSARA, P., Anisotropic proton conduction in aligned block copolymer electrolyte membranes at equilibrium with humid air, Macromol. **43** (2010) 292.

[14] DAS, N.C., SOKOL, P.E., Hybrid photovoltaic devices from regioregular polythiophene and ZnO nanoparticles composites, Renew. Energy **35** (2010) 2683–2688.

[15] CHIANG, Y.M., Building a better battery, Science **330** (2010) 1485–1486.

[16] TSAO, C.S., et al., Characterization of pore structure in metal-organic framework by small-angle X ray scattering, J. Am. Chem. Soc. **129** (2007) 15997–16004.

[17] BONINO, F., et al., Local structure of CPO-27-Ni metallorganic framework upon dehydration and coordination of NO, Chem. Mater. **20** (2008) 4957–4968.

[18] SCHMIDT-ROHR, K., CHEN, Q., Parallel cylindrical water nanochannels in Nafion fuel-cell membranes, Nat. Mater. **7** (2008) 75–83.

[19] SACCA, A., et al., Structural and electrochemical investigation on re-cast nafion membranes for polymer electrolyte fuel cells (PEFCs) application, J. Memb. Sc. **278** (2006) 105–113.

[20] OYAMA, S.T., et al., Transition metal phosphide hydroprocessing catalysts: A review, Catal. Tod. **143** (2009) 94–107.

[21] KASTENGREN, A.L., et al., Measurement of biodiesel blend and conventional diesel spray structure using X ray radiography, J Eng. Gas. Turbines Power Trans. Asme **131** (2009) 1031–1044.

[22] GARDNER, C., et al., In situ measurements of soot formation in simple flames using small angle X ray scattering, Nucl. Instr. Meth. Phys. Res. **238** (2005) 334–339.

[23] DIXON, D., et al., Design of in-situ experimentation for the study of fuel cells with X rays and neutrons, MP Mater. Test. **10** (2010) 725–735.

[24] BRAS, W., et al., Nanocrystal growth in cordierite glass ceramics studied with X ray scattering, Cryst. Growth. Des. **9** (2009) 1297–1305.

[25] BRAS, W., et al., The development of monodispersed alumino-chromate spinel nanoparticles in doped cordierite glass, studied by in situ X ray small and wide angle scattering, and chromium X ray spectroscopy, J. Non-Cryst. Sol. **351** (2005) 2178–2193.

[26] AVRAMI, M., Kinetics of phase change I - General theory, J. Chem. Phys. **7** (1939) 1103–1112.

[27] BIRCH, F., Finite elastic strain of cubic crystals., Phys. rev. A **71** (1947) 809–924.

[28] GLATTER, O., KRATKY, O., Small Angle X ray Scattering, Academic Press, London (1982).

[29] IGLESIAS-JUEZ, A., et al., A combined in situ time-resolved UV-Vis, Raman and high-energy resolution X ray absorption spectroscopy study on the deactivation behavior of Pt and Pt-Sn propane dehydrogenation catalysts under industrial reaction conditions, J. Catal. **276** (2010) 268–279.

[30] BEALE, A.M., et al., A combined SAXS/WAXS/XAFS setup capable of observing concurrent changes across the nano-to-micrometer size range in inorganic solid crystallization processes, J. Am. Chem. Soc. **128** (2006) 12386–12387.

[31] DE SMIT, E., et al., Local and long range order in promoted iron-based Fischer-Tropsch catalysts: A combined in situ X ray absorption spectroscopy/wide angle X-ray, J. Catal. **262** (2009) 244–256.

REAL TIME STUDIES OF MATERIALS AT FLNR JINR CYCLOTRONS

V.A. SKURATOV, S.A. KOZLOVSKY

Flerov Laboratory of Nuclear Reaction,
Joint Institute for Nuclear Research,
Dubna, Russian Federation
Email: skuratov@jinr.ru

Abstract

This report summarizes the results of recent real time studies of materials using high energy ion beams at the FLNR JINR cyclotrons. Firstly, data on the radiation stability of CdTe/CdS thin film solar cells against damage induced by 1.2 MeV/amu xenon ions are discussed. The experiments consisted of evaluating radiation stimulated changes in optical properties (luminescence and absorption spectrums) of some polymers containing quantum dots to be used as planar converters on top of solar cells and measurements of solar cell parameters such as short circuit current as a function of dose. The second part of this paper is devoted to in situ analysis of mechanical stress in alumina under irradiation with high energy heavy ions simulating the fission fragments impact in nuclear ceramics. The stress level has been deduced from ionoluminescence spectrums using the piezospectroscopic effect. The experimental data have revealed different stages in stress accumulation associated with irradiation regimes producing overlapping and non-overlapping swift heavy ion tracks.

1. INTRODUCTION

Real time studies of materials using energetic ion beams are playing an increasing role in experimental radiation materials science, providing very important information about the kinetics of radiation damage accumulation and various property changes in irradiated materials. Regarding swift heavy ion bombardment, the utilization of real time methods may distinguish, in particular, transient processes accompanying the overlapping of isolated disordered regions formed via electronic excitations (latent tracks). The aim of this report is to discuss the results of real time evaluation of structural changes in some materials induced by 1.2 MeV/amu xenon ion irradiation. Firstly, we will consider the radiation induced degradation of electrical properties of CdTe/CdS thin film solar cells and optical properties of polymer luminescent filters used as planar converters. Secondly, the peculiarities of mechanical stress accumulation in Al_2O_3:Cr single crystals under swift heavy ion irradiation in the broad ion fluence range are discussed.

2. RADIATION STABILITY OF CdTe/CdS SOLAR CELLS AND LUMINESCENT FILTERS AGAINST SWIFT HEAVY ION IRRADIATION

Long term radiation stability of materials against particle irradiation remains an important requirement for solar cells which have been widely used as power sources in space devices. Usually, the solar power generators consist of high efficiency Si and III–V cells made of monocrystalline materials. Nowadays, increasing attention is given to thin film solar cell materials that are not so sensitive to irradiation damage. In particular, the excellent stability of thin film CdTe/CdS solar cells irradiated with low and high energy protons has been recently demonstrated [1, 2]. Here, we describe the changes in properties of such solar cells and luminescence filters under swift heavy ion irradiation. Experiments have been carried out at the IC-100 FLNR JINR cyclotron accelerating heavy ions energies of 1.2 MeV/amu. Ionoluminescence and optical absorption spectrums were obtained using a set-up for studies of ion beam induced luminescence [3]. We have studied the optical properties of luminescent converters and concentrators produced with the aid of CdSe/CdS/ZnS colloid quantum dots (CQDs). As a polymer matrix, we used polymethyl methacrylate and methacrylate co-polymers with other acrylic monomers [4].

Figure 1 shows the dose dependence of the ionoluminescence spectrums generated in luminescent converters and concentrators by 167 MeV Xe ions. The spectrums consist of broad bands, one of which peaks at 600 nm,
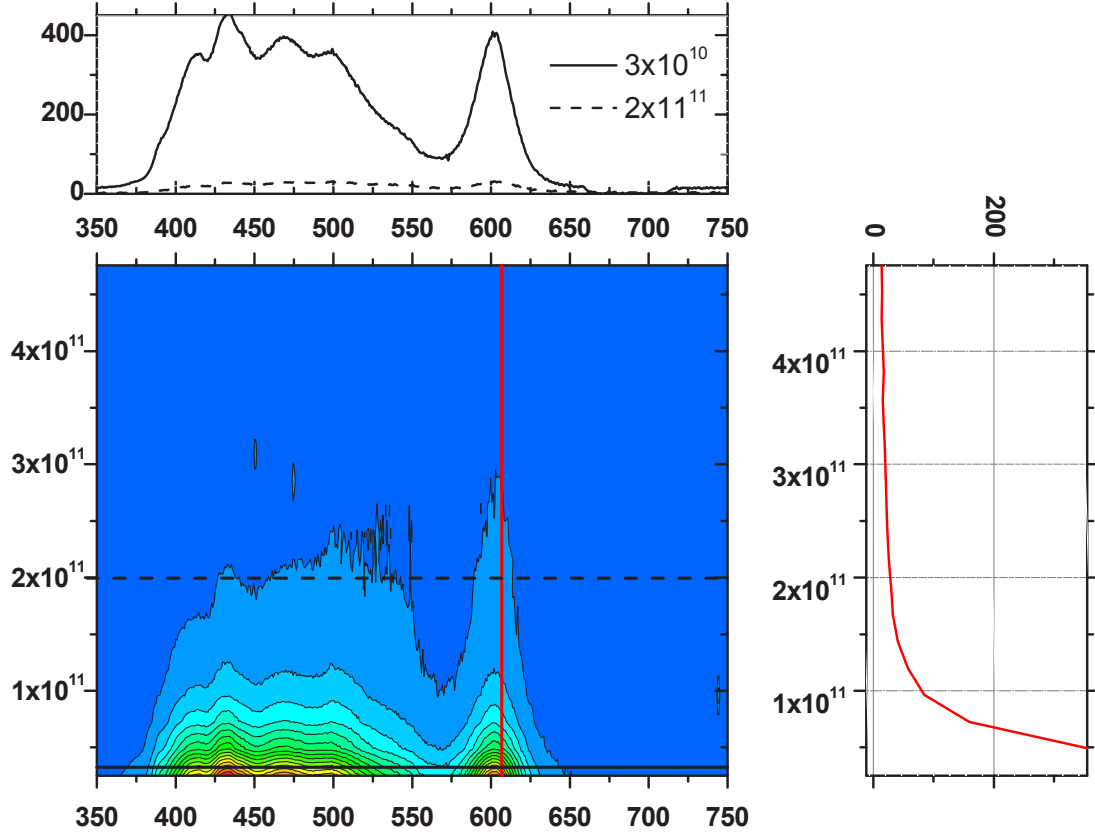
FIG. 1. Variation of ionoluminescence spectrums from luminescent converters and concentrators obtained during Xe irradiation. *Tirr.= 80 K. The spectrums on top are recorded at two selected ion fluences. Radiation induced degradation of the CQDs emission as a function of ion fluence is shown on the right side.*

and is associated with CdSe/CdS/ZnS CQDs emission. The luminescence intensity in the CQDs band decreases exponentially with ion fluence Φ and can be fitted by the following function:

$$I(\Phi) = A1 exp(-\pi Rh^2\, \Phi) + A2 exp(-\pi Rc^2\, \Phi) \tag{1}$$

where A1 and A2 are constants, Φ denotes the fluence in ions/cm^2, Rh and Rc are radii of the track halo and track core of regions surrounding the swift heavy ion trajectory in polymers [5]. Taking into account such a model of latent tracks, one can suggest that the first stage of this degradation is ascribed to the beginning of track halos overlapping, while the following degradation may be due to the overlapping of track cores.

This model leads to reasonable values of R_c= 19 nm and Rh= 39 nm [5]. We note that 167 MeV ion fluence $\Phi = 10^{11}$/cm^2 corresponds to the relatively high absorbed dose, 900 kGy, which much exceeds typical accumulated dose for a satellite mission, 100 kGy. The current (I_{sc}) observed under Xe ion bombardment is shown in Fig. 2.

As can be seen, a remarkable reduction in the values of the short circuit current is observed above 50 kGy that is evidence of very high radiation stability against swift heavy ion irradiation.

3. IN SITU EVALUATION OF MECHANICAL STRESS IN AL$_2$O$_3$:CR INDUCED BY SWIFT HEAVY ION IRRADIATION

Another research direction in real time studies of materials at the FLNR cyclotrons is the evaluation of mechanical stresses in radiation resistant insulators under heavy ion irradiation simulating fission fragment impacts. To monitor the evolution of stress in real time during ion bombardment, one can use the piezospectroscopic method,
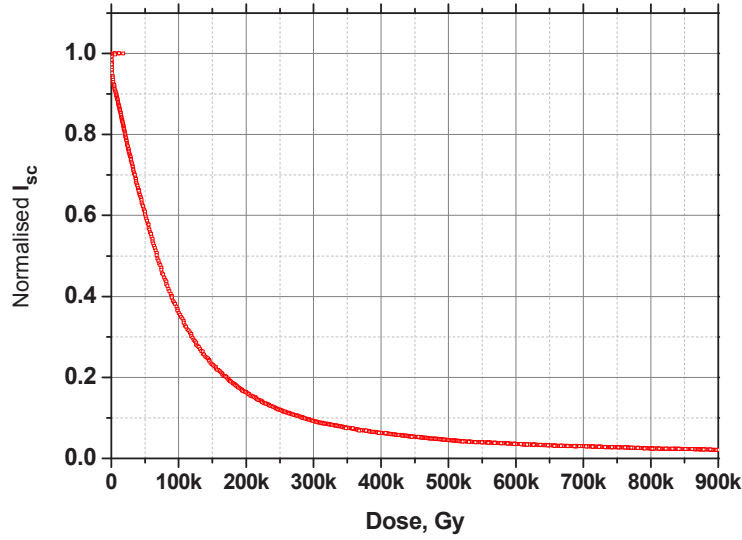
FIG. 2. *Short circuit current of the CdTe/CdS solar cells normalized to their initial value, measured during 167 MeV Xe irradiation as a function of absorbed dose.*

which utilizes the relationship between stress and changes in optical spectrums, for example, changes in the ion beam induced luminescence spectrums. The material most convenient for such measurements is alumina doped with chromium impurities in which the piezospectroscopic properties, namely the stress dependence of the *R* lines luminescence shift, is well investigated and even tabulated.

Mechanical stresses and their relationship to radiation damage in Al_2O_3 have been studied over the past decades by many researchers. Most of the experimental data have been obtained by using low energy ion beams in the range of hundreds of keV to some MeV [6]. Much less is known about stresses in material generated by swift heavy ion irradiation. Since even the first measurements revealed a strong sensitivity of integrated stress magnitude in Al_2O_3 on the ratio of electronic to nuclear stopping power [6], one could expect that large amounts of energy given to the electron subsystem of the crystal will crucially affect the stress state of alumina irradiated with high energy heavy ions. In our recent papers, we have reported estimates of stresses in ruby crystals during 1–3 MeV/amu Ar, Kr, Xe and Bi ion irradiation [3, 7, 8]. In this paper, we discuss the peculiarities of stress accumulation in Al_2O_3:Cr single crystals, revealed in real time measurements under 167 MeV Xe ion bombardment using a broad ion fluence range.

The optically polished *c* oriented ruby crystals used in our experiments were purchased from Roditi Ltd and have a size of $10 \times 10 \times 0.5$ mm and a chromium concentration of 0.3% Cr_2O_3 by weight. In situ accumulation of mechanical stresses at 80 K was monitored through the shift of the *R* lines in the Xe ion beam induced Cr^{3+} luminescence. Special care was taken to avoid possible temperature contribution in the R lines' shift by applying very low ion beam input thermal power, of several mW/cm^2, during ionoluminescence measurements. The temperature stability of the target holder during irradiation was in the range ± 0.5 K. Dispersion in the *R* line positions due to such instability is no more than ± 0.2 cm^{-1}. The *R* line positions, line widths and intensities were determined by fitting the spectrums recorded at 80 K to double pseudo-Voigtian profiles by the least squares method. The details of in situ measurements can be found elsewhere [3, 8].

The dose dependence of the *R* lines ionoluminescence spectrums of ruby detected during 167 MeV Xe ion bombardment is shown in Fig. 3. Together with a gradual decrease of the luminescence signal with ion fluence (not shown here), swift heavy ion irradiation induces a broadening of the *R* lines and the appearance of a 'shoulder' extending towards lower wave numbers. Besides these effects, a shift of positions and a following splitting of the *R* lines are observed.

The broadening of the *R* lines' is evidently due to radiation damage accumulation, while the observable asymmetry could be ascribed to the buildup of mechanical stress. The changes in the shape of the ionoluminescence spectrums can be interpreted by taking into account that the photon emission from each Cr^{3+} ion is independent of the other Cr^{3+} ions and each ion acts as an independent strain sensor, so the overall luminescence from a probed region is the sum of the photons that are emitted by individual Cr^{3+} ions [9]. Thus, the detected mechanical stresses

could be considered as independent contributions of separate differently stressed regions. Therefore, taking into account the direct proportionality between the *R* lines' shift and the magnitude of the stress, one can state that the stress state at a given fluence is characterized by stress fields composed of continuously distributed compressive stresses of different magnitudes. The wave number shift toward lower energies means that the irradiated target layer is under compression. The stress magnitude was evaluated through the shift of the R_2 line luminescence, Δv_2 [10, 11]. According to [11], the R_2 line shift and the approximate value of hydrostatic stresses, σh, are connected by the empirical relation:

$$\sigma h \ (GPa) = \Delta v_2 \ (cm^{-1})/7.61 \tag{2}$$

One should note that this effect had not been previously observed for 1.2 MeV/amu Kr ion irradiation, which has an incident electron stopping power lower than the threshold value ~ 20 keV/nm needed for damage production in alumina single crystals [12]. Therefore, lattice defects created via ionizing energy losses in Xe ion track regions generate local stress fields, the characteristic ion fluences correspond to maximum stress magnitude, and their interaction may result in stress relaxation. Two stage accumulation of the lattice disorder in α-Al_2O_3 irradiated with 0.7 MeV/amu Xe ions has been evidenced in Ref. [13] using Rutherford backscattering spectrometry channelling (RBS-C) and a surface profiling technique. It was suggested that partially disordered tracks first overlap, and, in a second step, an amorphous layer grows linearly with fluence from the sample surface. Very recent XRD studies of these specimens show that lattice strain increases with fluence until a maximum is reached of about $7.5 \times 10^{12}/cm^2$ [14], which is very close to our results. For higher fluences, the strain first decreases, indicating low stress relaxation in the material, and remains constant thereafter.

Summarizing these real time experiments, stress accumulation proceeds in several stages if the electron stopping power exceeds the threshold of radiation damage formation via electronic excitations. It is suggested that ion track region overlapping may stimulate the stress relaxation processes.

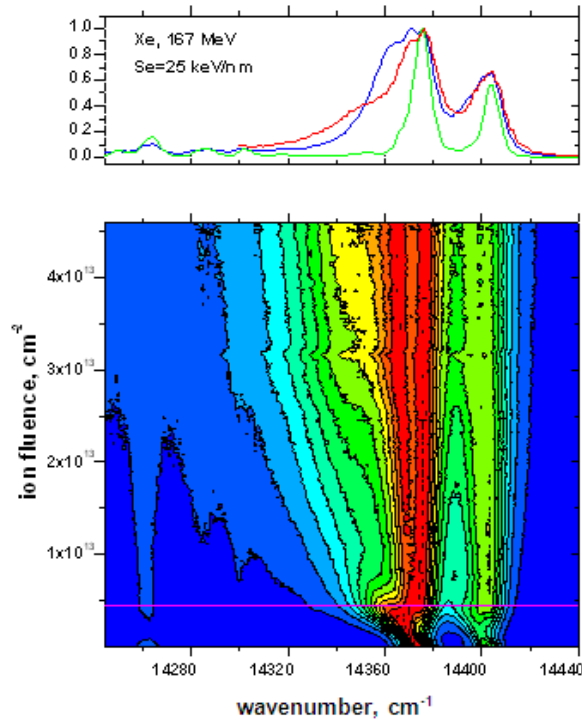*FIG. 3. The dose dependence of the R lines ionoluminescence obtained during Xe irradiation. Tirr.= 80 K. Spectrums are normalized on the maximum of the R1 line intensity. The spectrums on top (arbitrary units) are recorded at the very beginning of irradiation (green), at $4.0 \times 10^{12}/cm^2$ (red) and at $1.0 \times 10^{13}/cm^2$ (blue).*

REFERENCES

[1]   SHEEJA, K., et. al., Effect of 8 MeV electron irradiation on the performance of CSS grown CdTe/CdS solar cells, Semicond. Sci. Technol. **22** (2007) 1307–1311.

[2]   ROMEO, A., BÄTZNER, D.L., ZOGG, H., TIWARI, A.N., Influence of proton irradiation and development of flexible CdTe solar cells on polyimide, Mat. Res. Soc. Symp. Proc. **668**, (2001) H3.3.1–6MRS Symp.

[3]   BUJNAROWSKI, G., SKURATOV, V.A., HAVANCSAK, K., KOVALEV, Y., Accumulation of mechanical stress in Al_2O_3:Cr under swift heavy ion irradiation, Rad. Eff. & Def. in Solids **164** (2009) 409–416.

[4]   GLADYSHEV, P.P. et. al., "Thin film chalcogenides solar cells and luminescent filters of solar radiation on tha base of quantum dots and organic luminofors", Report of the 22nd ISTC Korea Workshop, Gumi Electronics & Information Institute, Republic of Korea (2010) 23–29.

[5]   APEL, P.Y., et. al., Track size and track structure in polymer irradiated by heavy ions, Nucl. Instrum. Meth. Phys. Res. B **146** (1998) 468–474.

[6]   ARNOLD, G.W., KREFT, G.B., NORRIS, C.B., Atomic displacement and ionization effects on the optical absorption and structural properties of ion-implanted Al_2O_3, Appl. Phys. Lett. **25** (1974) 540–542.

[7]   SKURATOV, V.A., KIM JONG GUN, STANO, J., ZAGORSKI, D.L., In situ luminescence as monitor of radiation damage under swift heavy ion irradiation, Nucl. Instrum. Meth. Phys. Res. B **245** (2006) 194–200.

[8]   SKURATOV, V.A., BUJNAROWSKI, G., KOVALEV, YU., S., O'CONNEL, J., HAVANCSAK, K., In situ and postradiation analysis of mechanical stress in Al2O3:Cr induced by swift heavy ion irradiation, Nucl. Instr. Meth. Phys. Res. B **268** (2010) 3023–3026.

[9]   XIAO, P., CLARKE, D.R., Piezospectroscopic analysis of interface debonding in thermal barrier coatings, J. Am. Ceram. Soc. **83** 5 (2000) 1165–1170.

[10]   GUPTA, Y.M., SHEN, X.A., Potential use of the ruby R_2 line shift for static high-pressure calibration, Appl. Phys. Lett. **58** (1991) 583–585.

[11]   PARDO, J.A., et al., Piezospectroscopic study of residual stresses in Al_2O_3–ZrO_2 directionally solidified eutectics, J. Am. Ceram. Soc. **83** (2000) 2745–2752.

[12]   CANUT, B., et al., Swift-uranium-ion-induced damage in sapphire, Phys. Rev. B **51** (1995) 12194–12201.

[13]   KABIR, A., et al., Amorphization of sapphire induced by swift heavy ions: A two step process, Nucl. Instr. Meth. B **266** (2008) 2976–2980.

[14]   KABIR, A., et al., Structural disorder in sapphire induced by 90.3 MeV xenon ions, Nucl. Instr. Meth. Phys. Res. B **268** (2010) 3195–3198.

CHEMICAL IMAGING OF MATERIALS WITH
SCANNING PHOTOEMISSION SPECTROMICROSCOPY

L. GREGORATTI, M. AMATI, M. KAZEMIAN ABYANEH, M. KISKINOVA
Sincrotrone Trieste SCpA,
Trieste, Italy
Email: luca.gregoratti@elettra.trieste.it

Abstract

With respect to the other photoelectron microscopy techniques, a scanning photoemission microscope (SPEM) uses the direct approach to photoelectron spectromicroscopy, which is the use of a small focused photon probe to illuminate the surface. The SPEM at the Elettra synchrotron light source can operate in two modes: imaging and spectroscopy. In the first mode, the sample surface is mapped by synchronized scanning of the sample with respect to the focused photon beam and collecting photoelectrons with a selected kinetic energy. The second mode is photoelectron spectroscopy from a microspot. The well-known capabilities of photoemission to chemically probe the surface of conducting and semiconducting, and to a certain extent of insulating, materials can be exploited at a submicrometre level for the investigation of spatially heterogeneous or confined systems, structures measured in micro- or nanometres, etc.

1. INTRODUCTION

In the last decades, the development of analysis techniques which can provide a wide range of information covering chemical, electronic and physical properties of probed samples together with their morphological and structural assets have attracted a great interest following the rapid advancement of materials science. This trend has influenced most of the analysis fields. Conventional electron microscopy machines (scanning electron microscopes (SEM) and transmission electron microscopes (TEM)) can be equipped with special detectors which can provide to a certain extent information on the chemical and electronic properties of the materials in addition to the traditional morphological or structural ones. On the other hand, scanning probe techniques (scanning tunnelling microscopes (STM) and atomic force microscopes (AFM)) have strongly improved their capabilities to probe the physical properties of samples. The maturity of Scanning Photoemission Microscopes (SPEMs) has offered the scientific community the possibility to combine photoemission, which is considered one of the most powerful techniques for the chemical and electronic characterization of materials, with lateral resolution. This opportunity was offered by the development of the third generation synchrotron sources where a large variety of photoemission based microscopes has been developed. They cover the vacuum ultraviolet (VUV), soft and hard X ray range taking advantage of the unique properties of the synchrotron radiation produced by modern accelerators (polarity, coherence, time structure, etc.). Photoemission microscopes can be divided into two main classes depending on whether they focus the incoming X ray beam and use the scanning to provide imaging (SPEMs) or if the lateral magnification is provided by the electronic and/or magnetic lens set-up (PEEMs). A SPEM can use different optical set-ups to demagnify the X ray beam; the most diffused are diffractive optics (zone plates (ZP)), pinholes, capillaries or reflective mirrors which ultimately define the main features of the microscope [1].

The final lateral resolution achievable with a microscope represents its most important quality; nevertheless, in most of the cases, a large number of limiting factors can degrade the spatial resolution, allowing other important possibilities. In the case of ZP, for instance, the maximum possible lateral resolution achievable by these optics is far beyond what is reached by SPEMs; geometrical constraints, a limited number of photons and other factors impose the use of zone plates with relaxed demagnification rate. As an example, the best achieved lateral resolution for a ZP based SPEM is approximately 50 nm, while scanning X ray transmission microscopes (STXM) which also use ZP have recently reached sub 10 nm spatial resolutions [2].

2. EXPERIMENTAL SECTION

2.1. SPEM layout

The SPEM layout built at Elettra is schematically shown in Fig. 1. A photon beam of high brightness is provided by an insertion device (undulator), then tailored and monochromatized using appropriate mirrors, gratings, entrance and exit slits, in order to meet the requirements of the photon focusing optics, which provide the microprobe. The SPEM uses zone plate optics, which have recently become the most widely used optical element in X ray microscopes. The optical system generating the X ray microprobe and the sample are mounted on appropriate stages, which enable positioning in the x, y and z directions and x–y scanning. A hemispherical sector electron analyser (HEA) is used for detecting and energy filtering of the emitted photoelectrons (PE). The lens system in front of the analyser entrance slit has to allow PE collection using different acceptance angles in order to optimize the signal count rate and spectral resolution for integral or angle resolved measurements. A more technical detailed description of the beamline and the microscope can be found in Refs [3, 4].

The main advantage of scanning instruments is that imaging and small spot spectroscopy are separate experiments. This allows independent optimization of each mode concerning energy resolution, lateral resolution and acquisition time. In the imaging mode, one can obtain element concentration maps or element chemical state maps by scanning the sample and collecting the preselected PEs.

2.2. Photoelectron detection system

A view of the detector is shown in Fig. 2(a). The base flange is a CF 100, modified with four high voltage connectors mounted at the side of the flange and a 48-pin connector in the centre for the signals. Two connectors supply the voltages to the microchannel plates (MCP); one supplies the anodes and the fourth is not connected. The large base visible in the picture is the insertion mechanism for the central connector. The case with the counting electronics is directly connected to the flange of the detector on the air side. The energy dispersed electrons are collected by the detector, which consists of two MCP in a chevron assembly, followed by an Al_2O_3 disk onto which 48 discrete gold anodes have been evaporated. The microchannel plates have been removed from the top part of the detector in Fig. 2(a) in order to show the 48 gold anodes. The ceramic disc with the 48 gold anodes is shown in Fig. 2(b). Forty-eight polarization resistors are directly laser trimmed on the Al_2O_3 disk in order to avoid the mixing of the signals. The anode voltage is very critical since noise pulses cannot be distinguished from real pulses: in order to keep this voltage 'clean' a strong RC filter is located within the vacuum very close to the anodes. The signals and the high voltage are decoupled by exploiting the electrical capacitance that exists between the metallic core and the metallic shield in coaxial wires. Owing to the high dielectric constant and strength of Kapton, a very thin coating of this material present in the coaxial cables is sufficient to achieve the necessary decoupling capacitance by overlapping a short length of the Kapton separated coaxial core and shield [5, 6].

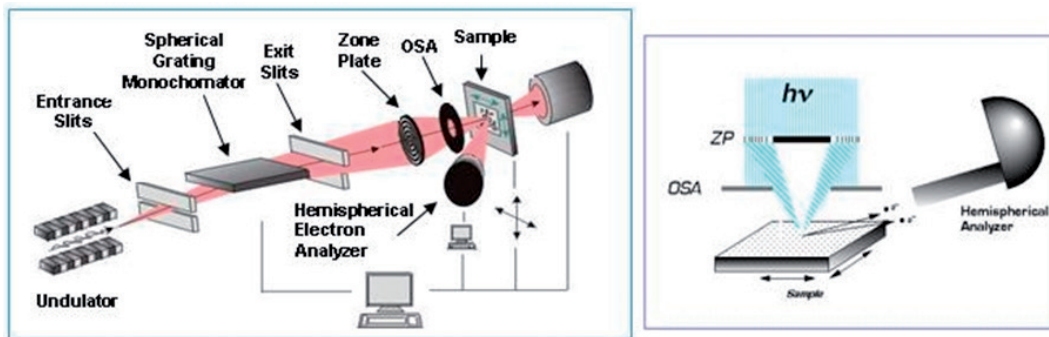
FIG. 1. (a) Layout of the ESCA microscopy beamline at Elettra which hosts the SPEM. The photon beam generated by a linearly polarized undulator is monochromatized by a spherical grating monochromator. The focusing optic system is formed by a zone plate and an order sorting aperture (OSA). (b) Detail of the focusing system and its effect on the photon beam. The take-off angle of the HEA is 30°.
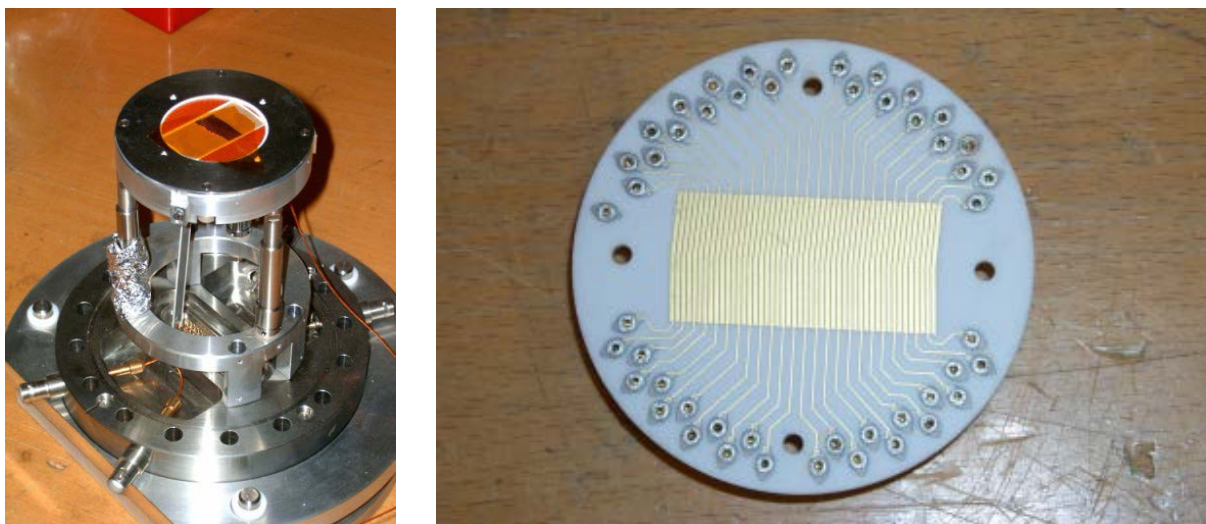
FIG. 2. (a) View of the electron detector of the hemispherical electron analyser of the SPEM. The microchannel plates have been removed from the top part of the detector. (b) Detailed illustration of the ceramic disc with the 48 gold anodes.
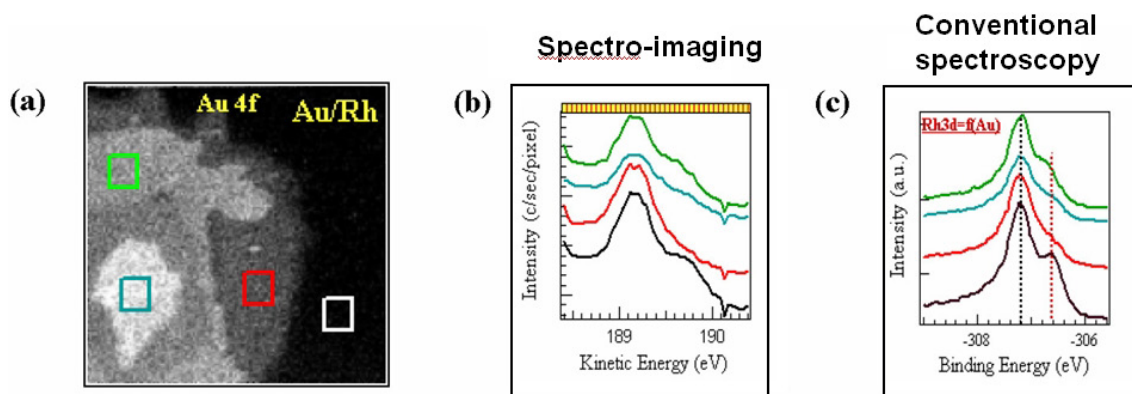

FIG. 3. (a) Au 4f map (64 × 64 μm²) illustrating areas with different Au coverage on a Rh(110) surface. (b) Reconstructed spectrums from the area corresponding to (a), Rh 3d5/2 image from the areas indicated with coloured squares in (a); (c) Rh 3d5/2 spectrums measured in spectroscopy mode from a microspot in the centre of the squares.

Figure 3 illustrates the most recent achievements in spectroimaging using 48 channel detector. The example is an Au/Rh(110) interface, where the Rh 3d spectrums undergo quite significant lineshape changes as a function of the local Au coverage. Part (a) shows the Au 4f map, where the contrast level reflects the lateral variations of the Au coverage. From a Rh 3d5/2 map of the same area (not shown) we reconstructed the Rh 3d5/2 spectrums from the indicated areas, which are shown in part (b). Part (c) shows the Rh 3d5/2 spectrums measured in a conventional spectroscopy mode from a spot within the indicated areas. The striking similarity in energy resolution achieved using spectroimaging is evident. It should be noted that by increasing the number of parallel counting channels, the pass energy of the analyser can be increased, accepting a much wider energy range of the emitted photoelectrons, while maintaining the same energy resolution on each channel.

2.3. SPEM performances and imaging contrast mechanism

In Fig. 4, an example of the achievable imaging lateral resolution of the SPEM at Elettra is shown. Part (a) is a test pattern used for ZP characterization. A line profile across the picture is shown in part (b), where the separation of the zones (50 nm) is well defined. (A qualitative indication of the capability of the SPEM to resolve structures below 100 nm is also visible below in Fig. 7, where 70 nm diameter multiwall carbon nanotubes is shown.)
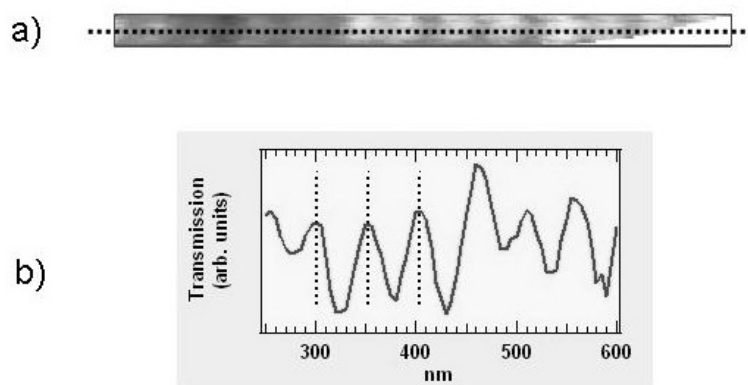
FIG. 4. *(a) Image of a test pattern composed by vertical structures spaced by 50 nm. (b) Linescan across the image shown in (a).*
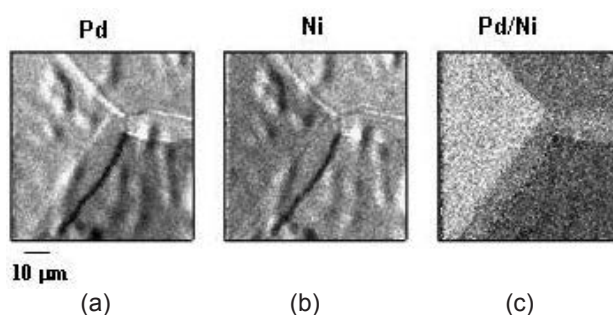

FIG. 5. *(a) and (b) Pd and Ni photoelectron maps acquired on Ni polycrystalline foils covered with a few Å of Pd atoms. To remove the topographical contribution, the ratio of the two images has been performed; image (c) shows the artefact free elemental distribution.*

In SPEM systems, the incident focused beam is normal to the sample surface as shown in Fig.1(b) and the analyser is usually positioned at a grazing take off angle with respect to the normal. In this geometry, one gains surface sensitivity, but also enhances the topographic artefacts. In particular, owing to the angular dependent probing depth of the emitted PEs, the more pronounced 'curved' topographic features appear brighter on the side facing the analyser, in contrast to the PEs emitted from the back side. PEs emitted from the areas behind a protruding feature are hindered in reaching the analyser and result in a shadowing effect. The processing procedures for 'removing' the topographic artefacts are described in details in Refs [6, 7]. Most often they involve subtraction of the background and division by the background image.

An example is reported in Fig. 5; a Ni polycrystalline foil not atomically flat has been covered with a few Angstroms of Pd atoms. Both photoelectron images acquired on the Pd and Ni core levels are dominated by the topographic features of the Ni substrate and appear very similar with the typical bright and dark areas produced by the geometrical SPEM set-up. Only the ratio of the two images can reveal the real concentration of the Pd atoms over the different Ni grains.

3. APPLICATIONS

3.1. Initial oxidation stage of a Ru(0001) surface

This example tackles the microscopic structure of transition metal catalysts under reaction conditions. A question that has barely been addressed is what determines the catalyst activity and selectivity in oxidation reactions — the properties of the bare metal surface or the metastable, e.g. 'oxide' microphases which can be formed in the presence of oxidizing reagents. Ru, along with Pt and Rh, is among the catalysts that have attracted the interest of surface scientists in an attempt to verify the mechanism of catalytic CO oxidation and NO reduction in the automobile exhaust converters. The first important step to understanding the mechanism of catalytic action

is the verification of the microscopic morphology of the Ru catalyst surface under reaction conditions. The pioneering studies combining structural imaging techniques, such as STM, I-V LEED and PEEM, with XPS, suggested that the 'active' Ru surface is O rich and consists of different phases with microscopic dimensions including non-stoichiometric oxide phases and dissolved oxygen [8–10]. However, neither of the methods used has provided sufficient qualitative and quantitative data confirming the assignment of the phases coexisting on the O rich Ru surface and their catalytic activity. Recent SPEM study on the development, spatial distribution and actual chemical state of the phases present on the so-called 'O rich' Ru surface, has identified for the first time the local composition of the phases coexisting in the initial stages of the Ru(0001) oxidation, quantitatively new information which is a solid base to verifying their actual role in CO oxidation [10]. For obtaining contrast in the chemical imaging, the chemical shift undergone by the Ru 3d core levels of the Ru atoms, which are bonded to oxygen, was used. As a result, the Ru 3d spectrums contain a contribution of the photoelectrons emitted from the Ru atoms, which are in a metallic state (below the formed oxide), Ru-M and Ru atoms bonded to oxygen. Since the oxygen coordination number determines the core level energy shift, this has allowed us to distinguish between stoichiometric RuO_2, intermediate Ru sub-oxides and chemisorption phases. Figure 2 shows two Ru 3d5/2 maps measured after exposure of the Ru(0001) sample to 105 Langmuirs of oxygen at 625 K and 675 K, respectively, which 'visualize' the spatial anisotropy of the initial stages of oxide growth and the dependence of the morphology on the oxidation temperature. The images in Fig. 6 are obtained measuring only the Ru 3d signal from the metallic substrate (Ru M), which decreases exponentially with increasing thickness of the O containing layer, so that the intensity profiles taken along the oxide patches reflect the spatial variation in their thickness. This has allowed us to quantify the thickness of the Ru oxide formed under varying oxidation conditions normalizing the intensity profiles against the Ru 3d emission measured for the clean Ru surface before oxidation. The elucidated thickness is shown in the right y scale of the line profile graphs. They indicate that the oxide like phase formed at 625 K is at most 2 layers thick, whereas its thickness exceeds 3 layers in the phase formed at 675 K. An interesting feature of the 675 K growth is that after nucleation the oxide growth expands in a preferred crystallographic direction. The profiles taken across the protruding oxide features of the 675 K phase reveal the expected decrease of the thickness of the film in the oxide growth direction (from left to right). However, closer inspection distinguishes breaks in the slope on the side of the growth direction between 5 and 6 Angstroms and around 8 Angstroms, corresponding to 2 and 3 oxide layers, respectively. This apparently reflects a layer by layer growth of RuO_2. Note also that for a thickness of less than two layers, the initial slopes of all profiles are similar and do not show directional anisotropy. Another notable feature of this earliest oxidation stage is that the oxide nucleus is decorated by O depleted areas, which we tentatively ascribed to the finite mobility of the O atoms or RuO_x clusters [10, 11].

3.2. Multi-wall carbon nanotubes

The second example is about our recent achievements in the imaging of multi-wall (MW) carbon nanotubes (CNTs) using SPEM. The unique electronic, mechanical and transport properties of the CNTs due to the covalent sp2 bonds and tubular structure with large length/diameter ratios make them excellent candidates for many potential applications. CNTs have raised great interest and found applications in various devices such as electronic
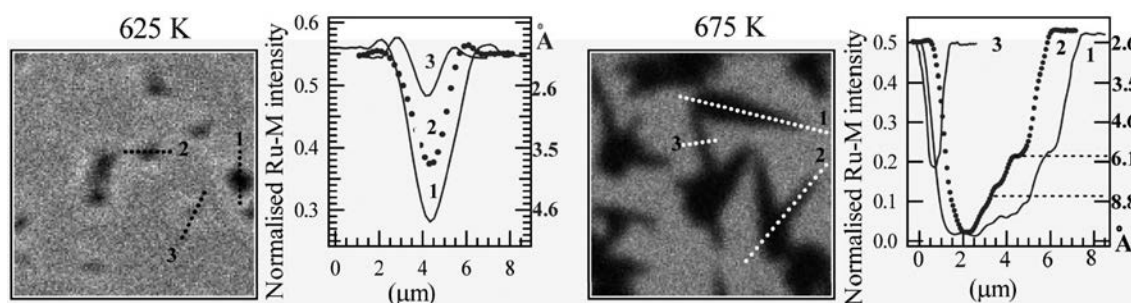
FIG. 6. Ru-M chemical maps ($25.6 \times 25.6 \ \mu m^2$ and $12.8 \times 12.8 \ \mu m^2$) and plots of selected intensity profiles taken along the lines indicated by the numbers 1, 2 and 3 in the images, normalized with respect to the intensity of the Ru 3d5/3 emission of clean Ru(0001) before oxidation: The right y scale of the profile plots indicates the calculated oxide thickness. The O depleted zones around the oxide islands formed at 625 K are evidenced by the two small maxima on both sides of the Rh-M profiles.

devices, sensors, actuators, field emitters and energy storage media. The high stability of the CNTs in an oxidative environment renders them not only excellent catalyst support materials but also high performance catalysts for hydrocarbon oxidation [12]. Moreover, their adaptive functionalization by adsorption of foreign atoms have made them a key material in nanotechnology [13, 14].

We have already studied the oxidation of CNTs [15] and carried out many experiments to investigate the mass transport of metals deposited on them [16]. At present, we are able to take SPEM images of CNTs down to 50 nm in diameter. The spatial resolution of SPEM in our beamline is high, but is limited to 150 nm due to photon spot size. The goal was to image CNTs less than 150 nm. To achieve this goal, we have used the low density aligned CNTs which allow us to detect the ejected photoelectrons from the CNTs even if the spot size is bigger than the NTs diameter. Figure 7 shows a typical SPEM image of aligned MWCNTs which have grown vertically on a Si substrate. The image is taken at the C1s core level, hence the CNTs appear in bright contrast and the vacuum background appears as dark contrast. In this image, the MWCNTs length is around 10 mm and their tip diameter is around 70 nm.

By using a special set-up, a single MWCNT can be partially covered with a metal, producing μm sized patches. Examples have been performed on MWCNT partially covered with gold around the middle. The XPS spectrums which have been taken inside and outside of the gold patch confirm the presence of the gold only inside the patch. We are able to deposit, in situ and partially, any metal on the CNTs. This technique facilitates sharp borders between metal and CNT surfaces which can help to properly study the transport properties of CNTs.
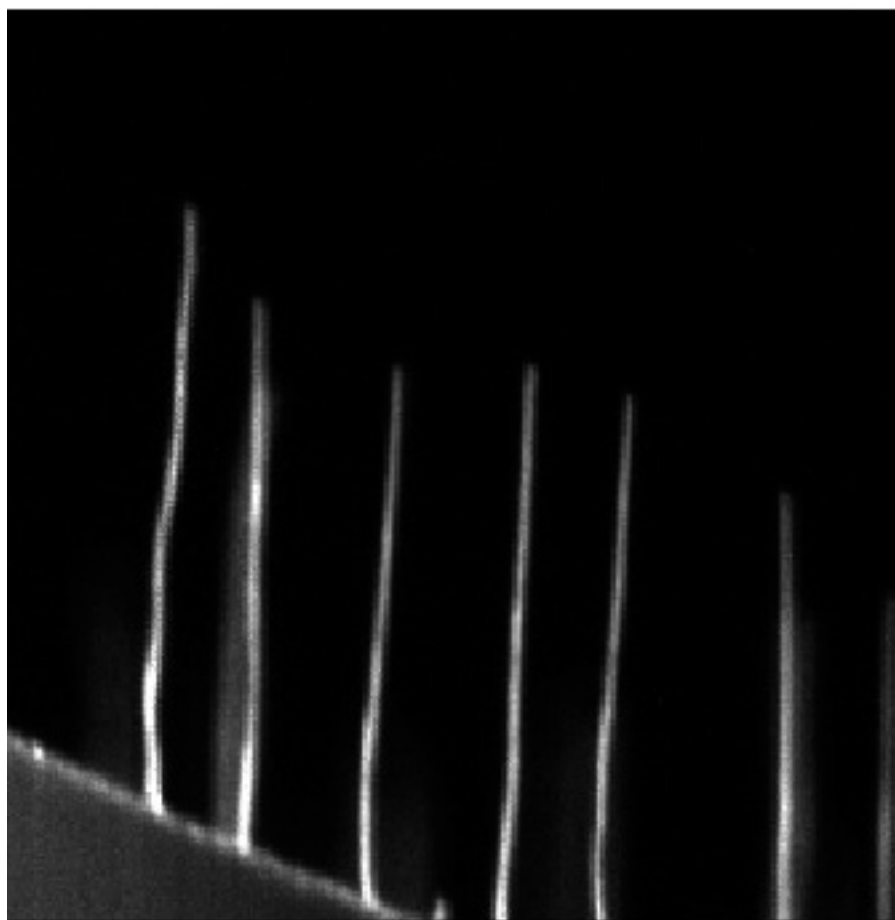

FIG. 7. Typical SPEM image of aligned MWCNTs which have grown vertically on a Si substrate. The width of each nanotube is 70 nm.

3.3. Real time experiments

SPEM and PEEM techniques are to a certain extent complementary from the point of view of time resolution, which in this context means the time needed to acquire one image or one spectrum. Owing to the intrinsic slowness of the mechanical raster of the sample, taking good images with the SPEM requires, in general, at least a few minutes. Of course, in several cases a proper design of the samples, for instance, by creating a 1-D structure where linescans can provide the desired information, can shorten the data acquisition times. As shown in Section 2.2, using inherent energy dispersion spectroscopy can, in well-defined cases, replace the acquisition of photoemission spectrums in the conventional way, which usually takes at least a few tens of seconds. The imaging speed of PEEM is much faster. The projection of the chemical maps on electron sensitive screens is acquired with digital cameras supporting at least the video rate. From this point of view, PEEM is ideal to image chemical reactions occurring on surfaces up to msec temporal resolution. The acquisition of spectrums is in general very slow, since, at least for the submicrometre resolution, it can be performed only by acquiring the a full image for each energetic point of the spectrum.

Examples of real time characterization performed with the SPEM of the electrochemically induced oxygen spillover at the Pt/YSZ (yttria-stabilized zirconia) interface can be found in Refs [17, 18] and for chemical waves on surfaces, see Refs [19, 20].

4. CONCLUSIONS

Photoelectron spectromicroscopy has undergone a fast paced development at third generation synchrotron radiation light sources, becoming a microscopic tool for probing material properties. The present paper has reviewed some of our recent achievements that have filled the information gap by examining the chemical and electronic properties of nanostructured materials, and identified local surface processes related to chemical interactions or mass transport. Although the selected results cover only some of the fields where synchrotron based photoelectron microscopy has become the most desired tool, they demonstrate the high performance level of the instruments.

Some of the near future upgrades for improving the performance of the photoelectron microscopes are increasing the lateral resolution and time resolution by developing new optical elements and aberration correction systems, and faster and more efficient detection systems.

REFERENCES

[1] GUNTHER, S., et al., Photoelectron microscopy and applications in surface and materials science, Prog. Surf. Sci. **70** 4–8 (2002) 187.

[2] VILA COMAMALA, J., et al., Advanced thin film technology for ultrahigh resolution X ray microscopy, Ultramicrosc. **109** (2009) 1360.

[3] MARSI, M., et al., ESCA Microscopy at ELETTRA: What it is like to perform spectromicroscopy experiments on a third generation synchrotron radiation source, J. Elec. Spec. & Relat. Phenom. **84** 1–3 (1997) 73.

[4] KISKINOVA, M., et al., Synchrotron radiation scanning photoemission microscopy: Instrumentation and application in surface science, Surf. Rev. Lett. **6** 2 (1999) 265.

[5] POTTS, A.W., et al., The exploitation of multichannel detection in scanning photoemission microscopy, Surf. Rev. Lett. **9** 2 (2002) 705.

[6] GREGORATTI, L., et al., 48-Channel electron detector for photoemission spectroscopy and microscopy, Rev. of Sci. Instr. **75** 1 (2004) 64.

[7] GUENTHER, S., et al., Artifact formation in scanning photoelectron emission microscopy, Ultramicrosc. **75** (1998) 35.

[8] OVER, H., et al., Atomic scale structure and catalytic reactivity of the $RuO_2(110)$ surface, Science **287** (2000) 1474.

[9] BOTTCHER, A., et al., Reactivity of oxygen phases created by the high temperature oxidation of Ru(0001), Surf. Sci. **452** (2000) 125.

[10] BOTTCHER, A., et al., Spectral and spatial anisotropy of the oxide growth on Ru(0001), J. Chem. Phys. **117** 17 (2002) 8104.

[11] BLUME, R., et al., Identification of subsurface oxygen species created during oxidation of Ru(0001), J. Phys. Chem. **B 109** 29 (2005) 14052.

[12] ZHANG, J., et al., Surface-modified carbon nanotubes catalyze oxidative dehydrogenation of n-Butane, Science **322** (2008) 73.

[13] FELTEN, A., et al., Gold clusters on oxygen plasma functionalized carbon nanotubes: XPS and TEM studies, Nanotechnology **17** (2006) 1954.

[14] TASSIS, D., et al., Chemistry of carbon nanotubes, Chem. Rev. **106** (2006) 1105.

[15] BARINOV, A., et al., Imaging and spectroscopy of multiwalled carbon nanotubes during oxidation: defects and oxygen bonding, Adv. Matter. **21** (2009) 1916.

[16] BARINOV, A., et al., Defect-controlled transport properties of metallic atoms along carbon nanotube surfaces, Phys. Rev. Lett. **99** (2007) 046803.

[17] ESCH, F., et al., Chemically resolved dynamical imaging of catalytic reactions on composite surfaces, Cat. Lett. **52/1 2** (1998) 85.

[18] LUERSSEN, B., et al., Photoelectron spectromicroscopy of electrochemically induced oxygen spillover at the Pt/YSZ interface, Chem. Phys. Lett. **316** 5–6 (2000) 331 335.

[19] ESCH, F., et al., Chemical waves and adsorbate induced segregation on a Pt(100) surface microstructured with a thin Rh/Pt film, Surf. Sci. **443** 3 (1999) 245.

[20] SCHAAK, A., et al., Elementally resolved imaging of dynamic surface processes: Chemical waves in the system Rh(110)/ NO+H$_2$, Phys. Rev. Lett. **83** 9 (1999) 1882.

DEVELOPMENT OF FACILITIES FOR
THE IN SITU CHARACTERIZATION OF MATERIALS
IN THE MATERIALS SCIENCE BEAMLINE
AT THE IUAC PELLETRON ACCELERATOR

D.K. AVASTHI, S.A. KHAN, P.K. KULRIYA, F. SINGH, A. TRIPATHI
Inter University Accelerator Centre,
New Delhi, India
Email: dka4444@gmail.com

Abstract

Ion beams play an important role in the characterization and engineering of materials. Two materials science beamlines exist at the Inter University Accelerator Centre (IUAC) facilities (15 MV Pelletron and superconducting LINAC). There are two large area position sensitive gaseous telescope detectors in these two beamlines, which, apart from light elements depth profiling and compositional analysis, are used for the on-line measurement of electronic sputtering. An in situ X ray diffractometer is set up in the LINAC beamline for in situ investigations of phase transitions, growth of embedded nanoparticles in a matrix etc. under swift heavy ion irradiation. An in situ quadrupole mass analyser is installed in the ultra-high vacuum (UHV) chamber of the Pelletron beamline for in situ investigations of the chemistry within the ion track by measurements of evolved gases or molecules under swift heavy ion bombardment. An ionoluminescence set up at the Pelletron beamline is installed and utilized for studies of light emitted during ion irradiation, which is useful for materials characterization. It can also reveal materials modification by ion beam.

1.   INTRODUCTION

Ion beams play a crucial role in the synthesis, characterization and modification of materials. Ion bombardment of solids results in the scattering of ions, producing recoil; the emission of photons such as X rays, gamma rays and visible light, emission of gases for polymer targets, etc. All these events are utilized in the characterization of materials and the methods for these have been standardized over the years by the efforts of researchers around the globe. Recoils are used in the technique of elastic recoil detection analysis (ERDA) for light elements depth profiling, which is complementary to Rutherford backscattering and suitable for depth profiling of high Z elements. Ionoluminescence uses the analysis of emitted UV and visible light and gives useful information, particularly about optoelectronic materials. The emitted gases during impingement of ions on polymers are analysed by the residual gas analyser or quadrupole mass analyser. These three characterization tools are set up in the beamlines of the Pelletron accelerator facility at IUAC Delhi. The Pelletron accelerator (under the Phase I plan) provides various ion beams including Li, C, N, F, Si, Ti, Ni, Ag, I and Au, with energies typically ranging from 50 MeV to 200 MeV and the ion fluence varying from 1010 to 1014 ions/cm^2. The energy of ions can be roughly doubled with the superconducting linear accelerator LINAC under the Phase II plan. The ions from Pelletron and LINAC are available for experiments in Beam Hall I and Beam Hall II respectively for research in various fields, including materials science.

The incident ions have the unique feature of depositing a large energy density which can result in the formation of ion tracks, explainable by Coulomb explosion [1] or thermal spike [2]. Both these mechanisms can cause a transient temperature rise and/or a pressure spike. Such conditions cause phase transformation in the materials. It is therefore interesting to study the phase transformation in situ to study the ion induced phase transformation, an in situ XRD facility has been set up in the beamline.

The present paper discusses the following on-line / in situ characterization tools developed and set up in the last several years, along with some examples of experiments performed with them:

(a)   On-line ERDA dedicated set-up [3–5] in Phase I and II beamlines;
(b)   In situ XRD [6];
(c)   Ionoluminescence [7];
(d)   On-line quadrupole analyser (QMA).

The basic aim of experiments in the materials science beamline has been to perform studies on the characterization and modification of materials with ion beams. Since the ion beam can deposit a large energy density in materials, there are possibilities of the creation of exotic phases, interface modifications, creation of ion track in materials etc., which can be exploited for materials engineering. Therefore, the motivation of experiments has been to study the consequences of large energy density deposition in materials by studying the materials either during ion irradiation (in situ/on-line) or after ion irradiation. On-line investigations are those which are performed during ion irradiation such as studies of recoils by ERDA and evolved gases by QMA. In situ investigations are those which are used intermittently immediately after different fluences at the beamline, such as X ray diffraction.

2. ON-LINE ERDA DEDICATED SET-UP IN PHASE I AND II BEAMLINES

The ERDA facility is regularly used for (a) conventional depth profiling studies and (b) monitoring changes in the elemental concentration of the films as a result of ion irradiation. The ERDA facility using the indigenously developed large area position sensitive detectors along with required electronics are established in the beamlines of Phase I and II. A few investigations that have been carried out, are briefly summarized.

2.1. H depth profiling in Pr-Pd layers

An investigation was carried out on the role of ion tracks formed in Pr-Pd layers on an all round enhancement in the hydrogenation properties of these films. Ion irradiation was performed with 120 MeV Ag^{+10} ions with the maximum fluence of 1×10^{13} ions/cm^2. The same ion beam was used to record hydrogen concentration in the hydrogenation (absorption of hydrogen) and dehydrogenation (removal of hydrogen by creating a vacuum) processes of these films by ERDA. The hydrogenation property has been found to be strongly influenced by the ion fluence. About 17.8% increase in the hydrogen stoicheiometry during hydrogenation and near maximal removal (about 31%) during dehydrogenation was observed for the highest ion fluence. The formation of nanotracks throughout the film thickness appeared to be providing two way transport routes for H diffusion [8].

2.2. Estimate ion track diameter using H loss studies

The swift heavy ion irradiation of polymers and H containing materials results in a decrease in hydrogen content. The data on hydrogen loss dependence on ion fluence can be used to estimate the ion track diameter. It was shown that 120 MeV Au irradiation of methyltriethosilane thin film on Si substrates resulted in hydrogen loss from a narrow cylindrical zone of a few nm. The formation of C rich cylindrical zones occurred in this process [9].

2.3. ERDA with large area position sensitive telescope detector

Since the swift heavy ion irradiation causes the modification of material, whereas the recoils produced in irradiation can be used by ERDA for characterization, it provides a possibility of using ERDA as a probe to characterize changes (in elemental concentration and depth profile) during irradiation. To exploit such a possibility, it is desirable to record the recoil spectrum with sufficient statistics using only a small fluence so that fluence dependent changes can be recorded. For the accomplishment of this objective, it becomes necessary to increase the solid angle of the telescope detector. However, the increase in the acceptance angle of the detector results in larger kinematic broadening, which hampers the depth resolution. A large area position sensitive detector and making kinematic correction by software, utilizing the position of detected recoils, makes it possible to keep a large solid angle without affecting the depth resolution [10, 11]. A telescope detector essentially consists of two electrodes in a SS304 vacuum chamber with a thin entrance window foil of a polymer. The typical pressure of gas (isobutane) used for operation is typically 2 to 5 kPa The anode is split in two or three parts to provide ΔE and E residual energies of recoil atoms. ΔE provides information on the atomic number of the detected recoil. The cathode is given a backgammon shape so that the left and right side signals are created by the passage of recoil in the gas medium of the detector, which provides information on the position of recoil and hence the recoil angle.

On-line monitoring of ion induced modifications using a large area position sensitive detector with kinematic correction is one of the most interesting aspects of ERDA. Electronic sputtering is an area which can be investigated by on-line monitoring in specific cases. The stoicheiometric changes in the film, especially the elemental constituents of the film, are also investigated by on-line ERDA which helps in the determination of electronic sputtering. The photograph of the on-line ERDA facility is shown in Fig. 1.

2.4. N depletion studies by on-line ERDA

Another interesting study has been on the formation of nanoscale metallic structures in cupric nitride thin films by the impact of 200 MeV Au ions [12]. It was revealed by ERDA that the nitrogen content reduced by 4.5 times owing to irradiation at a fluence of 1.8×10^{13} ions/cm^2. The presence of conducting regions in the irradiated films was confirmed by conducting AFM, and they could be due to the formation of a copper rich region, resulting from the large nitrogen loss.

The measurements on electronic sputtering performed by on-line ERDA are given in Section 2.7.

2.5. Oxygen content measurements

Most of the oxide materials studied by on-line ERD [13–18] show that significant electronic sputtering may exist. There is no preferential sputtering of oxygen and therefore the stoichiometry of the irradiated material is not disturbed in swift heavy ion irradiation. The above conclusion is based on the irradiation on several oxides such as ZnO [13], Fe_2O_3 [14], $NiMn_{0.05}Ti_{0.2}MgFeO_4$ [15], $Li_{0.25}Mg_{0.5}Mn_{0.1}Fe_{2.15}O_4$ [16], CuO [17] and nickel oxide [18]. A similar result is obtained in the case of 100 MeV Au ion irradiation of oxygen deficient germanium oxide ($GeO_{1.7}$) [19], despite the fact that the system shows Ge phase separation owing to SHI irradiation with the same beam [20]. In contrast to the observation in the oxygen deficient Ge oxide system, oxygen deficient indium oxide film irradiated with 120 MeV Ag ions shows a preferential decrease of oxygen as well as phase separation leading to the formation of indium clusters of 35–45 nm in size [21].

2.6. On-line monitoring of swift heavy ion induced mixing at interface

Swift heavy ions (SHI) are capable of causing mixing at the interface and the recoils produced during irradiation can provide information about the changes at the interface [22]. The kinematic correction of the recorded recoil spectrums using the position information from the position sensitive detector results in improvement in depth resolution, which allowed the on-line study of ion beam mixing in a Fe/Ti bilayer system using 135 MeV Au projectiles at room temperature. The decrease in the slope of the recoil spectrums corresponding to the Fe/Ti interface indicates mixing. The mixing rate was found to be 147 ± 9 nm^4 for this system [23].
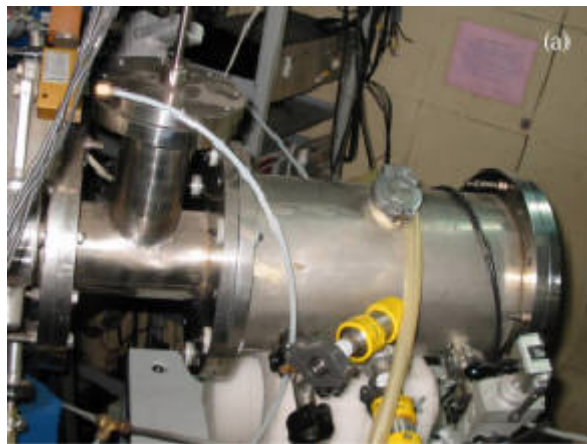

FIG. 1. Photograph of large area position sensitive detector (LAPSDT) installed in Beam Hall I.

2.7. Electronic sputtering measurements by on-line ERDA

The large area gaseous telescope detector allows the measurements of the elemental concentration in the film at different fluences, which in turn is used to determine the electronic sputtering. The sputtering yield of carbon and hydrogen from amorphous C film was found to be dependent on the structural properties of the film [24]. The electronic sputtering of LiF, CaF_2 and BaF_2 thin films [25–27] were studied by on-line ERDA. Typical two dimensional recoil spectrums of CaF_2 thin films on Si substrate are shown [28] in Fig. 2. The sputter yield of both the elements in the film was found to be stoicheiometric. The total sputter yield was determined to be 1.3×10^5, 2.5×10^4 and 1.2×10^4 atoms/ion, respectively for LiF, CaF_2 and BaF_2 films deposited on Si substrates, whereas the sputter yield for same films on glass substrate were 3.8×10^5, 7.8×10^4 and 3.7×10^4 atoms/ion, respectively for LiF, CaF_2 and BaF_2 films deposited on glass substrates as shown in Fig. 3. The sputtering yield for film deposited on glass substrate was thus found to be nearly three times higher than that on Si substrate for the halide thin films. It was found that the sputtering yield increased with the increase in band gap of the halide films.

3.   ON-LINE QMA

Swift heavy ions are known to produce a loss of elements, such as hydrogen and nitrogen and to produce electronic sputtering in a variety of materials. These phenomenons have been utilized to understand the mechanism of ion–solid interactions. An ERDA facility had existed in the centre for over a decade and this gives quantitative information on the lost elements in the studied materials indirectly. However, the information about the ejected species and particularly about the cluster emissions could not be derived. Also, the information related to charge carried by these ejecta was missing. To get answers to these questions, an experimental apparatus based on a quadrupole mass spectrometer has been set up in the materials science beamline. It collects ejected species from the samples, which are tilted at an angle of 20° with respect to the beam direction. The probe, consisting of 3-lens optics, is nearly 5 mm from the sample surface during the measurements. The quadrupole mass spectrometer instrument (QMG 422 with SIMS option from Pfeiffer Vacuum) operates at 2.25 MHz and can mass analyse in the range 1–1024 amu.
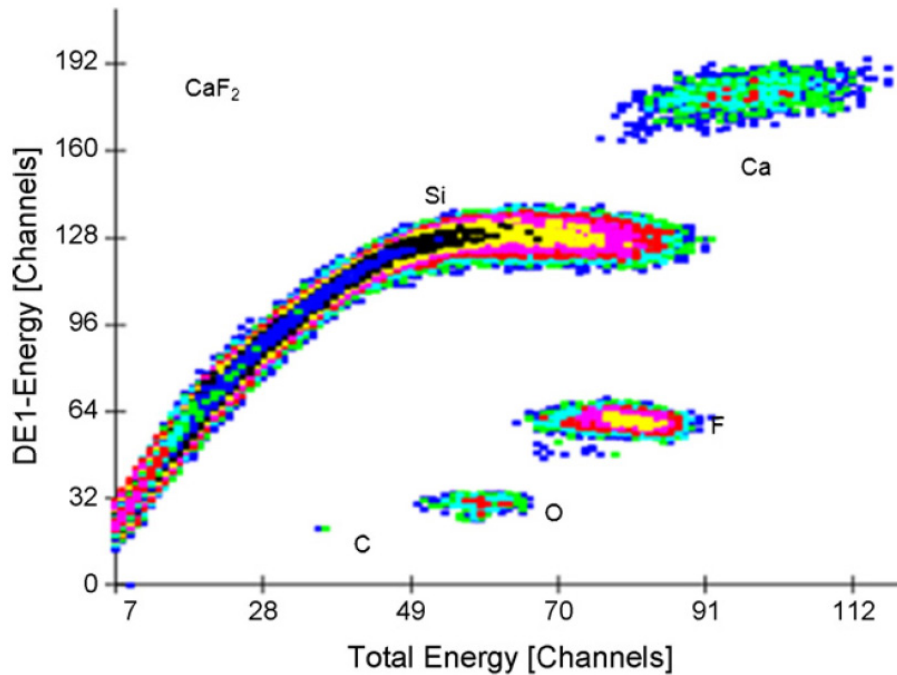

FIG. 2. *Primary ERDA spectrums of CaF$_2$ thin films deposited on Si substrate, bands of Si, F, O, C and Ca recorded with LAPSDT are shown [28].*
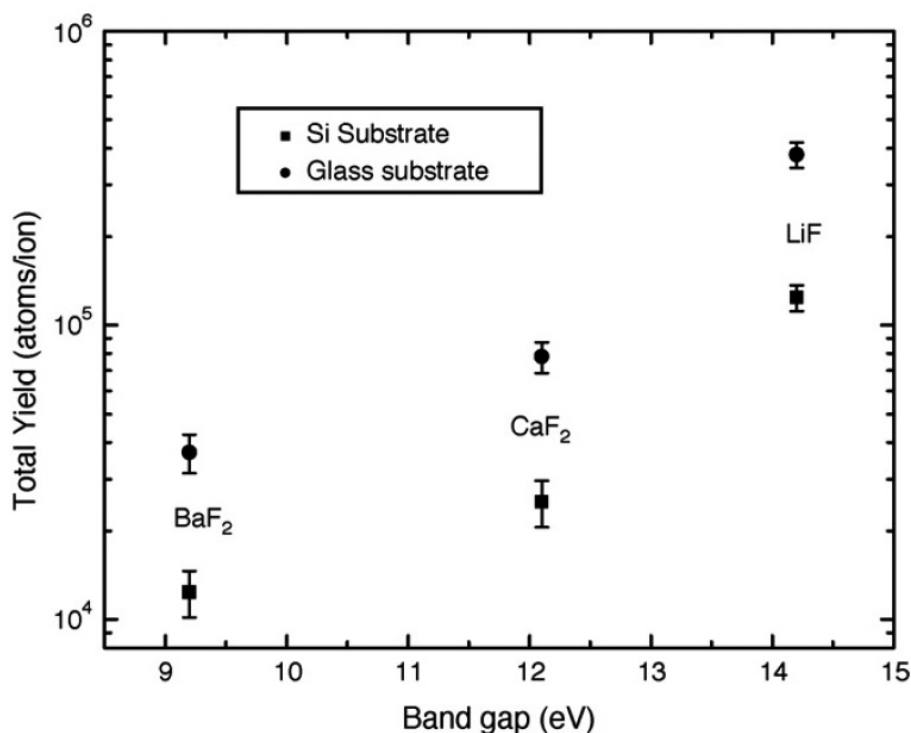
FIG. 3. *Comparison of yield for LiF, CaF$_2$ and BaF$_2$ deposited on glass and Si substrate. Higher yield is observed (~3 times more) for insulator substrate for all the materials [28].*

The UHV chamber, pumped by a turbo-molecular pump and an ion pump, has a base pressure of the order of 10^{-7} Pa. However, during experiments with SHI beams, the pressure in the chamber is only of the order of 10^{-5} Pa owing to the coupling of the chamber with the high vacuum chamber which precedes it in the beamline. There is a load lock system, evacuated by a separate turbo-molecular pump, to introduce samples into the main chamber without disturbing its vacuum. There is a provision to bias the spectrometer with respect to the sample in order to collect the charged ejected species more efficiently. The total ions falling on the sample can be determined by calibrating the ladder current with suppressed faraday cup in the beamline. The data can be recorded either for selected mass numbers or for selected mass range with the help of the software provided by Pfeiffer. A photograph of the on-line QMA facility is shown in Fig. 4.

The experimental apparatus described above enables the measurement of the ejection of molecules during SHI irradiation and the effect of ion energy, ion fluence and its charge state on the ejection process. The detailed analysis of the ejection process may give an insight into the fragmentation process occurring due to SHI and the indirect determination of the size damaged zones produced by each impinging ion.

In situ QMA investigations in a 100 nm Ni on PTFE (polytetrafluoroethylene) bilayer system induced by 120 MeV Au ions with fluences varying from 1×10^{12} to 5×10^{13} ions/cm^2 have been performed. The QMA analysis shows the emission of fluorine (F) and different fluorocarbons (C_xF_y) such as CF, CF$_3$, C$_2$F$_3$ etc. during irradiation. The loss of volatile elements from Teflon in the Ni-Teflon system suggests that desorption of the fluorocarbon gases takes place during ion irradiation [29], as shown in Fig. 5. The on-line facility of QMA provides a possibility to study the chemistry within an ion track core region.

4. IN SITU XRD

An in situ XRD set-up has been installed and tested [30] in the materials science beamline of Beam Hall II, as shown in Fig. 6. The X ray diffractometer is a Bruker D-8 Advanced system, with a horizontal goniometer in a theta–theta configuration, can be operated at a power of max output 1.6kW, at 40kV. The instrument employs
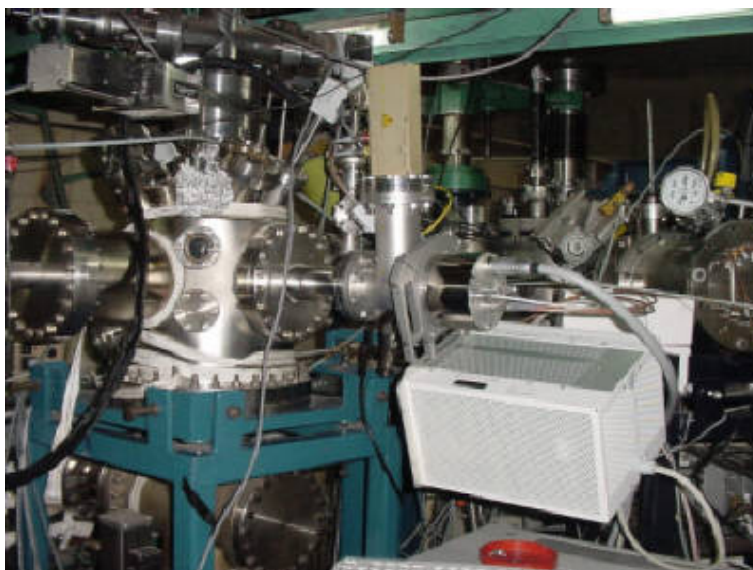
FIG. 4. Pfeiffer QMA 422 quadrupole mass analyser system with SIMS option.
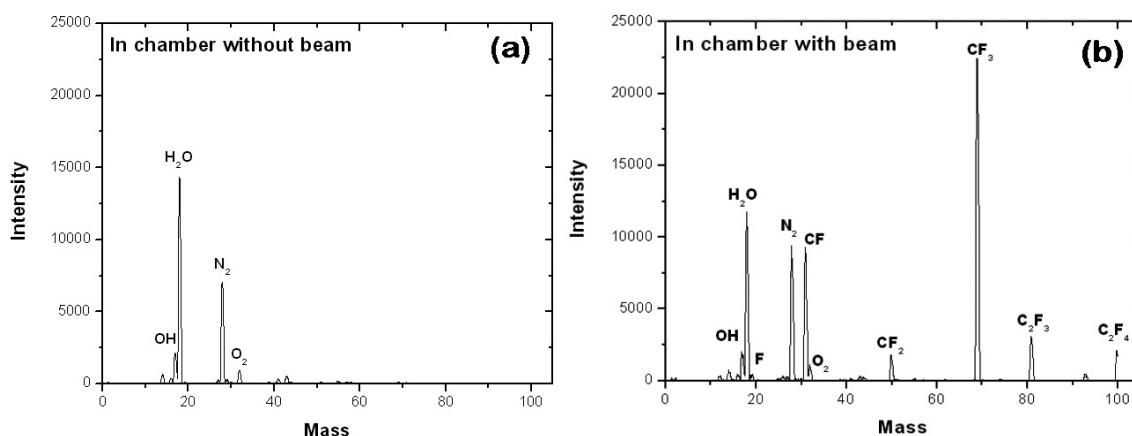

FIG. 5. Residual gas spectrums (a) without and (b) with ion beam on the Ni/Teflon system [29].

Cu $K_{\alpha 1}$ radiation from a sealed tube generator (Bruker AXS). The XRD system is equipped with a conventional NaI detector and a very fast Vantec detector. The Vantec detector (owing to its position sensitivity) makes the data acquisition sixty times faster than the conventional scintillation detector, which is desirable for in situ studies. XRD studies in controlled atmospheres (gas, air and vacuum) can be carried out at temperatures varying from 105 K to 300 K. There have been a large number of ex situ experiments to study ion irradiated samples. There have been three in situ XRD experiments with an ion beam. A photograph of the facility is shown in Fig. 6. The facility is regularly used for structural characterizations of ion irradiated materials. A few of the most interesting studies are described below.

4.1. Snap shots of the growth of Au during ion irradiation

The kinetics of the growth of Au nanoparticles embedded in thin silica films during 90 MeV Ni ion irradiation has been investigated using in situ XRD [30]. Irradiation has been found to result in a controlled growth of embedded Au nanoparticles with ion fluence. This Au silica nanocomposite was irradiated by 90 MeV Ni ions and the XRD was recorded in situ during the experiment, as shown in Fig. 7, to study the growth kinetics of the Au particle under ion bombardment. This was explained in light of the thermal spike model.
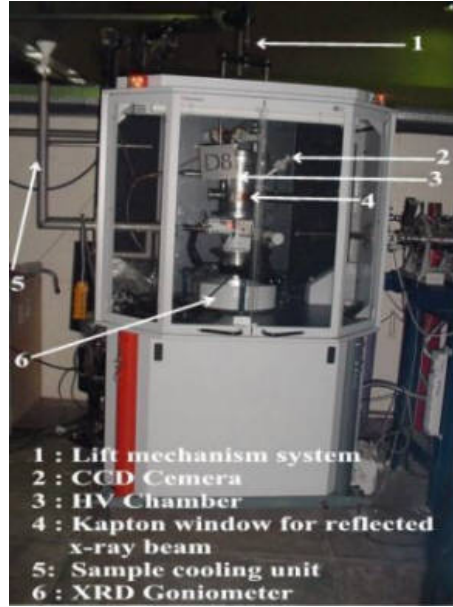
FIG. 6. A photograph of the in situ X ray diffraction set-up with its sample cooling unit [6].
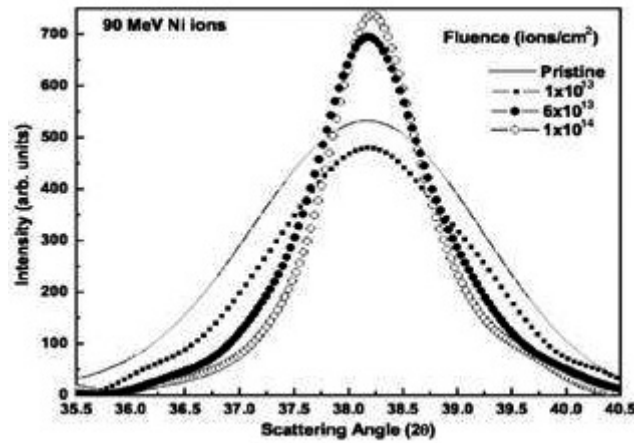
FIG. 7. In situ XRD spectrums show the growth from 4 nm (for pristine) to 9 nm at a fluence of 1×10^{14} ions/ cm² of Au nanoparticles on the ion irradiation [30].

4.2. Phase transformation under SHI irradiation

In situ X ray diffraction to study the structural modifications of zircon and scheelite phases of $ThGeO_4$ induced by swift heavy ion (93 MeV Ni^{7+}) irradiation at different fluences was reported [31]. X ray diffraction (at room temperature) of the irradiated zircon phase of $ThGeO_4$ indicates that the ion beam induced stresses led to a reduction of the cell volume up to 2% and its transformation to a mixture of nanocrystalline and amorphous scheelite phases. Irradiation of the zircon phase at liquid nitrogen temperature results in amorphization at a lower fluence (7.5×10^{12} ions/cm²), as compared to the fluence (6×10^{13} ions/cm²) required for amorphization when irradiation is at room temperature. The scheelite type $ThGeO_4$, irradiated at room temperature, undergoes complete amorphization at a lower fluence of 7.5×10^{12} ions/cm² without any volume reduction. The track radii determined from X ray diffraction measurents on room temperature irradiated zircon, scheelite and low temperature irradiated zircon phases of $ThGeO_4$ are 3.9 nm, 3.5 nm and 4.5 nm, respectively.

4.3. Low temperate ion irradiation induced studies in $YBa_2Cu_3O_{7-y}$

An in situ XRD study of 200 MeV Ag ion irradiation induced structural modification in c axis oriented $YBa_2Cu_3O_{7-y}$ thin films at 89 K was carried out [32]. Figure 2 shows the evolution of the low temperature (T = 89 K) in situ XRD pattern of an $YBa_2Cu_3O_{7-y}$ thin film with 200 MeV Ag ion irradiation. It is observed that the films remained c axis oriented up to a fluence of 2×10^{13} ions/cm, where complete amorphization occurs. This observation is explained on the basis of SHI induced secondary electrons, which create oxygen disorder by an electron capture process in the CuO chains of a fully oxygenated $YBa_2Cu_3O_{7-y}$ structure. The FWHM of XRD peaks and the microstrain around ion tracks showed an incubation effect up to a fluence of 1×10^{12} ions/cm, and subsequently these parameters increased due to the proximity of strained regions around ion tracks. This study suggested that SHI induces three different types of defects in $YBa_2Cu_3O_{7-y}$ at LT: (a) amorphous ion tracks provided $S_e > S_{e\,th}$, (b) strained region around ion track and (c) oxygen disorder (point defects) in the CuO basal plane.

4.4. Study on stresses in oxide semiconductors

In situ XRD measurements are carried out at incremented fluences under 120 MeV Ag ions. The average grain size, lattice constant c and stress in the film are determined from the diffraction pattern at different fluences. The issue of stress is addressed in view of its strong implications in the origin of ferromagnetism in oxide materials such as ZnO. The nature of the stress is intrinsic and the origin is attributed to the strong density of defects, such as dislocations at the grain boundaries, as evidenced by other experimental studies [33].

5. IONOLUMINESCENCE

It is well known that when an ion beam with an energy of a few MeV/u impacts on a crystalline or organic specimen, visible light is often observed. This light induced by the energetic ions is termed ionoluminescence (IL). The analysis of the emitted light provides a better tool for studying materials phenomenons, such as ion matter interaction, for various properties of materials such as impurities, local symmetry of optically active dopants and defects [7]. An IL facility has been set up at the materials science beamline at IUAC and has been used for several experiments. It has been shown that the IL spectrum of natural cyanite mineral exhibits sharp peaks at 689, 694, 705, 713 and 716 nm, along with a broad emission peak at 530 nm. The sharp emission peaks at 689 and 694 nm are attributed to R_2 and R_1 lines of Cr^{3+} impurities, while the peaks from 705 to 716 nm are attributed to Fe^{3+} impurities. The evolution of amorphization was understood by performing fluence dependent studies and their effect on luminescence intensity and was corroborated with vibration techniques such as FTIR to understand the kinetics of bond breaking by such energetic Au ion irradiation [34]. The nature of sharp IL peaks at 689 and 706 nm, along with broad emission in the region 710–800 nm, were studied further in natural and laboratory synthesized cyanite samples under Ag and Si ion irradiation [35, 36]. The reduction in IL and PL band intensity with increasing ion fluence was attributed to the degradation of Si–O bonds present on the surface of the sample. Recently, IL has been used to study the nanophosphors to have an insight into fundamental interactions and their stability under energetic ion irradiation [37].

6. SUMMARY

A brief description of the in situ facilities at the beamlines of the 15 MV Pelletron accelerator is presented. A few examples are quoted detailing experiments and results obtained using these in situ characterization tools.

REFERENCES

[1] FLEICHER, R.L., et al., Nuclear Tracks in Solids, University of California Press, Berkeley, CA (1975).

[2] WANG, Z.G., et al., The S_e sensitivity of metals under swift-heavy-ion irradiation: a transient thermal process, J. Phys. Condens. Matter **6** (1994) 6733.

[3] GHOSH, S., et al., Heavy ion elastic recoil detection analysis set up for electronic sputtering studies, Rad. Eff. & Defects in Solids **161** (2006) 247.

[4] RAO, S.V.S.N, et al., Development of a large area two-dimensional position sensitive $\Delta E-E$ detector telescope for material analysis, Nucl. Instr. and Meth. B **212** (2003) 545.

[5] KHAN, S.A., et al., Development of a position sensitive detector telescope for ERDA based on-line monitoring of swift heavy ions induced modifications, Nucl. Instr. & Meth. B **266** (2008) 1912.

[6] KULRIYA, P.K., et al., Setup for in situ X ray diffraction study of swift heavy ion irradiated materials, Rev. Sci. Instrum. **78** (2007) 113901.

[7] SINGH, F., "Report on Swift heavy ions in materials engineering and characterization", Proceedings of the Conference on Swift Heavy Ions in Materials Engineering and Characterisation (SHIMEC 2010), (Proc. Conf. New Delhi, 2010), Taylor & Francis, New Delhi (2010).

[8] KALA, S., Nanotracks as transport routes for enhanced and reversible hydrogen diffusion in swift heavy ion irradiated Pd–Pr layers, Appl. Phys. Lett. **90** (2007) 153121.

[9] KUMAR, A., Oxygen intake in ion irradiated fullerene films, Nucl. Instr. & Meth. B **266** (2008) 1709.

[10] ASSMANN, W., ERDA with very heavy ion beams, Nucl. Instr. & Meth. B **118** (1996) 242.

[11] AVASTHI, D.K., Online monitoring of ion induced modifications by ERDA using a large area position-sensitive detector telescope, Nucl. Instr. & Meth. B **142** (1998) 117.

[12] GHOSH, S., et al., Formation of nanoscale metallic structures on cupric nitride thin film surface by the impact of 200 MeV Au^{15+} ions, Nucl. Instr. & Meth. B **248** (2006) 71.

[13] AGARWAL, D.C., et al., Formation of self-affine nanostructures on ZnO surfaces by swift heavy ions, J. Appl. Phys. **104** (2008) 24304.

[14] CHAUDHARY, Y.S., et al., Modified structural and photoelectrochemical properties of 170 MeV Au^{13+} irradiated hematite, Thin Solid Films, **492** (2005) 332.

[15] DOGRA, A., et al., Influence of 190 MeV Ag ion irradiation on structural and magnetic properties and oxygen content of $NiMn_{0.05}Ti_xMg_xFe_{1.95-2x}O_4$ (x = 0.0, 0.2) ferrite thin film, Nucl. Instr. & Meth. B **225** (2004) 283.

[16] GHOSH, S., et al., In-situ monitoring of electrical resistance of nanoferrite thin film irradiated by 190 MeV Au^{14+}ions, Nucl. Instr. & Meth. B **212** (2003) 510.

[17] CHAUDHURY, Y.S., et al., A study on 170 MeV Au^{13+} irradiation induced modifications in structural and photoelectrochemical behavior of nanostructured CuO thin films, Nucl. Instr. & Meth. B **225** (2003) 291.

[18] JOSHI, U.S., et al., Resistance switching properties of planner Ag/Li:NiO/Ag structures induced by swift heavy ion irradiation, J. Appl. Phys. **105** (2009) 73704.

[19] BATRA, Y., et al., Ion-beam-induced phase separation in GeO_x thin films, J. Phys. D: Appl. Phys. 40 (2007) 4568.

[20] BATRA, Y., et al., Elastic recoil detection (ERD) analysis of GeO_x thin films, Nucl. Instr. & Meth. B **266** (2008) 1697.

[21] TRIPATHI, N., et al., Swift heavy ion induced structural modifications in indium oxide films, Nucl. Instr & Meth. B **268** (2010) 3335.

[22] AVASTHI, D.K., et al., On-line study of ion beam induced mixing at interface by swift heavy ions, Nucl. Instrum. Meth. B **156** (1999) 143.

[23] KUMAR, S., et al., Swift heavy ion induced mixing in metal/metal system, Nucl. Instrum. Meth. B **244** (2006) 194.

[24] GHOSH, S., et al., Electronic sputtering of carbon allotropes, Nucl. Instr. and Meth. B **219–220** (2004) 973.

[25] KUMAR, M., et al., Swift heavy ion induced effects in LiF thin films, Phys. Stat. Solidi C **4** (3) (2007) 1075.

[26] KUMAR, M., et al., Influence of grain size on electronic sputtering of LiF thin films, Nucl. Instr. Meth. B **256** (2007) 328.

[27] KUMAR, M., et al., Size effect on electronic sputtering of LiF thin films, J. Appl. Phys. **102** (2007) 083510.

[28] KUMAR, M., et al., Substrate effect on electronic sputtering yield in polycrystalline fluoride (LiF, CaF_2 and BaF_2) thin films, Appl. Surf. Sc. **256** (2010) 2199.

[29] PRAKASH, J., et al., Ion beam induced interface mixing of Ni on PTFE bilayer system studied by quadrupole mass analysis and electron spectroscopy for chemical analysis, Vacuum **84** (2010) 1275.

[30] MISHRA, Y.K., et al., Controlled growth of gold nanoparticles induced by ion irradiation: An in situ X ray diffraction study, Appl. Phys. Lett. **90** (2007) 073110.

[31] PATEL, M.K., et al., Swift heavy ion induced structural modifications in zircon and scheelite phases of $ThGeO_4$, Nucl. Instr. & Meth. B **268** (2010) 42.

[32] BISWAL, R., et al., 200 MeV silver ion irradiation induced structural modification in $YBa_2Cu_3O_{7-y}$ thin films at 89 K: An in situ X ray diffraction study, J. Appl. Phys. **106** (2009) 053912.

[33] SINGH, F., et al., Ion beam-induced luminescence and photoluminescence of 100 MeV Si[8+] ion irradiated kyanite single crystals, Solid State Commun. **150** (2010) 1751.

[34] NAGABHUSHANA, H., et al., Determination of the chemical states of impurities in natural Kyanite by the Ionoluminescence technique, Phil. Mag. **89** (2009) 995.

[35] NAGABHUSHANA, H., et al., Ionoluminescence and photoluminescence studies of Ag[8+] ion irradiated kyanite, J. Luminescence **128** (2008) 7.

[36] NAGABHUSHANA, H., et al., Ion beam-induced luminescence and photoluminescence of 100 MeV Si[8+] ion irradiated kyanite single crystals, Solid State Commun. **147** (2008) 377.

[37] NAGABHUSHANA, K.R., et al., Luminescence studies on swift heavy ion irradiated nanocrystalline aluminum oxide, J. Luminescence **131** (2011) 764.

IMAGING OF TEXTURE, CRYSTALLITE SIZE AND STRAIN IN MATERIALS USING ACCELERATOR BASED PULSED NEUTRON SOURCES

Y. KIYANAGI[*], H. SATO[*], K. IWASE[**], T. KAMIYAMA[*]

[*] Faculty of Engineering, Hokkaido University, Kita, Nishi, Sapporo, Hokkaido,
Email: kiyanagi@qe.eng.hokudai.ac.jp
[**] Frontier Research Center for Applied Atomic Sciences, Ibaraki University, Tokai-mura,

Japan

Abstract

The pulsed neutron transmission method can give position dependent information on crystallographic microstructure, such as preferred orientation, crystallite size and strain for thick materials, for which the X ray cannot be applied, since the pulsed neutron measurements enable researchers to obtain neutron transmission spectrums depending on position by using a position sensitive detector. Furthermore, the transmission spectrums reflect the total neutron cross-section containing information of the crystallographic structure. By analysing the transmission spectrums, spatially dependent information can be obtained. An in situ transmission measurement was performed during a tensile test of an iron sample with notches. The results clearly showed changes of anisotropy, crystallite size and strain dependent on the load.

1. INTRODUCTION

Neutrons can measure the crystallographic microstructure in a relatively thick material, since the X ray diffraction and the electron beam scattering cannot observe the crystallographic information inside the material. Energy resolved transmission imaging using neutrons is attracting attention since it gives more detailed information compared with traditional imaging using a white neutron beam. Such transmission imaging has been performed at reactor sources and also at pulsed sources based on an accelerator. Especially at a pulsed neutron source, the time of flight method to decide the wavelength of the neutron passed through a sample gives a great advantage to the energy resolved measurement since it makes the spatially dependent measurement much easier than measurements using the methods employed at the reactor sources. The spatially dependent transmission spectrums as a function of the flight time of the neutrons are easily transformed to the wavelength dependent spectrums. The wavelength dependent spectrum has structures relating to Bragg scattering in the sample material. By analysing this spectrum using the Rietveld imaging of transmission spectra (RITS) code [1], we deduce spatially dependent information such as preferred orientation, crystallite size and strain or lattice spacing.

The strain is base data for evaluating the stress that is very important for structural materials, although the pulsed neutron transmission method cannot directly give information on the stress in the material. However, the method can observe the strain over a wide area of a sample simultaneously. On the other hand, neutron diffraction can evaluate the stress but it requires scanning over the area of the sample to obtain the position dependent strain. Therefore, it is impossible to get the crystallographic information over the wide area of sample at the same time during the transient process. Simultaneous measurement over a wide area is one of the important merits of the pulsed neutron method in crystallographic structure analysis. The change in the crystallographic structure depending on load is important information for assessing the material soundness. Usually, the tensile test is performed using a small piece of material. However, pulsed neutron imaging can measure a material for practical use, so we have tried to measure the change in the crystallographic structure of the iron plate with notches, since it may show a complicated behaviour around the notches. Here, we present the principle of pulsed neutron imaging, and as an example of real time measurements, we introduce in situ imaging of crystallographic structure change during the tensile test of an iron sample.

2. PRINCIPLE OF PULSED NEUTRON IMAGING

Pulsed neutron imaging uses the characteristic structure of the total neutron cross-section. Therefore, it is very important to know the components composing the cross-section. The total neutron cross-section at a long wavelength region is expressed by the following formula.

$$\sigma_{tot}(\lambda) = \sigma_{coh}^{ela}(\lambda) + \sigma_{incoh}^{ela}(\lambda) + \sigma_{coh}^{inela}(\lambda) + \sigma_{incoh}^{inela}(\lambda) + \sigma_{abs}(\lambda) \tag{1}$$

where tot signifies total, coh signifies coherent, incoh signifies incoherent, abs signifies absorption, ela signifies elastic and inela signifies inelastic. For deducing the crystallographic structure, the coherent elastic cross-section is important. However, the formula given in textbooks is not suitable for an actual material, since it is usually intended for the ideal case. We studied the effect of the texture (preferred orientation) and the crystallite size on the coherent elastic cross-section experimentally, and confirmed that the texture changes the shape of the cross-section of the Bragg scattering, and the larger crystallite size reduces the cross-section [2–4]. This indicated that we could obtain information on the crystallographic structure. In the analysis of the diffraction experiments, these effects have been taken into account. For the transmission experiments, it was required to develop a similar data analysis code. For the description of a Bragg edge transmission spectrum of an actual material, we have to consider the effect of the pulse shape of neutrons emitted from the moderator, extinction relating to the crystallite size and the preferred orientation. These three parameters are included in the following formula as $R_{hkl}(\lambda, d_{hkl})$, $P_{hkl}(\lambda, d_{hkl})$ and $E_{hkl}(\lambda, F_{hkl})$;

$$\sigma_{coh,p}^{ela}(\lambda) = \frac{\lambda^2}{2V_0} \sum_{d_{hkl}=0}^{2d_{hkl}<\lambda} |F_{hkl}|^2 d_{hkl} R_{hkl}(\lambda, d_{hkl}) P_{hkl}(\lambda, d_{hkl}) E_{hkl}(\lambda, F_{hkl}) \tag{2}$$

where V_0 is the unit cell volume, d_{hkl} is the d spacing, the distance between the crystal lattice planes $\{hkl\}$, and F_{hkl} is the crystal structure factor including the Debye-Waller factor. The first factor, $R_{hkl}(\lambda, d_{hkl})$, is called the resolution function or the edge profile function. This function describes the edge asymmetric broadening due to the neutron pulse shape and the strain, etc. The second factor, $P_{hkl}(\lambda, d_{hkl})$, is the modified March-Dollase preferred orientation distribution function [5], and the third factor, $E_{hkl}(\lambda, F_{hkl})$, is Sabine's primary extinction function [6, 7].

Figure 1 shows a diagram of the experimental set-up for the pulsed neutron imaging. The arrangement is very simple. The neutrons emitted from the pulsed source are incident on a sample with a wavelength spectrum $I_0(\lambda)$, transmit through the sample with a wavelength spectrum $I(\lambda)$ and are finally detected by a two dimensional (2-D) position sensitive detector (PSD) as a function of flight time. By using the incident wavelength spectrum $I_0(\lambda)$ and the transmitted one $I(\lambda)$, we can obtain the total neutron cross-section by using following formula.

$$\sum_{tot} = \sigma_{tot}\rho = \ln\left[\frac{I_0(\lambda)}{I(\lambda)}\right]\bigg/t \tag{3}$$

Here, λ is the neutron wavelength, $\sigma_{tot}(\lambda)$ is the neutron total cross-section, ρ is the density and t is the thickness of the sample. The neutron transmission $Tr(\lambda)$ is found by:

$$Tr(\lambda) = \exp(-\sigma_{tot}(\lambda)\rho t) \tag{4}$$

By implanting the three factors mentioned above in the neutron cross-section and combining a non-linear fitting method, we have developed a data analysis code RITS for the pulsed neutron transmission experiment to obtain the crystallographic structure information.
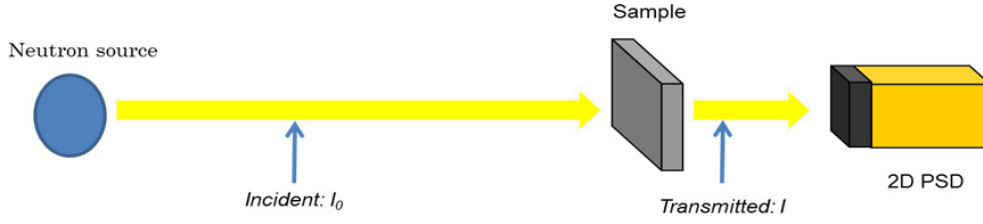
FIG. 1. Diagram of the pulsed neutron transmission experiment. A 2-D PSD is placed to measure the position dependent time of flight spectrums.
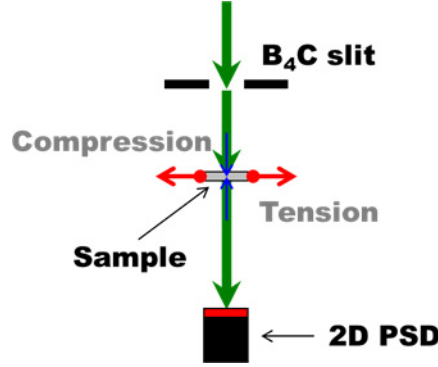

FIG. 2. Experimental arrangement of the transmission measurements.

By analysing the wavelength transmission with the RITS code, we can obtain the information on the preferred orientation and the crystallite size. Furthermore, in the high wavelength resolution measurement, we can observe the shift of the Bragg edges and estimate the strain at each lattice plane.

3. IN SITU EXPERIMENT DURING TENSILE TEST

3.1. Experimental

We performed real time measurements on an iron plate with notches during a tensile test at the beamline of the spectrometer TAKUMI [8] at J-PARC. The experimental set-up is shown in Fig. 2. The flight path length is about 40 m. A tensile jig was placed in a way that compression was measured by the transmission method. The load studies were 0 kN, 10 kN, 20 kN, 25 kN, 27.5 kN, 30 kN, 32.5 kN, 40 kN and 49.5 kN, and further measurements were performed after releasing the load. A 2-D PSD was placed 9 cm behind the sample. The 2-D PSD consists of 16×16 Li glass scintillator plates 2.1×2.1 mm^2 in size [9]. The gap between the adjacent pixel plates is 1.0 mm. Thus, the total detector area is approximately 48×48 mm^2. A photograph of the sample is shown in Fig. 3. The area shown is the centre part of an iron plate with a size of 200 mm $\times$ 100 mm. The distance between two notches is 30 mm and the angle of the notch is 45° for one side. The thickness of the iron is 5 mm. We chose this sample since it was expected that inhomogeneous distribution would appear around the notches.

3.2. Results and discussions

We first measured the transmission spectrum of a sample with no load to obtain the basic data for all other measurements; after that, the load was increased in stepwise way. Figure 4 shows examples of transmission spectrums around the notch at three kinds of loads. The spectrum at 49 kN is different from the other two spectrums around every lattice plane observed, which may indicate transition to plastic deformation.
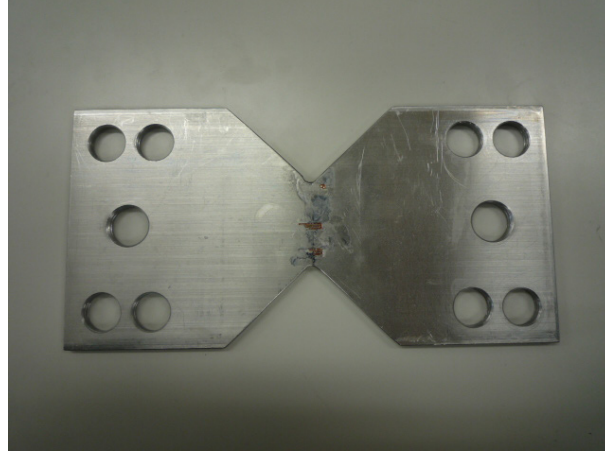
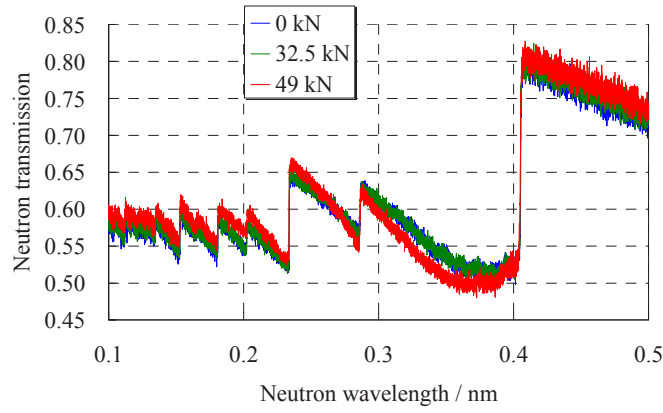FIG. 3. *Photograph of an iron sample with two notches.*

FIG. 4. *Transmission spectrums near a notch at 0 kN, 32.5 kN and 49 kN.*

We analysed transmission data by using the RITS code in order to deduce the degree of anisotropy, crystallite size and strain. In strain evaluation, we assumed that the lattice spacing with no load was strain free. So, we obtain strain as follows. When the lattice spacing (d) changes from d^0_{hkl} to d_{hkl}, the lattice strain, ε_{hkl}, is defined as $\varepsilon_{hkl} = (d_{hkl} - d^0_{hkl})/d^0_{hkl}$.

Here, d^0_{hkl} and d_{hkl} are the d spacing before the tensile test and during the tensile test, respectively. Figure 5 shows the results of strain, anisotropy (March-Dollase coefficient) and crystallite size at 10 kN, 25 kN, 40 kN and 49 kN. The March-Dollace coefficient is a measure indicating the anisotropy. The value of unity for the March-Dollase coefficient corresponds to isotropic case, and departing from unity, the anisotropy become strong. Strain was indicated in units of $\mu\varepsilon = 10^{-6}$. The effect of compression, namely minus strain, first appears around notches and gradually spreads out over the whole area observed with increasing load. The anisotropy and crystallite size show a similar tendency. Changes appear mainly in upper part of the sample and a sudden large change in the distribution occurred at 49 kN. In order to explain such characteristic changes, we need detailed consideration of the crystallographic mechanism, with which we are now proceeding.

4.   SUMMARY

We are now developing a pulsed neutron imaging method that can evaluate various material characteristics. Here, we have introduced the imaging of the crystallographic structure over a wide area, in which the image was obtained at one measurement without scanning. Therefore, it is suggested that this method may be a unique one that can measure information on the actual material during the same period as the real time measurement.
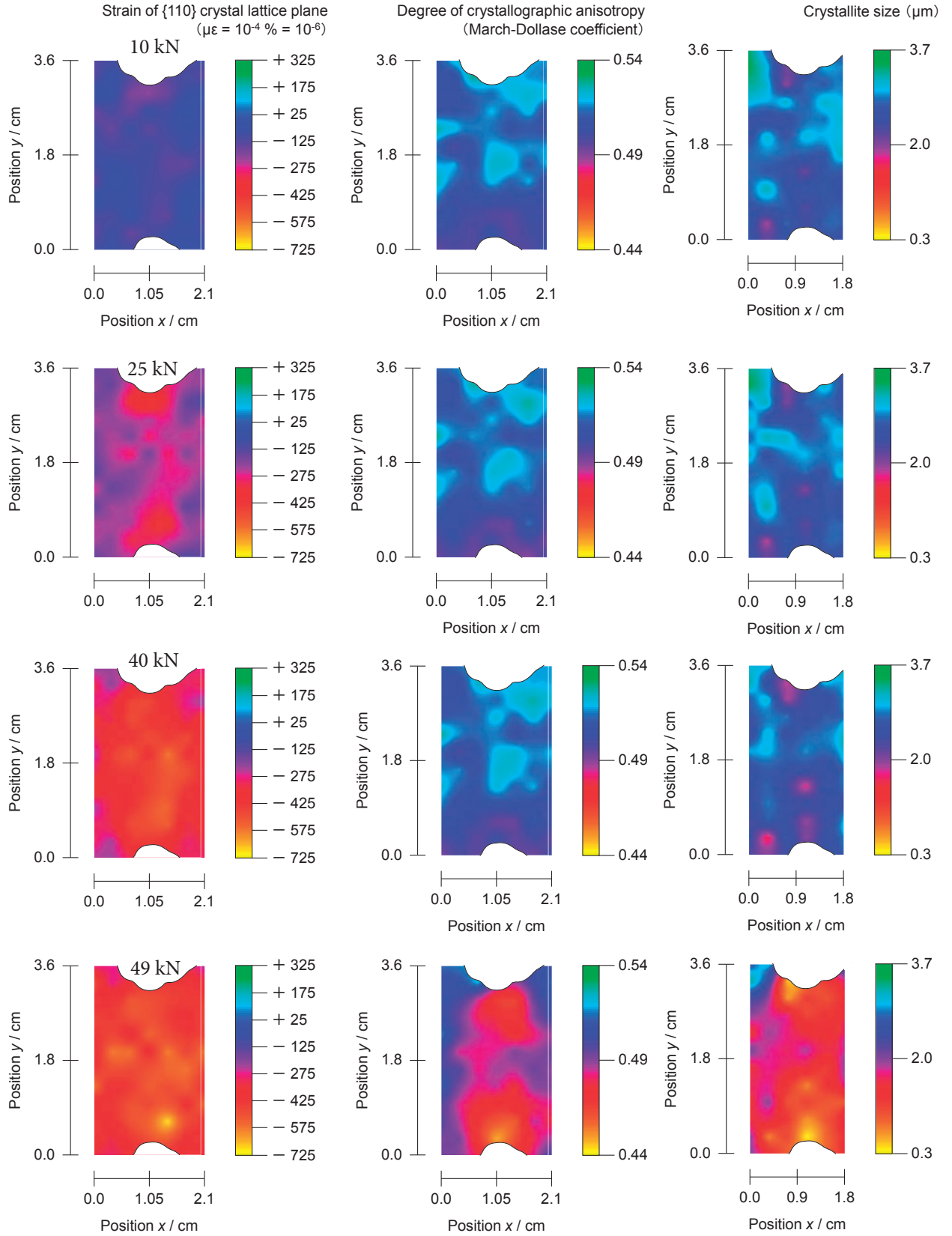
FIG. 5. *Spatial distributions of strain, anisotropy and crystallite size at loads of 10 kN, 25 kN, 40 kN and 49 kN.*

REFERENCES

[1]   SATO, H., KAMIYAMA, T., KIYANAGI, Y., A Rietveld-type analysis code for pulsed neutron bragg-edge transmission imaging and quantitative evaluation of texture and microstructure of a welded α-iron plate, Mater. Trans. JIM **52** (2011) 1294.

[2]   KIYANAGI, Y., KAMIYAMA, T., IWASA, H., HIRAGA, F., Characteristics of a new type neutron radiography using time-of-flight method, Key Eng. Mater. **270–273** (2004) 1371.

[3]   KIYANAGI, Y., KAMIYAMA, T., NAGATA, T., HIRAGA, F., Material characterization using cold neutron transmission spectroscopy, Physica B Cond. Mat. **385–386** 2 (2006) 930.

[4]   IWASE, K., SAKUMA, K., KAMIYAMA, T., KIYANAGI, Y., Bragg-edge transmission imaging of strain and microstructure using a pulsed neutron source, Nucl. Instr. Meth., Phys. Res. A **605** (2009) 1.

[5]   DOLLASE, W. A., Correction of intensities for preferred orientation in powder diffractometry: application of the March model, J. Appl. Crystallogr. **19** (1986) 267–272.

[6]   SABINE, T.M., VON DREELE, R.B., JØRGENSEN, J.-E., Extinction in time-of-flight neutron powder diffractometry, Acta Crystallogr. Sec. **A 44** (1988) 374.

[7]   SABINE, T.M., A reconciliation of extinction theories, Acta Crystallogr. Sec. A **44** (1988) 368.

[8]   MORIAI, A., et al., Development of engineering diffractometer at J-PARC, Physica B **385–386** (2006) 1043.

[9]   MIZUKAMI, K., et al., Measurements of performance of a pixel-type two-dimensional position sensitive Li-glass neutron detector, Nucl. Instr. Meth., Phys. Res. A **529** (2004) 310.

SPALLATION NEUTRONS USED FOR IMAGING IN THE TIME AND ENERGY DOMAIN

E.H. LEHMANN[*], P. BOILLAT[**], C. GRÜNZWEIG[*], L. JOSIC[*], R. ZBORAY[***], J. KICKHOFEL[****]

[*] Spallation Neutron Source Division, Paul Scherrer Institute, Villigen PSI,
Email: eberhard.lehmann@psi.ch
[**] Electrochemistry Laboratory, Paul Scherrer Institute, Villigen PSI,
[***] Laboratory for Thermalhydraulics, Paul Scherrer Institute, Villigen PSI,
[****] Laboratory for Nuclear Energy Systems, Swiss Federal Institute of Technology Zürich, Zürich,

Switzerland

Abstract

SINQ, the Swiss national source for neutron research, is based on the principle of spallation, where protons from a 590 MeV cyclotron are sent to a lead target with highest possible beam intensity. The proton beam current from the PSI's cyclotron is of the order of 2 mA, corresponding to about 1 MW deposited beam power in the target region. SINQ is a large scale user facility. The spallation neutrons with initial energies of up to 100 MeV are slowed to thermal energies within the moderator tank filled with heavy water (D_2O). Further reduction of the neutron energy can take place in the cold source, which is operated at about 25 K and is filled with liquid deuterium. Unlike similar spallation sources (SNS, Oak Ridge, United States of America; JPARC, Tokai, Japan; ISIS, Didcot, United Kingdom), SINQ is not a pulsed source but provides a constant neutron flux level. As such, it compares to a research reactor with about 15 MW of thermal power. Neutron imaging as an advanced technique for neutron research, applied studies and industrial testing is established at SINQ with two beamlines: NEUTRA for thermal neutrons and ICON for cold neutrons. This capability has only minor representation compared to the scattering facilities at SINQ, with about 15 such installations. Modern neutron imaging techniques are exclusively based on digital systems, where each pixel can be considered an individual neutron counter. Neutron imaging experiments are mainly performed in transmission mode where the comparison between the initial and transmitted radiation is used to describe the properties of the sample material in the beam. For standard applications, the full incident neutron spectrum is used, which delivers an energy average attenuation value. Recent developments at the SINQ imaging beamlines permit time dependent investigations, in particular of cyclic processes, with frames in the millisecond range. This option is of high interest for studying the injection of fuel into running combustion engines, to follow the lubricant distributions in different engines and to study two phase flow phenomenons in technical devices such as heat exchangers. Energy selective studies have become more common since new approaches were introduced, such as phase contrast neutron imaging, studies with polarized neutrons or strain measurements with mono energetic neutrons. Suitable devices such as turbine type selectors, crystal based monochromators or time of flight methods will enable the realization of these new and promising methods.

1. INTRODUCTION

Neutron research in Switzerland is based on the utilization of the spallation neutron source SINQ located at the Paul Scherrer Institute. It was built in the 1990s as an extension of the already existing 590 MeV proton accelerator complex, a synchronous cyclotron in the MW class of beam power. SINQ replaced the MTR research reactor SAPHIR (10 MW), which was in operation successfully for over 37 years. This new approach with the spallation source presented the unique opportunity to install state of the art scientific devices for research with thermal and cold neutrons overcoming the limitation of the SAPHIR reactor in space and performance (in particular in respect to the cold neutrons).

The new trend in the production of spallation neutrons has some advantages compared to those generated using reactor technology. First of all, no delicate nuclear fuel has to be handled, therefore there is no risk of criticality, and core meltdown due to coolant loss is impossible. This much lower risk potential is also the reason to enable a much easier and liberal access of users to the research facilities. Only radiation protection has to be considered carefully and on the same level as at reactor based sources.

When the power per produced neutron is compared with the neutron production rate (2–3 fission neutrons compared to 10–15 spallation neutrons), cooling power needs are much less. Finally, the target can be operated for two years (6000 hours/year) without replacement. There are no real limitations imposed by the target burnup. Only the material damage in the target window and some target rods need be considered carefully and conservatively. Activation and radiation levels are dominated by short lived spallation and activation products. After a cooling phase of about two years, the main target components can be safely stored in an onsite repository facility.

Thermal and cold neutron beamlines are equipped with almost all advanced techniques for neutron research, mainly in neutron scattering but also for neutron imaging, fundamental neutron research and radiochemistry. Material characterization takes place by the study of atomic features with neutron scattering methods on the microscopic level, whereas neutron imaging is more of a macroscopic method in materials research.

This article will describe the main properties and parameters of the accelerator driven spallation source SINQ. It will focus on the neutron imaging capabilities at SINQ and their utilization for studies in energy related applications such as electric fuel cells and combustion engines.

2.   THE SPALLATION NEUTRON SOURCE SINQ AT PSI

The bombardment of heavy element targets by high energy particles such as protons results in the destruction of the target nuclei (spallation), while a relatively high number of neutrons are emitted. The neutron yield is directly related to the mass number of the target material, the energy of the injected particles and the proton beam intensity.

Defined by the properties of the two stage cyclotron accelerator complex at PSI, the final proton energy cannot be higher than 590 MeV. Only the beam intensity, which is currently of the order of 2 mA, can be increased in order to raise the neutron output.

The target material at SINQ is lead inside cladding tubes made out of Zircaloy. This material has proven to be very radiation resistant and has been preferentially used in nuclear power plants for many years. Within a European project (MEGAPIE [1]), a successful trial was made to operate SINQ with a liquid metal target (Pb-Bi alloy) resulting in a considerable increase in the neutron production rate when compared to the previously used rod type solid state targets.

In the meantime, solid state target technology was further improved, resulting in a neutron output of nearly 80%, compared with that of the liquid metal option. Being the less demanding and safer approach, future SINQ targets will be made out of rod bundles surrounded with a special blanket.

Compared to other spallation sources (SNS — USA, JPARC — Japan, ISIS — UK), SINQ is not a pulsed one but operates in a continuous mode. This behaviour is determined by the properties of the accelerator. Therefore, the time of flight technique is not possible due to limitations in energy selection.

SINQ is in operation for about 8 months per year with cycles of at least 3 weeks with short breaks for maintenance and beam development. An open solicitation for beamtime proposals (scientific proposals) is made twice a year (15 May, 15 Nov). There is an oversubscription for most facilities indicating the high demand for neutron research.

3.   NEUTRON IMAGING AS RESEARCH TOOL FOR MATERIAL CHARACTERIZATION

As shown in Fig. 1, SINQ delivers beam to eight ports with thermal neutrons, two ports for cold neutrons and a bundle of seven cold neutron guides. These beamlines are aligned tangentially to the spallation target region in order to avoid contaminating radiation contributions from high energy neutrons and gamma rays.

Neutron imaging installations have been performed for thermal neutrons with the NEUTRA facility [2] and with the ICON beamline [3] for cold neutrons. An overview image is shown in Fig. 2 for the ICON beamline. The main components are aperture and shutter devices, an evacuated flight tube (modular), beam limiters, remotely controlled sample manipulators and several digital neutron imaging detection systems. All installations are well shielded with protected and controlled access to the beamline when all shutters are closed. The beam can be tuned by filters or energy selective devices on request. A third option for neutron imaging is under preparation at the BOA beamline where polarized cold neutrons will be delivered.
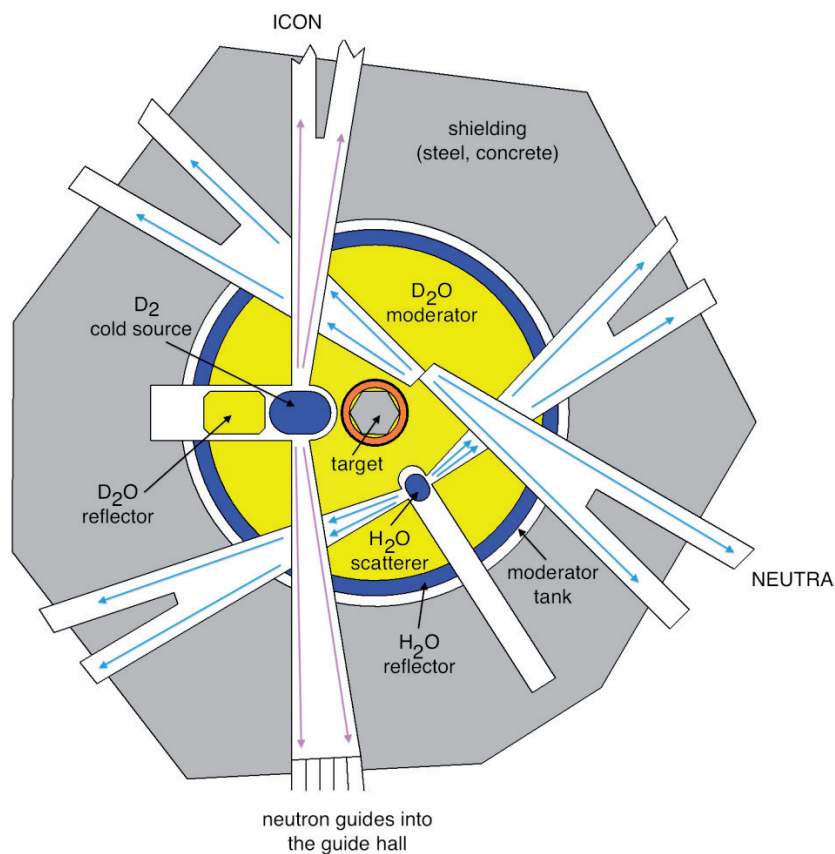
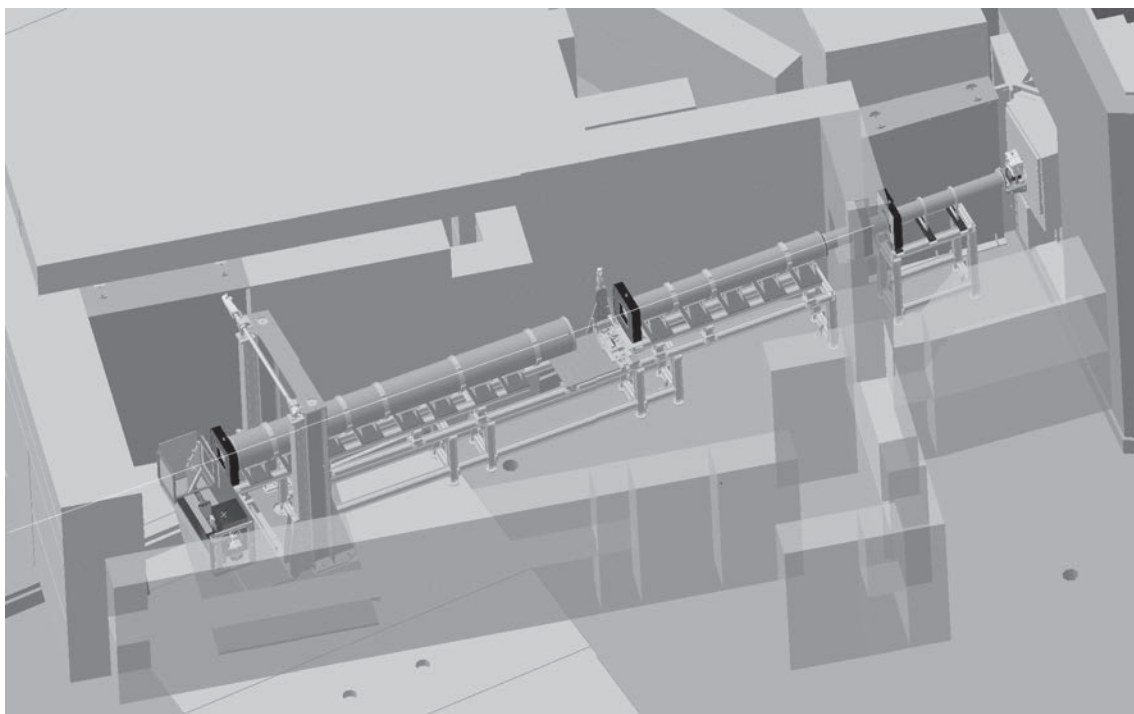*FIG. 1. Layout of the spallation neutron source SINQ at the Paul Scherrer Institute, Switzerland.*

FIG. 2. Overview of the ICON facility for imaging with cold neutrons.

TABLE 1. PERFORMANCE PARAMETERS OF THE NEUTRON IMAGING FACILITIES AT SINQ

NEUTRA	ICON	BOA
Thermal neutrons	Cold neutrons	Very cold neutrons, polarized
High penetration	High contrast	High intensity
Homogenous beam profiles	Variable apertures, Bi filter	Polarizing bender
Two beam positions	Two beam positions	
XTRA option 320 kV tube	Microtomo set-up	Under construction
NUERAP for fuel inspection	Turbine energy selector	
	Fuel cell infrastructure	

High flexibility is required in neutron imaging to satisfy the different demands from scientific and industrial users. This holds with respect to the sample size (field of view), the required spatial resolution, the time resolution, the dynamic range needed and the image frequency. The basic features of the neutron imaging facilities at SINQ are summarized in Table 1.

Compared to the simple and direct approach of transmission radiography with a parallel beam and a white spectrum, several new techniques have been developed in recent years. Most of them are also established at SINQ.

— *Neutron tomography:* the full three dimensional structure and content of an object can be observed with this method, in which a sequence of individual projections is used for the mathematical reconstruction of the behaviour in the third dimension. This technique works only with digital and stationary (position fixed) neutron imaging systems. At SINQ, neutron tomography can be done on the macro level (up to 40 cm sample size) down to the micro level (up to 3 cm sample size). Accordingly, the spatial resolution is between 0.2 mm and 0.01 mm per voxel.
— *Phase based imaging:* considering neutrons as waves (with wavelengths in the order of the atomic distances in solid state lattices), there is the option to derive phase information from the neutron–sample interaction in addition to the transmission contrast. This approach enables us to distinguish materials with similar attenuation properties or to study magnetic features in specific materials directly. A set-up of such a grating interferometer is established at ICON as a user insert, optimized for 4 Å neutrons.
— *Energy selective neutron imaging:* Whereas almost all studies for neutron imaging have been performed with a broad thermal or cold spectrum, the selection of variable narrow energy bands will enable a direct visualization of textures and internal stress in the sample material. This technique is also of high relevance at the new pulsed spallation sources, where time of flight techniques can be used efficiently.
— *Imaging with polarized neutrons:* This new technique has been proven successfully [4, 5] for the study of magnetic fields in and around related materials. At SINQ, we are in the preparative phase of the beamline BOA which will deliver polarized neutrons with high intensity and already has an imaging option available.
— *Microscopic studies with neutrons:* It is a real challenge to improve the spatial resolution in neutron imaging as much as possible. At present, 10 μm is a realistic goal, which is nearly realized within the microtomo set-up [6] at the ICON beamline. Further improvements are hindered by the two step (capture, secondary excitation) detection process for neutrons, the limited beam collimation and also the required beam intensity. However, there is an increasing demand for studying objects with sizes of the order of cm^3, where the resolution can be exploited and the specific neutronic contrast (in particular for hydrogen) utilized.

Neutron imaging can be generally considered a complementary tool to X ray techniques. In the last years, there have been enormous developments at both laboratory and synchrotron sources. Because neutron sources with the required performance can never be made mobile, the role of advanced neutron imaging facilities as user labs becomes more and more important. The beamtime allocation is done at SINQ either based on high scientific impact within the normal user programme or by commercial relevance with respect to industrial paying customers.

4. REAL TIME STUDIES OF RUNNING ENGINES

One challenging problem in combustion engines, which still dominate the transportation of people and goods, is the optimization of the combustion process and the reduction of environmental pollutants. For this purpose, some insight into the engines is required while the fuel distribution needs to be visualized. Neutron imaging has several advantages in this kind of study: the metallic structures of the engines are more or less transparent and the fuel (containing large amounts of hydrogen) has some visibility with the neutrons. However, there is a problem in the time domain: the engines have speeds of the order of thousands of rotations per minute, which would result in a blurring when using standard imaging techniques, as one image requires seconds of exposure. The solution was found by using detection systems which can be synchronized to the rotation of the engine with the help of electronic triggering. Because one single frame in the triggering mode has only milliseconds of exposure, a stacking of many frames with the identical engine rotation position is required. This technique was used and proven successfully with engines driven by an external electric motor [7] where we inspected it with the aim of visualizing the time dependent lubricant distribution.

Recently, we used the same principle with the engine of a two stroke chainsaw operating at about 3000 rpm [8]. As shown in Fig. 3, the snapshot is very clear, exhibiting no motion blurring. Surprisingly, the high level of engine vibration during operation does not influence the image quality at all because this motion is well determined and very repetitive. A full run movie was produced of 16 individual valve positions of the engine.

The only problem within these studies was the lack of contrast for the injected fuel inside the combustion zone. The amount of injected fuel per cycle for this engine is only a few mg and therefore the contrast of hydrogen alone is not high enough. A project was initiated to develop a specific fuel containing a neutron absorbing tracer to maximize attenuation. The two candidate materials were seen in either Gd or ^{10}B. Although the absorption cross-section of Gd (49 000 b) compared to ^{10}B (3840 b) is much higher, the real attenuation power is compensated by the lower nuclear density achievable with Gd. Both lines were followed with some success. In the case of a Gd tracer, we were able to produce a substrate based on nanoparticles with an efficient attenuation coefficient of 100 cm^{-1}. The chemical option with a Gd based fuel composition provides an attenuation of only 7 cm^{-1}.
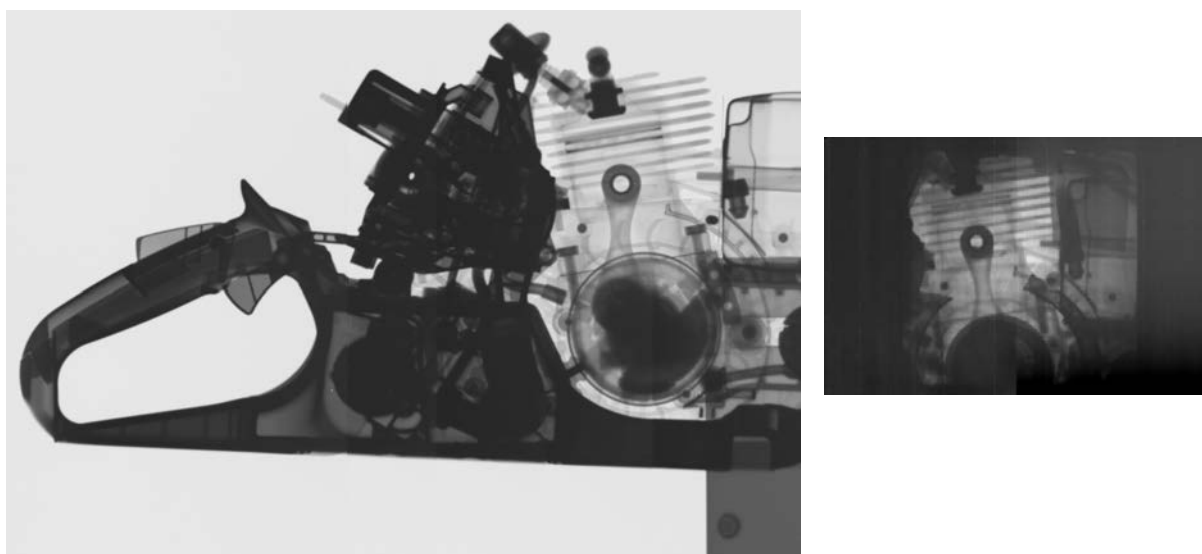

FIG. 3. Radiograph of a chain saw and one snapshot of the image sequence of a two stroke combustion engine operating at 3000 rpm.

The next approach will be test runs using the new tracers in the real combustion process. Theoretical considerations have shown that the attenuation contrast should be sufficient to reach the visibility limits for the small amount of injected fuel.

5. FUEL CELL RESEARCH WITH NEUTRONS

Electric fuel cells (FC) based on the hydrogen–oxygen interaction within a polymer electrolyte (PE) device are considered as potential substitutes for the common combustion process with gasoline or diesel oil. This technique has been known for many decades but an optimization process is needed to increase performance and reduce the price to a competitive level.

The fuel cell itself is relatively simple in its construction (see Fig. 4) but its performance is strongly dependent on the water balance in the cell. Although a certain amount of water is required to keep the conductivity through the membrane high enough, the electrochemical process produces liquid water and vapour which might hinder the efficient gas flow through the cell.

Since the PE FC is constructed with solid outer plates, making the cell gas tight and enabling the extraction of electric power from the cell, a view into the cell using optical means is nearly impossible. A non-invasive inspection of the water distribution in the cell can only be done successfully and with high sensitivity by means of neutron imaging methods. Common X ray methods are not sensitive enough to see low amounts of water and have problems penetrating the fuel cell walls. Although neutron imaging has become a routine technique for scientific and industrial investigations of fuel cells, there is the potential and the need for further methods development.
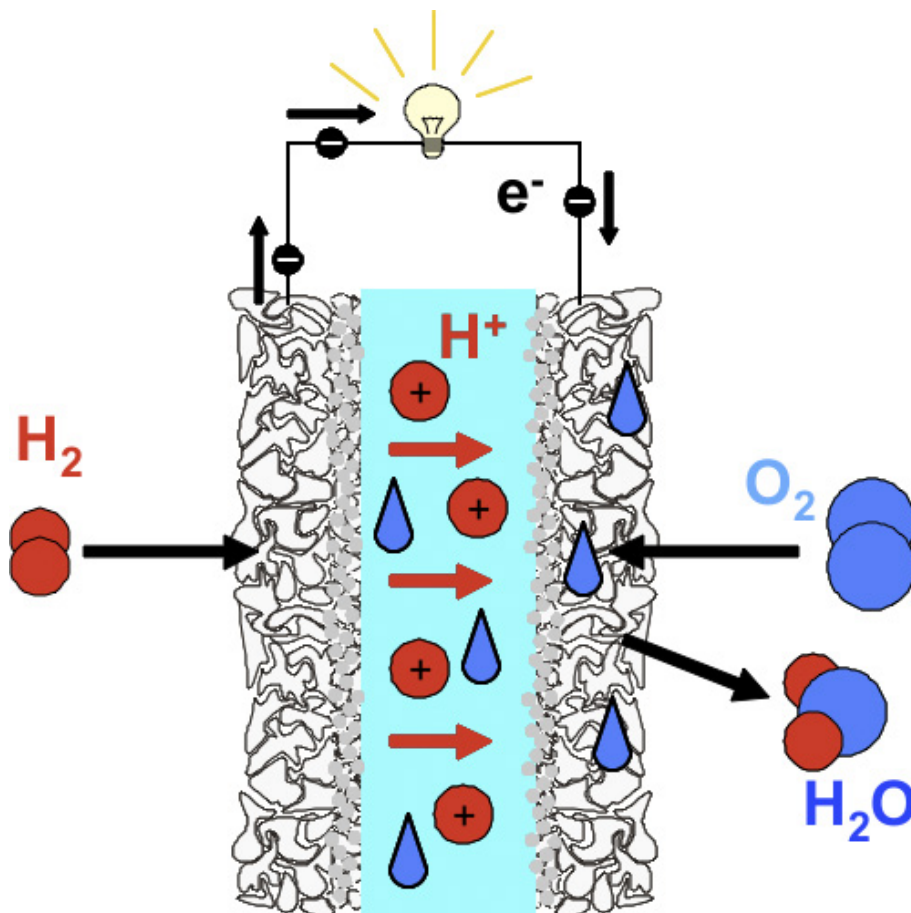

FIG. 4. Principle layout and operational scheme of the PE fuel cell: the two gases, hydrogen and oxygen, are combined in the membrane in the middle and the electrochemical reaction enables the extraction of charge (free electrons) and produces water, which can be investigated comfortably with neutrons.

In the time domain we have to consider two levels: the one which is related to the speed of the gas flow, the other one by the buildup and decrease of the water content in the membrane region or in the flow channels. Because neutron imaging can be performed with reasonable image quality (high dynamic, low noise) under reasonably high neutron intensity with exposure time in the order of few seconds, the first timescale can barely be covered. However, it was found that only a few droplets are moved in the fast regime while the most important processes happen in slower time domains. There are presently two main avenues for PEM FC research: the performance characterization of real industrial devices on the macroscale during a variable operational regime and studies of the behaviour inside and next to the membrane with the highest possible spatial resolution. For this last option, well designed so-called differential cells [9] have been built and operated. Because the spatial resolution is inherently limited (see above), a detector arrangement was developed which extended the resolution range in one direction by tilting the neutron sensitive device [9]. Figure 5 shows some results of microlevel investigations, which are directly linked to the power generation within the cell.

6. OPTIMIZING NUCLEAR FUEL BUNDLES USING NEUTRON TOMOGRAPHY

In the upper part of the fuel pin bundles of a nuclear boiling water reactor (BWR), the dominant flow regime is annular flow of the liquid coolant. Annular flow is characterized by the presence of a continuous liquid film flowing on the wall of the fuel pins, surrounding a central gas core laden with liquid droplets entrained from the liquid film. The water film, though very thin, provides efficient heat transfer from the fuel pins. A dry out of the liquid film endangers the integrity of the pins (burn out) and clearly represents a safety concern. It is also an economical constraint as the maximum fuel temperature allowed and the heat flux from the fuel to coolant is limited by this condition, which in turn limits the thermal power output of a BWR. Functional spacers, which also serve to enhance the stability of the fuel pin bundles, and spacer vanes, are developed to increase the dry out margin by influencing the flow. They aim to provide a maximal effectiveness for phase separation to transfer the droplets from the gas core onto the fuel rod surfaces, thereby increasing the liquid film thickness (LFT).

Annular flows and the effect of functional spacers on the LFT have been investigated by cold neutron tomography at the ICON beamline at SINQ in a scaled up model of two neighbouring subchannels as found in BWR fuel assemblies. The test section is constructed of aluminium, and adiabatic experiments with air–water annular flows have been performed as a generic representation of actual BWR conditions. The sensitivity of cold neutrons to water enables imaging of the typically 2–300 μm thick water films with a high contrast, as is shown in the left image of Fig. 6 for an experiment without a spacer. It shows the geometry of the test section, imitating two half fuel pins and four quarter pins surrounding the two neighbouring subchannels. The right image in Fig. 6 shows the LFT distributions on the surface of a spacer vane for another experiment. Details on the experiments are given in Ref. [10].
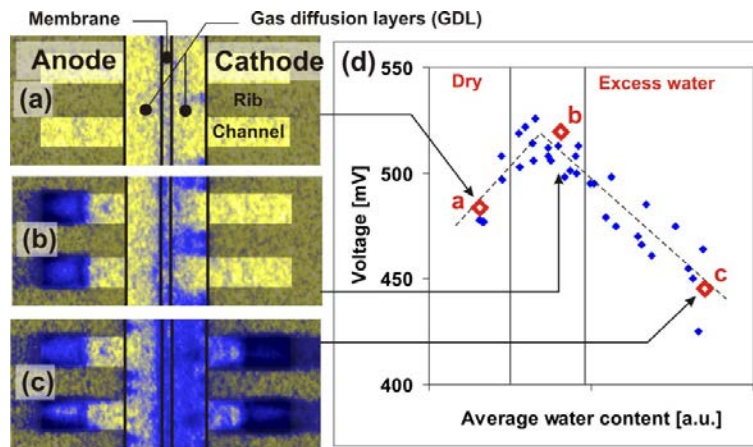

FIG. 5. Visualization and quantitative determination of the water distribution around the membrane of a differential PEM fuel cell obtained with a high resolution detection system. The neutron image shows the fuel cell structure in yellow; the produced water is shown in blue. The observed region is only 3 mm wide.
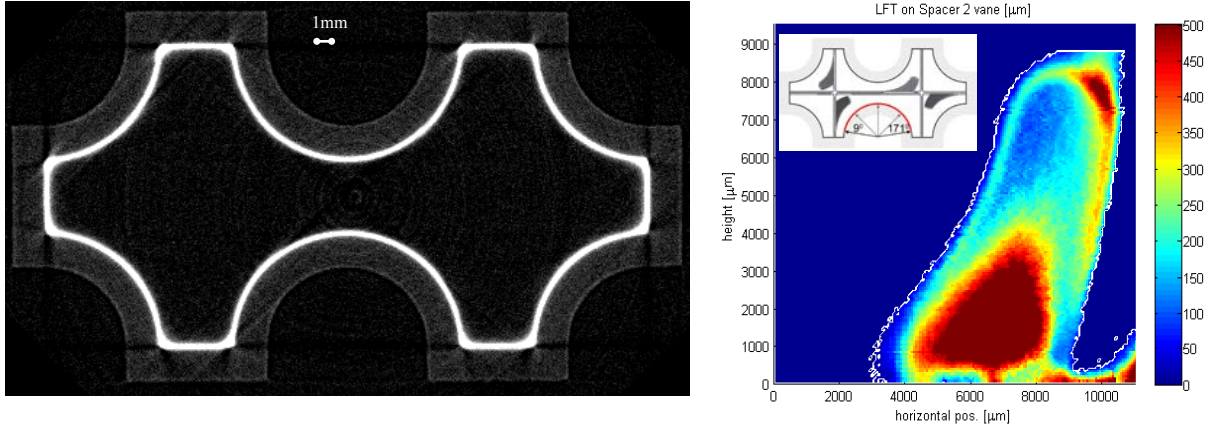
FIG. 6. Reconstructed cross-section of the double subchannel geometry providing the water film on the inner wall surface with high contrast (left). The LFT (liquid film thickness) distribution on a spacer vane is shown on the right side. The inset shows the whole spacer structure inside the double subchannel.

Cold neutron tomography is shown to excel for investigating air–water annular flows and could be a useful tool for optimizing the design of functional spacers. The high resolution, high contrast measurements provide the spatial distributions of the coolant LFT (liquid film thickness) on the fuel pin surfaces as well as on the surfaces of the spacers, including the vanes.

7. ENERGY SELECTIVE STUDIES FOR MATERIAL CHARACTERIZATION

Non-destructive testing of structural materials with neutrons has had a long tradition ever since reasonably intense neutron sources were made available and neutron detection systems were developed. Over more than three decades, until the middle of the 1990s, photographic film methods dominated routine imaging. Film is still in use for some specific and certified applications.

The invention and introduction of digital imaging systems has provided many advantages in the field of neutron imaging. A summary of this topic can be found in the literature, e.g. Ref. [11].

Thermal and cold neutrons have a higher transmission probability through metals than X rays which typically have 150 keV photon energy. This enables the study of thicker samples and transmission geometries in particularly heavy elements such as lead, bismuth and even uranium.

It is quite common to perform neutron imaging with a broad thermal neutron spectrum where a superposition of all neutron wavelengths contributes to the resulting neutron image.

Besides, in some characteristic neutron absorbing materials (e.g. Cd, Gd and Co), the dominant interaction of the neutrons with the metals is by neutron scattering. Owing to the crystalline structure of the metals, elastic coherent scattering plays an important role, in particular in the cold energy range between 2 and 5 Å. Given the angularly random orientation of the metal crystallites, scattering takes place at lattice planes with different distance d, following Bragg's law, with the reflection angle θ.

$$2d \sin \theta = \lambda \tag{1}$$

The total cross-section for the metals is dominated by this Bragg behaviour in the cold energy range. The example for iron in its body centered cubic (BCC) phase is shown in Fig. 7.

These interaction properties have also some impact to the neutron imaging techniques if it is possible to narrow the energy ranges in the region close to the major Bragg edges. There is a high slope in the cross-section indicating strong contrast variation when a measurement takes place above and below the Bragg edge. A gain in transmission or in contrast, respectively, might be achievable. In combination with other materials which are not influenced by Bragg scattering, or have Bragg peaks at other neutron energies, there is the high potential to distinguish different materials efficiently.
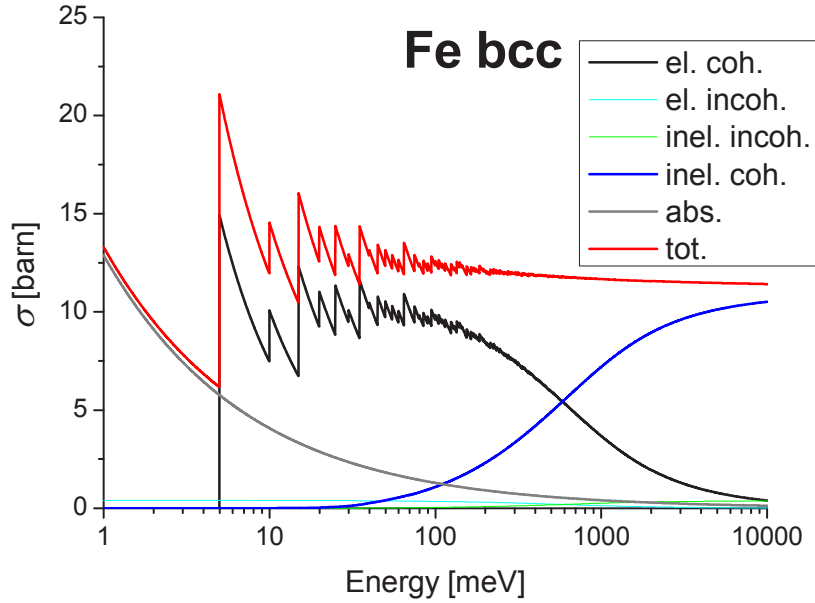
FIG. 7. Cross-section data for BCC structured iron with the characteristic Bragg edges (caused by the coherent elastic scattering at the lattice planes) in the cold energy range.
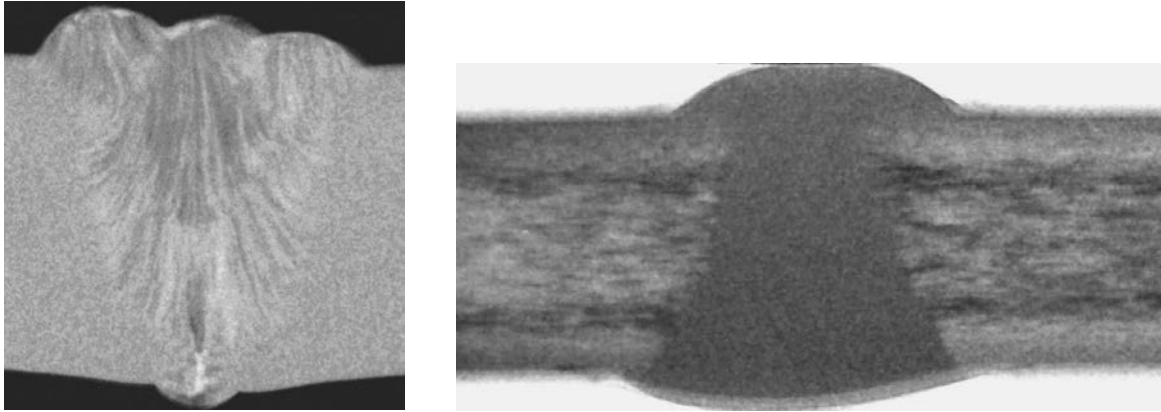

FIG. 8. Results of energy selective imaging with a steel weld (left) and a rolled aluminium plate (right) where the preferential orientation of crystallites becomes directly visible.

Neutron imaging investigations have been done in energy selective mode by using a either turbine type energy selector device [12] or a double crystal monochromator set-up [13]. As well as contrast variations, as mentioned above, the investigation of either steel welds or rolled aluminium provided new insights into material structure by directly showing the texture in different zones (see Fig. 8). The given contrast strongly depends on the chosen wavelength during the experiment and is caused by the preferential orientation of the crystallites in the different zones. With the white beam, outside the Bragg region, only homogenous sample attenuation can be recognized. This new method has potential for other structural materials if the conditions are chosen well with respect to the selected neutron energy and the sample orientation.

Energy selective imaging will be used in the future for the visualization and determination of internal stress in structural materials. This type of imaging requires higher energy selectivity on the one hand and the right energy position of the Bragg conditions of the particular material on the other hand.

8. FUTURE DEVELOPMENTS AND TRENDS

Spallation neutron sources and other accelerator driven neutron sources with lower intensity will be the future in neutron generation for research purposes. Despite the drawbacks with the handling of nuclear fuel (see above), there is mainly the advantage of a dedicated time structure in neutron delivery which can directly be used for the selection of particular neutron energies. Such time of flight techniques are also of high importance for neutron imaging applications when the energy selection has to be made for the highest performance and flexibility. Much improvement is expected in comparison to the present possibilities at continuously running sources.

That is the reason why neutron imaging facilities are under construction and consideration at the pulsed spallation sources in Japan, the UK and the USA. They can also be combined with a detection system observing the scattered neutrons around the sample.

REFERENCES

[1] WAGNER, W., et al., The first liquid metal target driven by a megawatt class proton beam, J. Nucl. Mater. **377** 1 (2008) 12–16.

[2] LEHMANN, E., PLEINERT, H., The new neutron radiography station at the spallation source SINQ, INSIGHT **40** 3 (1998) 515–640.

[3] KÜHNE, G., et al., ICON The new facility for cold neutron imaging at the swiss spallation neutron source SINQ, Swiss Neutron News **28** (2005) 20–29.

[4] KARDJILOV, N., et al., Tree dimensional imaging of magnetic field with polarized neutrons, Nature Phys. **4** (2008) 399–403.

[5] SCHULZ, M., "Quantum Criticality: Radiography with polarized neutrons", Neutron Radiography: Proceedings of the 9th World Conference (Proc. Conf. Kwa Maritane, South Africa, 2010), Elsevier, Amsterdam (2010).

[6] LEHMANN, E.H., et al., The micro-setup for neutron imaging: A major step forward to improve the spatial resolution, Nucl. Instr. Meth. in Phys. Res. A **576/2–3** (2007) 389–396.

[7] BRUNNER, J., LEHMANN, E., SCILLINGER, B., "Dynamic neutron radiography of a combustion engine", Neutron Radiography: Proceedings of the 7th Word Conference (Proc. Conf. Rome, 2002), Italian National Agency for New Technologies, Energy and Sustainable Economic Development, Rome (2002).

[8] GRÜNZWEIG, C., et al., Visualization of a Fired Two Stroke Chain Saw Engine Running at Idle Speed by Dynamic Neutron Radiography, SAE Technical Paper 2010-32-0013, Warrendale, PA (2010).

[9] BOILLAT, P., et al., In situ observation of the water distribution across a PEFC using high resolution neutron radiography, Electrochem. Commun. **10** (2008) 546–550.

[10] LEHMANN, E.H., VONTOBEL, P., FREI, G., BRÖNNIMANN, C., Neutron Imaging – detector options and practical results, Nucl. Instrum. Meth. Phys. Res. A **531** (2004) 228–237.

[11] KAESTNER, A.P., et al., Cold neutron imaging at SINQ – The ICON facility, Nucl. Instr. Meth.Phys. Res. A **659** 1 (2011) 387–393.

[12] HILGER, A., et al., The new cold neutron radiography and tomography instrument CONRAD at HMI, Physica B **241** 243 (1998) 82.

[13] KICKHOFEL, J., et al., "Cold Neutron Tomography of Annular Coolant Flow in a Double sub-channel Model of a Boiling Water Reactor" Neutron Radiography: Proceedings of the 9th World Conference (Proc. Conf. Kwa Maritane, South Africa, 2010), Elsevier, Amsterdam (2010).

ESTABLISHMENT OF AN ASEAN ION BEAM ANALYSIS CENTRE FOR MATERIAL CHARACTERIZATIONS AT CHIANG MAI UNIVERSITY

T. KAMWANNA[*, **], P. JUNPHONG[*, ***], L.D. YU[*, +], S. INTARASIRI[++],
D. SUWANNAKACHORN[*], S. SINGKARAT[*, +]

[*] Plasma and Beam Physics Research Facility, Department of Physics and Materials
Science, Faculty of Science, Chiang Mai University, Chiang Mai
Email: yuld@fnrf.science.cmu.ac.th
[**] Department of Physics, Faculty of Sciences, Khon Kaen University, Khon Kaen
[***] Department of Physics, Faculty of Science, Maejo University, Chiang Mai
[+] Thailand Center of Excellence in Physics, Commission on Higher Education, Bangkok
[++] Science and Technology Research Institute, Chiang Mai University, Chiang Mai

Thailand

Abstract

A comprehensive ion beam analysis centre unique in the ASEAN (Association of Southeast Asian Nations) region has been established at Chiang Mai University, Thailand. The centre is equipped with a 1.7 MV Tandetron tandem accelerator and a 300 kV medium energy ion beam accelerator for ion beam analysis. The Tandetron accelerator employs two ion sources, a duoplasmatron ion source and a sputter ion source, capable of producing ion beams of both light species (hydrogen and helium) and heavy species. The beamline is currently able to perform ion beam analysis techniques, such as Rutherford backscattering spectrometry (RBS), RBS/channelling, elastic backscattering (EBS), particle induced x ray emission (PIXE) and ionoluminescence (IL) with the assistance of commercial and self-developed software. The medium energy ion accelerator features an ns pulsed beam so that time of flight (ToF) RBS analysis using medium energy ion beams is available for detailed analysis of materials. Ion beam analysis experiments and applications have been vigorously developed for the real time characterization of various materials. Examples are presented and qualities of the ion beam analysis techniques are discussed.

1. INTRODUCTION

The laboratory Plasma and Beam Physics Research Facility (PBP), formerly known as the Fast Neutron Research Facility (FNRF, http://www.fnrf.science.cmu.ac.th/), [1] was established about 30 years ago at Chiang Mai University (CMU). Its main mission is to promote research projects related to accelerator technology applications for fulfilling Thailand's need for more qualified young physicists and useful technological spin offs. On the basis of previous work on neutron analysis, detector techniques, ion beam and plasma modification of materials, and linac electron beam with intensive X ray generation, the laboratory has recently developed ion beam analysis (IBA) techniques to complete the establishment of a comprehensive IBA centre unique in the ASEAN (Association of Southeast Asian Nations) region. The centre is currently equipped with a 1.7 MV HVEE (High Voltage Engineering Europa [2]) Tandetron tandem accelerator and a 300 kV self-developed low/medium energy ns pulsed beam accelerator. The former is for routine and conventional ion beam analyses while the latter is for high resolution analyses, particularly of very near surface regions. The analytical techniques developed include Rutherford backscattering spectrometry (RBS), RBS/channelling, elastic backscattering (EBS), time of flight RBS (ToF RBS), particle induced X ray emission (PIXE), ionoluminescence (IL) and microbeam writing/reading. These analysis techniques have been applied in various fields such as materials science, environment, biology, agriculture, gemmology, archaeology and criminology. The centre also trains students and young researchers in order to increase the national research levels. This paper provides an overview of the IBA centre at CMU.

2. FACILITIES

2.1. 1.7 MV Tandetron tandem accelerator

2.1.1. Beamline

As shown in Fig. 1, the entire beamline consists of an ion source terminal which includes two ion sources, a duoplasmatron ion source (Peabody Scientific) and a Cs sputter ion source (Peabody Scientific), a switching magnet with two entrances and one exit, the accelerator including the high voltage supply, the beam transportation line, a 30° mass analysing magnet and an analysis chamber. The duoplasmatron ion source allows the extraction of alpha particles and protons, and the negative ion sputter source is capable of producing heavy species. The tandem accelerator has a terminal voltage of up to 1.7 MV. At the terminal electrode, a nitrogen gas stripper converts negative ions to positive ones and allows a second acceleration of the ions with the same voltage. The accelerated ions are transported in the beamline through focusing lenses and the mass analysing magnet to enter the target chamber.

2.1.2. Analysis chamber

The chamber contains a sample stage on a 2-D translatable and 2-D rotatable goniometer and detectors such as a SSB (silicon surface barrier) detector, Si(Li) detector and optical fibres for RBS, EBS, PIXE and IL analyses, respectively. Figure 2 shows the arrangement of the detecting and associated devices. The incident beam intensity ranges between 0.1 and 200 nA, depending on the energy and type of ions, and can be controlled by several parameters such as stripper gas pressure, quadrupole triplet and collimators. The beam spot size is about 2 mm in
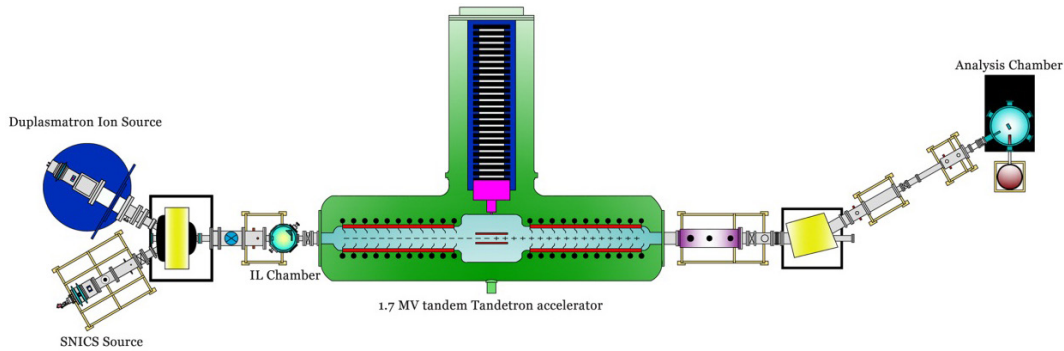

FIG. 1. Schematic diagram of the beamline of the 1.7 MV Tandetron accelerator for ion beam analysis at PBP, CMU. The beamline length is about 10 m.
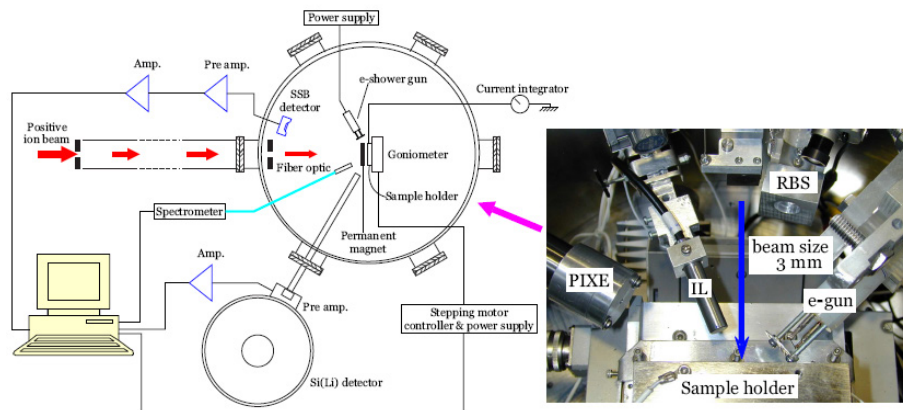

FIG. 2. The analysis chamber at the target terminal of the 1.7 MV Tandetron accelerator beamline. Left: schematic of top view. Right: photograph of the inside.

diameter when focused by the quadrupole triplet lens. The sample holder is electrically isolated from the chamber and acts as a Faraday cup. Two permanent magnets are placed in parallel in front of the sample holder as a secondary electron suppressor, in order to have an accurate measurement of the charge. Backscattered particles from samples are detected by the SSB detector which can be adjusted up to 170° with respect to the beam direction. The detector has a 25 mm^2 active area, 100 μm thick silicon crystal and an energy resolution of 12 keV at FWHM (full width at half maximum). The X ray emission from samples is detected using a Si(Li) detector with an energy resolution of 150 eV (FWHM of Mn k$_\alpha$ 5.9 keV), situated at 120° relative to the beam direction. The active area of the detector is 30 mm^2 with a 25 μm thick beryllium widow. For PIXE measurements on insulating samples, an electron shower placed closely in front of the sample is used to neutralize the charge buildup on the sample. In addition, a 1000 μm core HOH UV (high OH, or hydroxyl, content for ultraviolet) optical fibre is situated at 150° relative to the beam direction, allowing simultaneous measurements using the IL technique.

The SSB detector was calibrated with the RBS measurement of a standard sample of thin layer of Cu, Ag and Au sequentially deposited on Si substrate, and the Si(Li) detector calibration was performed using the X rays of the [109]Cd radioactive source. For the spectrometer, the calibration was performed using the HG-1 mercury argon calibration source [3]. In the PIXE measurement calibration, SRM (standard reference material) 610 Trace Elements in Glass Matrix [4] was analysed as a quality control. Table 1 shows the certified and experimental values of the elemental composition, obtained by using 2 MeV protons and Mylar funny filter [5] in front of the Si(Li) detector for the most necessary elements in one run. The measurement demonstrates the accuracy of the experimental set-up to be within ±10%.

For the inside of the analysis chamber, we are developing a micro aperture, as shown in Fig. 3. The aperture system is capable of varying the aperture size down to 1 μm by full computer control. Cooperating with X-Y translation of the sample stage, the system allows for microproton beam writing and reading [6].

2.1.3. *Data acquisition system*

A pre-amplifier and amplifier from Canberra and Tennelec are used to amplify the signals from the detectors. After amplification, the signal is delivered through a coaxial cable to a multichannel analyser (MCA, made by Ortec), where spectrums are acquired with the MAESTRO code. For RBS and EBS measurements, the obtained backscattering spectrums are analysed with SIMNRA code [7]. The GUPIXWIN software is used to fit and simulate PIXE spectrums [8]. For IL measurements, an optical fibre leads the emitted light to an Ocean Optic S2000 Spectrometer. The spectrometer is connected to a computer where spectrums are acquired with the OOIBase32 Ocean Optics software [9].

TABLE 1. COMPARISON OF THE CERTIFIED AND EXPERIMENTAL (EXP.) VALUES OF SUPPORT MATRIX (%) AND TRACE ELEMENTS (ppm) OF SRM 610

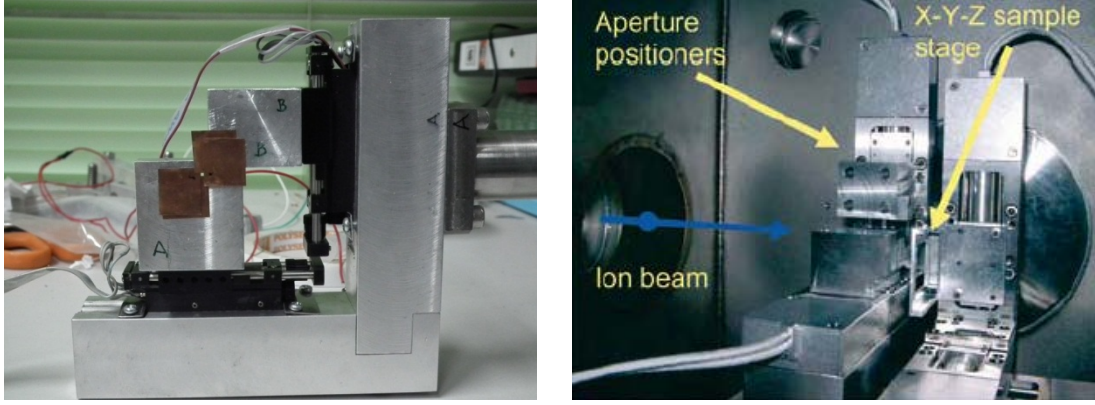| Major matrix	Certified value	Exp. Value	Traces	Certified value	Exp. Value
SiO$_2$	72	73.08	Fe	458 ± 9	416.7
CaO	12	11.58	Mn	485 ± 10	456.2
Na2O	14	13.14	Ni	458.7 ± 4	437.7
Al$_2$O$_3$	2	2.20	Sr	515.5 ± 0.5	506.8
			Th	457.2 ± 1.2	493.8
			Pb	426 ± 1	455.5
			Rb	425.7 ± 0.8	391.6
			U	461.5 ± 1.1	507.1

FIG. 3. Photographs of the microaperture system for MeV microbeam writing/reading applications. (a) The aperture system. (b) Installation inside the chamber.
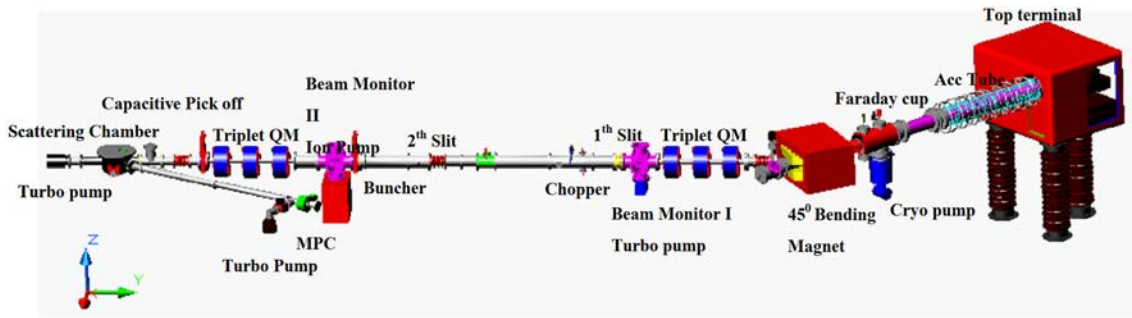

FIG. 4. Schematic diagram of the 300 kV ns pulsed beam accelerator for ToF RBS analysis. The total beamline length is about 14 m.

2.2. 300 kV medium energy ion beam accelerator

2.2.1. Beamline

The 300 kV ion beam accelerator, as shown in Fig. 4, has been developed in-house and installed with thorough upgrading and modification of a 150 kV pulsed deuteron accelerator for 14 MeV neutron generation [10, 11]. The accelerator is equipped with a compact filament driven multicusp ion source (MIS). The dc current applied to the filament is about 15–20 A and the electron emission current is about 2–2.5 A. The extracting voltage is 10 kV and an einzel lens focuses the extracted beam with 5–6 kV. The continuous beam can be accelerated up to 300 kV. A self-made 45° bending magnet after the accelerating tube analyses ion species. The analysed ion beam is further focused by a triplet quadrupole magnet, which was designed by the MAGNET program [12] and self-constructed. The beam is then chopped by a system that is composed of two orthogonal slits and X and Y deflectors. The first slit limits the beam diameter within a 3 cm diameter before entering the X deflector. The X deflector sweeps the beam in sinusoidal shape with a frequency of 2 MHz on the Y axis and the Y deflector connects with a fast switch to kick the beam out of the second slit. After that the beam is chopped to a 50 ns pulse width and then enters a bunching system. The buncher has 2 gaps and the distance between the gaps is 46 cm. It is connected to a 4 MHz radio frequency (RF) source with a high voltage of 13 kV. After the pulsed beam passes through the buncher, it is compressed when travelling along the drift space to produce a 2 ns pulse width at the target. The target position is 3.14 m from the centre of the buncher.

2.2.2. Analysis chamber

The target chamber, designed for surface analysis using the ToF RBS technique, is installed at the end of the beamline. The chamber has a 262 cm long backscattering ToF tube at an angle of 150° relative to the incident beam axis. At the end of the ToF tube, a micro channel plate (MCP) detector (Model F4655-10, Hamamastu

Company [13]) is installed. The MCP detector has an effective diameter of 14.5 mm with a channel diameter of 12 μm, and can be operated in vacuum with a pressure of 1×10^{-5} Pa or lower.

2.2.3. *Data acquisition system*

The ToF spectrometer measures the time from backscattered ions with various energies travelling over a fixed distance. The spectrometer consists of a MCP and a capacitive pick off. When a bunch of ions passes through the capacitive pick off in the target chamber, a current signal is induced. This signal is used for starting a timing clock, which is represented by a time to amplitude converter (TAC). The clock is stopped by a signal reaching the MCP at the end of the ToF tube. Data acquisition is performed by a multiparameter analyser, MPA 3 [14]. The signals are analysed by an analogue digital converter (ADC) and then displayed on the computer through the MPA–base interface. The ToF RBS spectrums are analysed with the SIMNRA code [7].

3.   APPLICATIONS

The IBA centre at Chiang Mai University has developed useful ion beam analysis techniques, supported by both commercial and self-developed software, for various applications in the fields of materials science, environment, biology, agriculture, gemmology, archaeology and criminology. Here, we briefly describe some examples. The traditional RBS technique was used for the investigation of the thickness and composition of F doped SnO_2 thin films [15] and amorphous ITO (indium-tin oxide) films [16]. Special RBS analysis was applied to determine the concentration distributions of implanted carbon ions in silicon wafers with assistance of self-developed programs [17], as shown in Fig. 5. The program was based on analysing the deficient part of the RBS spectrum due to the presence of the lighter element to extract the true elemental concentration depth distribution that was deconvoluted with the depth resolution. RBS/channelling was employed to analyse the crystalline quality of β-SiC formed by ion beam synthesis [18]. EBS, a particularly powerful method of analysing lighter elements in a heavier matrix owing to a large resonance cross-section of the light element, was applied to analyse the compositions of Pt-C nanofilms on Si deposited by the dual cathodic vacuum arc deposition (CVAD) technique. Both Pt and C were simultaneously deposited from two cathodic arc sources onto a Si substrate with various ratios of Pt/C to 100 nm. EBS analysed the carbon clearly, as shown in Fig. 6. The PIXE technique was developed for aerosol measurement to monitor environmental pollution and trace element analysis of biological, gemmological, archaeological and criminological samples. Figure 7 shows examples of the PIXE analyses which provided key information on the samples.

For example, the analysis of the PIXE spectrums from the seeds of our newly developed ion beam induced rice mutants [19] revealed increases in useful minerals for health in the mutated rice grains, and the spectrums from local gemstones showed a difference in the impurity elements between natural sapphire and ruby. IL was used for characterization of the formation of high quality single crystalline ZnO nanobelts from the peak at 389 nm, which was due to the exciton emission (*P* line) [20] (Fig. 8). Low/medium energy ToF RBS analysis was carried out to measure the thickness of thin nanofilms (Fig. 9). It was impossible to measure this thickness by high energy RBS owing to the fact that its depth resolution is insufficient. In a recent development, a microaperture system has been constructed and installed in the analysis chamber of the 1.7 MV accelerator beamline for applications in both MeV microbeam writing and reading. Employing the aperture technique to obtain a microbeam is more economical than purchasing quadrupole focusing lenses and thus more acceptable for developing countries. The aperture system is fully computer controlled to vary the aperture size and the minimum achievable aperture is 1 μm. Behind the aperture, the sample stage is capable of X-Y translation so that microbeam scanning of the sample can be available for writing patterns and scanning surfaces.
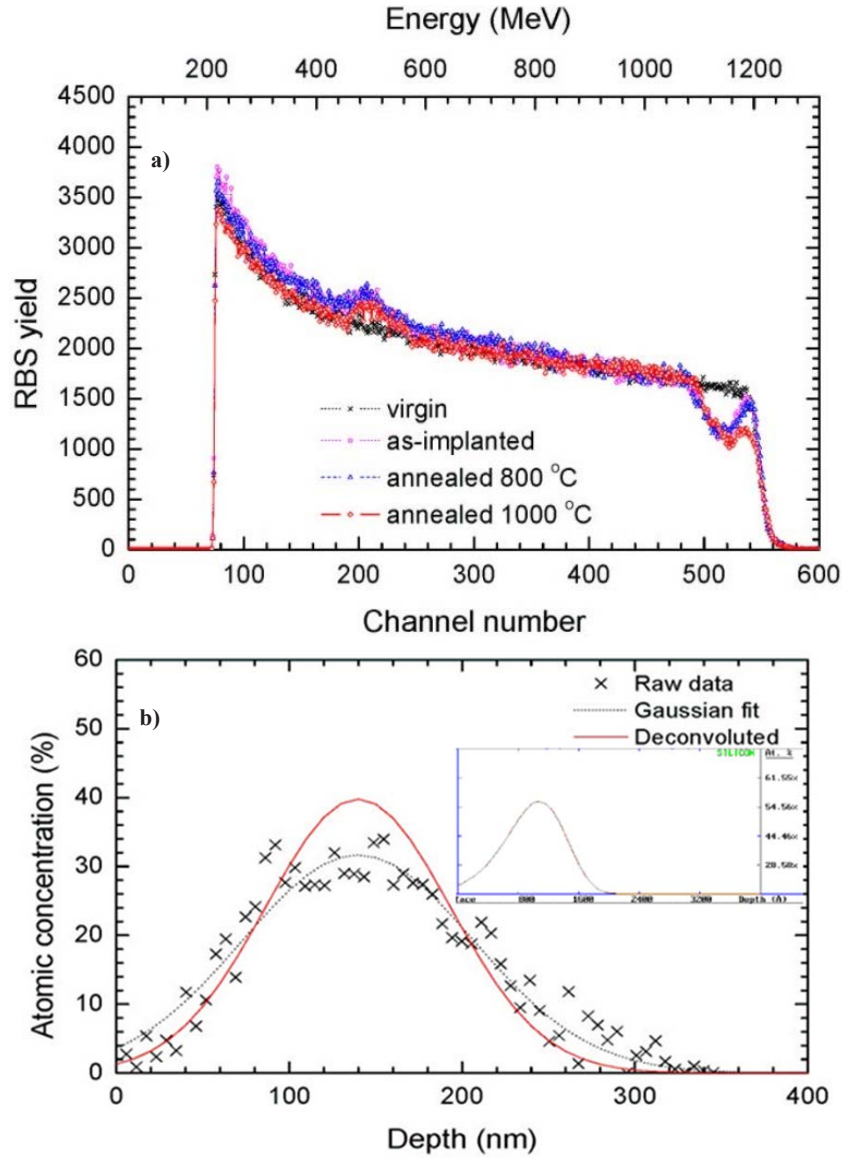
FIG. 5. *Special RBS analysis of the concentration distribution of lighter carbon ions implanted in a heavier silicon wafer for the study of ion beam synthesis of silicon carbide crystal. Top: RBS spectrums from a Si wafer sample implanted by C ions at 40 keV energy to a fluence of 6.5 × 1017 ions/cm2, measured by 2.13 MeV He++ beam. Bottom: Carbon concentration distribution as a function of depth in as implanted Si, extracted from the RBS spectrum shown in the top figure by the self-developed program. The inset is a PROFILE code calculated C ion depth profile in Si.*
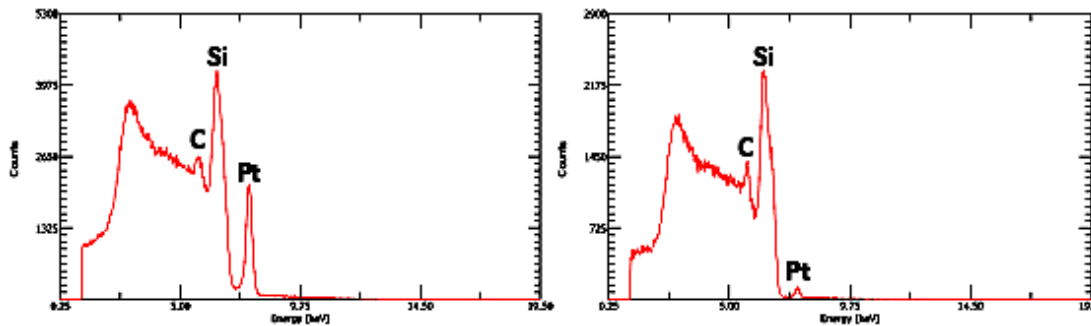
FIG. 6. *2.2 MeV proton beam analysed EBS spectrums of Pt C nanofilms on Si with different ratios of Pt/C, deposited using the dual vacuum cathodic arc technique.*
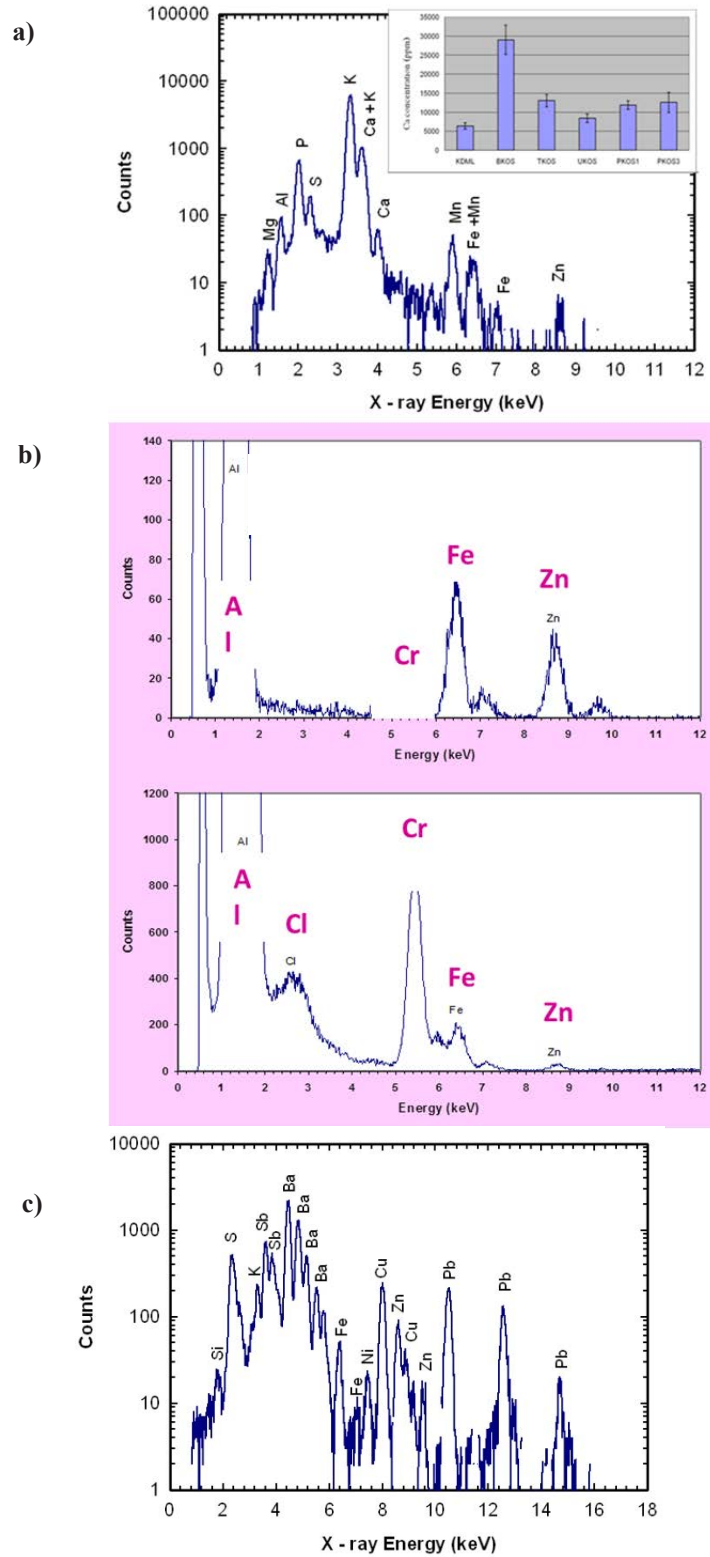
FIG. 7. Examples of PIXE spectrums applied for trace element analysis of (a) local Thai purple rice seeds of ion beam induced mutants; the inset is the Ca content in various rice mutants compared with that of the control (the left one), (b) local natural sapphire (top) and ruby (bottom) and (c) gun-shot residues on the hand.
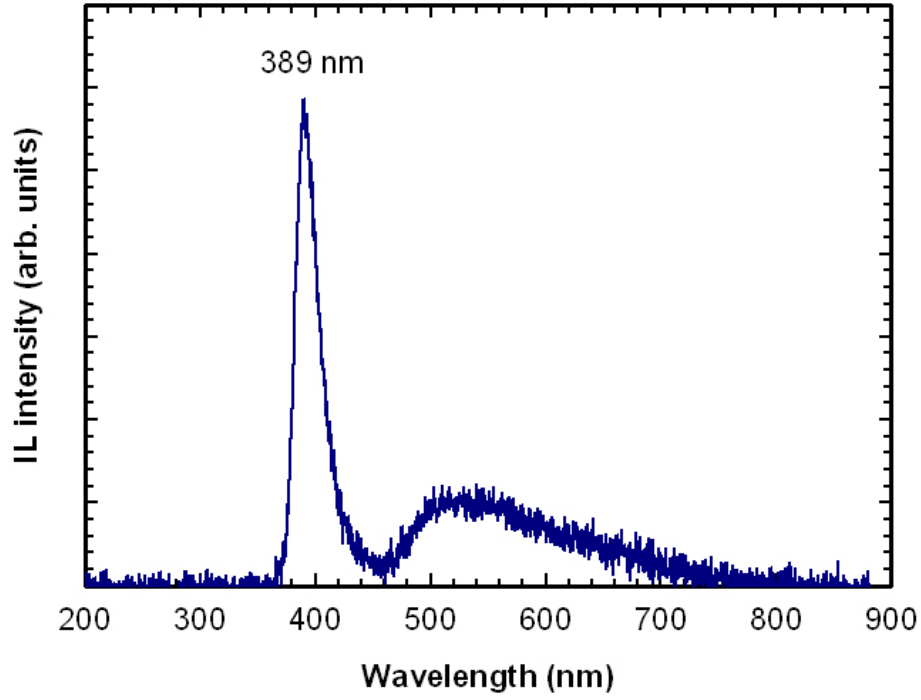
FIG. 8. *IL spectrum to characterize the formation of high quality single crystalline ZnO nanobelts deposited on Cu substrate. The peak at 389 nm is due to the exciton emission and the evidence of high quality of ZnO nanobelts.*

FIG. 9. *An example of low energy ToF RBS analysis of nanofilm of Au on Si. The analysing beam was 140 keV D+. (a) Original ToF RBS spectrum. (b) Converted normal RBS spectrum, from which the film thickness was measured to be 22 nm.*

4.   CONCLUSION

The accelerator based ion beam facilities composed of a high energy tandem accelerator and a medium energy pulsed beam accelerator have been developed and installed at Chiang Mai University to form a comprehensive ion beam analys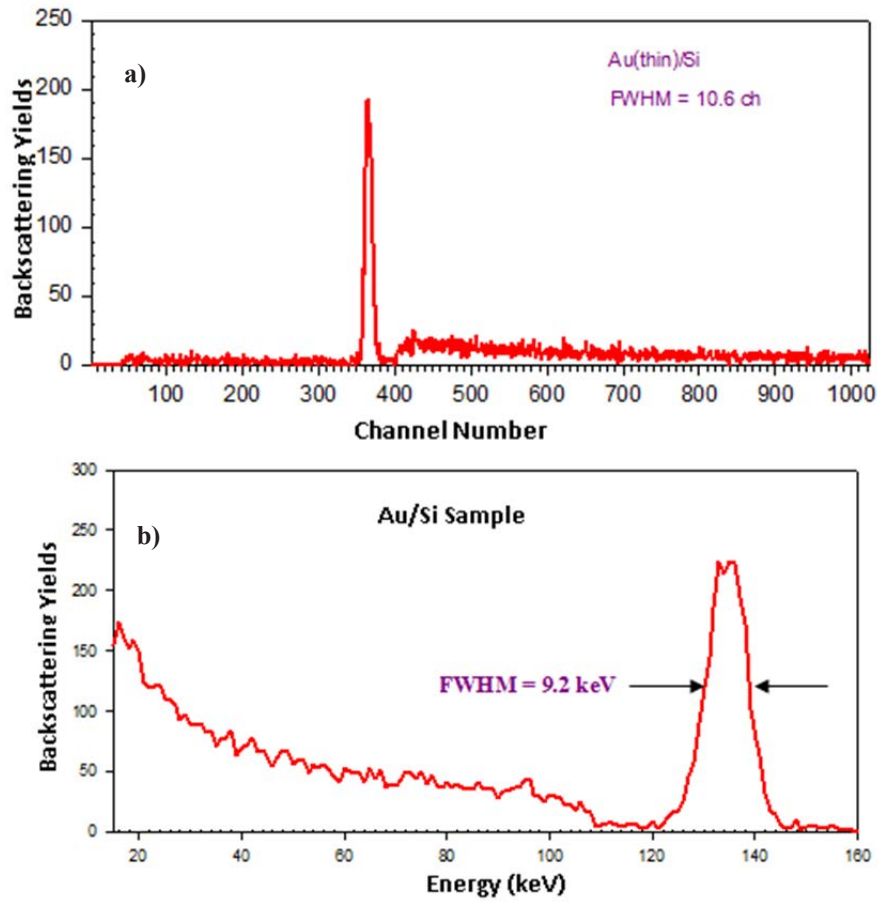is centre unique in the ASEAN region. The IBA centre has developed and applied key ion beam analysis techniques such as RBS, RBS/channelling, EBS, PIXE, IL, low/medium energy ToF RBS and microbeam writing/reading for applications in various fields. Applications of the ion beam analysis techniques have demonstrated the applicability of the IBA centre to a range of topics demonstrating its potential to serve regional and national scientific research.

ACKNOWLEDGEMENTS

REFERENCES

[1] PLASMA AND BEAM PHYSICS RESEARCH FACILITY (formerly Fast Neutron Research Facility) (2010),
http://www.fnrf.science.cmu.ac.th/

[2] HIGH VOLTAGE ENGINEERING, Welcome (2007),
http://www.highvolteng.com/

[3] OCEAN OPTICS, Homepage (2007),
http://www.oceanoptics.com

[4] NATIONAL INSTITUTE OF STANDARDS AND TECHNOLOGY, Physical Measurement Laboratory (2005),
http://www.eeel.nist.gov/oles/oles_forensic_srms.html

[5] HARRISON, J.P., ELDRED, R.A., Data acquisition and reduction for elemental analysis of aerosol samples, Adv. X ray Anal. **17** (1973) 560.

[6] PUTTARAKSA, N., et al., Fabrication of a negative PMMA master mold for soft lithography by MeV ion beam lithography, Nucl. Instr. Meth. B **272** (2012) 149–152.

[7] MAX PLANCK INSTITUT FÜR PLASMAPHYSIK, SIMNRA Home Page (2007),
http://www.rzg.mpg.de/~mam/

[8] UNIVERSITY OF GUELPH, GUPIX and GUPIXWIN (2005),
http://pixe.physics.uoguelph.ca/gupix/main/

[9] OCEAN OPTICS (2006),
http://www.oceanoptics.com/technical/softwaredowloads.sap

[10] CSIKAI, J., et al., Determination of the ratio of D^+ and D_2^+ ions in low energy neutron generators, Nucl. Instru. Meth. A **239** (1985) 641–643.

[11] JUNPHONG, P., et al., Modification of a pulsed 14 MeV fast neutron generator to a medium energy ion accelerator for TOF RBS application, Nucl. Instr. Meth. B **269** 24 (2011) 2895–2900.

[12] ISELIN Ch., computer code MAGNET, CERN, Geneva (1967).

[13] HAMAMATSU, Technical Information MCP Assembly (1994),
http://www.hamamatsu.com/jp/en/product/category/3100/3008/index.html

[14] FAST COMTEC, Homepage (2014),
http://www.fastcomtec.com

[15] KAMWANNA, T., et al., "Thickness and composition of F doped SnO_2 thin films as determined by Rutherford backscattering spectrometry", Proceedings of the Fourth Thailand Materials Science and Technology Conference (Proc. Conf. 2006), Thailand Science Park (2006).

[16] WANG, M.H., et al., Thermal change of amorphous indium tin oxide films sputter-deposited in water vapor atmosphere, Thin Solid Films **516** (2008) 5809–5813.

[17] INTARASIRI, S., et al., RBS and ERDA determinations of depth distributions of high dose carbon ions implanted in silicon for silicon–carbide synthesis study, Nucl. Instr. Meth. B **249** (2006) 859.

[18] INTARASIRI, S., et al., Characterization of the crystalline quality of b-SiC formed by ion beam synthesis, Nucl. Instr. Meth. B **249** (2006) 851.

[19] PHANCHAISRI, B., et al., Low-energy ion-beam-induced mutation in Thai jasmine rice, Surf. Coat. Technol. **201** (2007) 8024–8028.

[20] CHOOPUN, S., et al., Single crystalline ZnO nanobelts by RF sputtering, J. Crys. Growth **282** (2005) 365.

IN SITU CHARACTERIZATION OF NUCLEAR ENERGY MATERIALS BY SYNCHROTRON RADIATION AND ELECTRON MICROSCOPY

MEIMEI LI
Argonne National Laboratory,
Argonne, Illinois,
United States of America
Email: mli@anl.gov

Abstract

This paper presents the applications of in situ characterization techniques, including transmission electron microscopy (TEM) with in situ ion irradiation and high energy X ray diffraction with simultaneous thermal-mechanical loading, in the study of structural materials in advanced nuclear reactors. A good example cases is given here: a novel experiment of TEM with in situ ion irradiation of Mo thin films by 1 MeV Kr ion irradiation that was designed explicitly to improve and validate a computer model. A rate theory based cluster dynamic model was developed to model the ion irradiation induced damage in the thin film with temporal and spatial dependence of defect distribution. Experimental data were compared in detail with modelling results under exactly matched irradiation conditions. The interplay between experiments and modelling allowed an improved understanding of the physical process during irradiation and the development of an accurate physical model. Another area discussed is that of high energy X ray diffraction measurements of bulk materials under thermal/thermal-mechanical loading. This type of in situ characterization provides information on phase transformation and stability and the effect of microstructural changes on mechanical properties, essential to the development of predictive models of materials' long term performance in nuclear reactor environments. Currently, an in situ radioactive materials probe is being developed for measuring irradiated materials under temperature and loading conditions.

1.   INTRODUCTION

Advanced nuclear energy systems are envisioned to operate at high temperatures, with high burnup and subject to harsh neutron irradiation and corrosive environments. Advanced materials and nuclear fuels with significantly improved performance, safety and reliability are needed for the increasingly demanding operating conditions. The fundamental challenge in developing new materials with improved irradiation, temperature and corrosion resistance is to understand and control chemical and physical phenomenons in complex systems over multiple time and length scales. The sustainability of current light water reactors also largely relies on the development of the scientific basis for understanding and predicting the performance of nuclear fuel and structural materials and their long term environmental degradation behaviour. These scientific and technical challenges require a coordinated approach with all available computational and experimental tools.

Because of the very nature of radiation damage, research on nuclear energy materials must deal with the behaviour of matter far from equilibrium. Research relies heavily on computer modelling and simulations to study materials dynamic and transient behaviour with length and timescales spanning from atomistic to continuum and from sub-picoseconds to years. The importance of well controlled, in situ experiments explicitly conducted for model validation is more and more appreciated in the computational science field. With the exponential growth of computing power and sophistication of computational models, validation of computer model predictions may be the greatest challenge.

Advanced characterization and in situ experimental capabilities make it possible for direct comparisons between simulations and experiments. Transmission electron microscopy with in situ heavy ion irradiation is a valuable tool for understanding the physical processes of irradiation damage in nuclear energy materials. Well controlled irradiation experiments can be conducted to examine the effect of a number of variables including ion type and energy, irradiation dose, dose rate, temperature, specimen orientation, etc. Irradiation dose rates can be varied over several orders of magnitude. High dose rates allow high doses (e.g. 100 displacement per atom (dpa)) achieved in hours. Another important advantage of this in situ irradiation tool is real time observation of defect formation, motion and evolution in a single specimen area. Advances in video and camera recording capabilities and computer data processing make such dynamic experiments more viable and valuable to reveal damage kinetics. Transmission electron microscopy (TEM) with in situ ion irradiation technique has increasingly been used to

study radiation damage production, accumulation and evolution, radiation induced phase transformation, damage recovery and plastic flow, etc. A summary of TEM with in situ ion irradiation facilities and experiments can be found in the literature (examples in Refs [1–3]).

X rays are an invaluable tool for the non-destructive examination of nuclear fuels and materials. The use of synchrotron X ray radiation techniques has provided valuable insight into radiation damage in nuclear materials [4, 5]. The third generation synchrotron radiation sources provide high energy, high brilliance X ray beams, allowing deep penetration, high spatial and temporal resolution and in situ studies of bulk properties, which can provide critical information for the development of predictive models and innovative nuclear energy materials. Despite the great potential of synchrotron radiation techniques, the application of synchrotron radiation in the investigation of activated materials is still in its infancy.

This paper discusses the applications of state of the art in situ characterization techniques, including TEM with in situ ion irradiation and high energy X ray scattering under in situ thermal-mechanical loading in the investigation of nuclear energy materials and their role in enabling the integration of experiments and modelling.

2. TRANSMISSION ELECTRON MICROSCOPY WITH IN SITU ION IRRADIATION

Radiation damage involves atomic scale unit events within picoseconds to collective long term microstructural evolution at the mesoscale. A fundamental understanding of radiation damage requires the closed coupling of spatial temporal scales. This allows studies of displacement cascades within nanometres and picoseconds, to longer and larger scales of cascade evolution and point defect migration that leads to the formation of a large population of extended defects (dislocation loops, voids, bubbles and extended dislocation network, precipitates, etc.). These extended defects can drastically change the physical and mechanical properties of a material [6–8]. Modelling and simulation of this multiscale damage process is at the forefront of computational materials science under extreme conditions.

To be truly predictive, computer models of complex scientific and technological phenomenons in nuclear environments must be developed in close association with well controlled experiments. Current theoretical and computer models are not robust enough to provide a quantitative understanding and predictive capability, largely owing to a lack of high quality experimental validation. Although a significant experimental database from various neutron irradiation programmes exists, previous experiments were designed primarily for testing and certifying the performance of specific materials in nuclear reactors. Comparisons between modelling and reactor based experiments are difficult due to insufficient depth and low fidelity of available data and overly complex irradiation conditions. Ion beams provide an indispensable tool to probe radiation damage in situ over moderate time and length scales in a material. Despite a number of advantages of using ion beams and extensive studies of ion irradiations, there is a long standing question in the radiation damage community: How is the radiation damage produced by ions in accelerators related to that produced by neutrons in nuclear reactors? Large differences exist between ion irradiation and neutron irradiation in the recoil spectrum, damage production, dose rate and, in particular, surface effects of in situ ion irradiations of thin films. With increasing interest in using ion irradiation in the study of new materials and new phenomenons, the use of ion irradiation to assess in reactor performance is an important but challenging topic to address.

Our recent collaborative efforts of TEM with in situ ion irradiation experiments in combination with the rate theory based cluster dynamics modelling successfully highlighted the importance of a closely coordinated integration of in situ experimentation and computer modelling in a radiation damage study [9]. In situ ion irradiation experiments of molybdenum were designed explicitly for the development of a predictive model of defect kinetics in thin films. The experiments were performed at Argonne's IVEM Tandem Facility using 1 MeV Kr ions. This study took advantage of thin film specimens and used the thickness of a thin film as an important variable in describing the spatial dependence of defect distribution. For the first time, three dimensional diffraction contrast electron microscopy was conducted to image and measure the depth distribution of nanometre sized dislocation loops (Fig. 1(a)). The results showed that 3-D electron tomography can provide direct, quantitative measurements of the spatial dependence of defect concentrations and enable direct comparison with simulations of defect structures at different foil depths (Fig. 1(b)). This additional spatial dimension significantly improved the rate theory based cluster dynamic model of defect reaction kinetics in ion irradiated thin films. The success of modelling the free
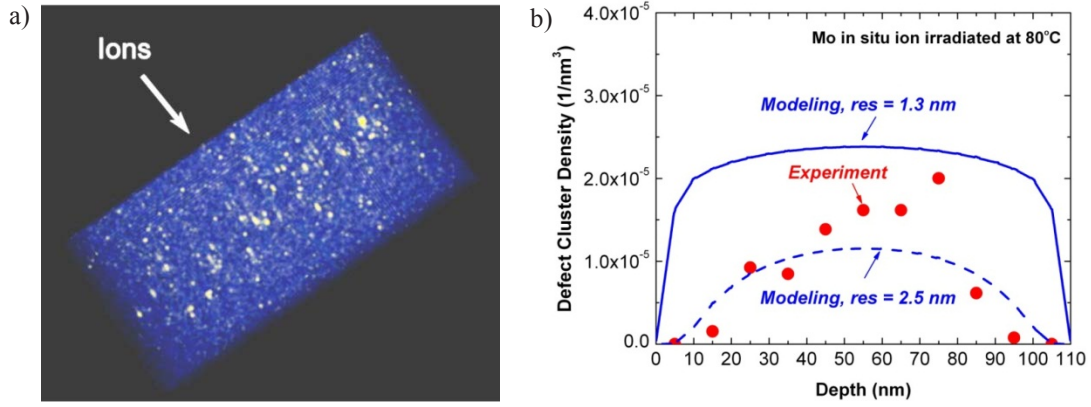
FIG. 1. (a) Cross-section view of reconstructed 3-D volume showing dislocation loops in a Mo thin film irradiated to 5×10^{12} ions/cm^2 (~0.015 dpa) at an ion flux of 1.6×10^{11} ions·cm^2·s (~5×10^{-4} dpa/s) with 1 MeV Kr ions at 80°C and (b) comparison between in situ ion irradiation experiment and the model calculations of spatial distribution through the foil thickness of visible defect clusters.

surface interfaces of a thin film allowed the extension of model predictions of neutron damage in bulk and is validated by the set of neutron irradiation data of the identical material.

3. IN SITU STUDIES WITH SYNCHROTRON RADIATION

The high energy, high brilliance and short pulse X rays together with state of the art X ray instrumentation at the Advanced Photon Source (APS) offer great opportunities for time resolved studies of dynamics over a range of time and length scales. Synchrotron X ray diffraction (XRD) measurements under in situ thermal-mechanical loading provide a state of the art capability to examine concurrent microstructural evolution and associated deformation and failure mechanisms in bulk materials, ideal for developing a microstructure based deformation and fracture understanding and predictive model. To explore the use of this advanced in situ synchrotron radiation technique, we have performed high energy XRD studies of ferritic-martensitic steels under in situ thermal or thermal-mechanical loading at beamline 1-ID-C and 11-ID-C at the APS. Time resolved XRD measurements during thermal annealing of mod.9Cr-1Mo and NF616 steels showed the precise temperatures of ferrite to austenite transformation and the reverse transformation, and growth behaviour of $M_{23}C_6$ carbide and MX carbonitride phases as functions of ageing, temperature and time. This dynamic microstructural information of phase transformation and stability was used to support thermodynamic calculations of phase equilibria and kinetic simulations of diffusion controlled precipitation and coarsening. As shown in Fig. 2, a sharp drop in intensity of the body centred cubic crystals (bcc) (200) and a sharp increase in intensity of the face centred cubic (fcc) (200) and (220) occurred at ≈805°C, indicating the start of austenite transformation, i.e. Ac_1 ≈ 805°C [10]. The Ac_1 predicted by Thermo-Calc is 848°C, higher than the measured value. During isothermal hold at ≈ 830°C, the bcc (200) intensity remained relatively constant, while the fcc (200) and (220) intensity slightly decreased with exposure time. The NbC (111) intensity increased significantly after ≈1 h annealing at ≈830°C, implying precipitation. On cooling from 830°C to room temperature, a multistage behaviour was observed for the bcc phase. A drastic decrease in intensity was observed for the fcc (200) and (220) reflections in the temperature range of 440–250°C, corresponding to the martensite transformation. The martensite transformation was completed at room temperature.

In situ high energy synchrotron XRD measurements during tensile loading provide information for linking the microstructural changes with associated deformation and failure mechanisms. Figure 3 shows the response of the lattice strain in the axial loading direction to the applied stress, up to the maximum load at 20°C for the diffraction peaks (110), (200), (211) and (310) of the bcc matrix of the mod.9Cr-1Mo steel [11]. Lattice strain was determined by a relative change of lattice spacing in a microscopic volume and it was used as an internal strain gauge to probe the mechanical response of various phases and crystallographic orientation dependent stress–strain behaviour during loading and unloading. The combined microstructural and thermomechanical information allows models to be established for accurate predictions of materials performance during long term service in nuclear environments.
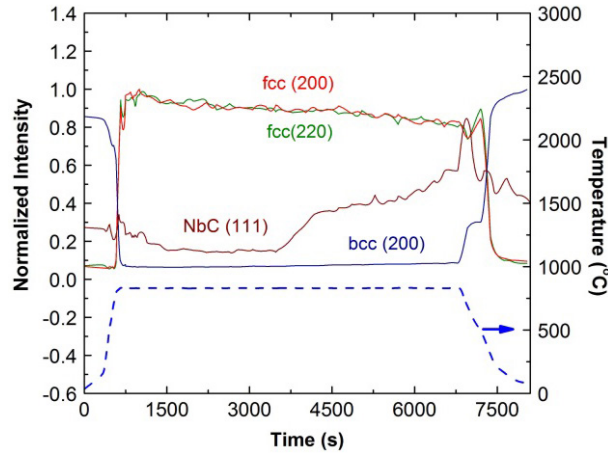
FIG. 2. *Normalized diffraction intensity as functions of exposure time and temperature for the bcc (200), fcc (200) and (220) and NbC (111) in NF616 steel.*
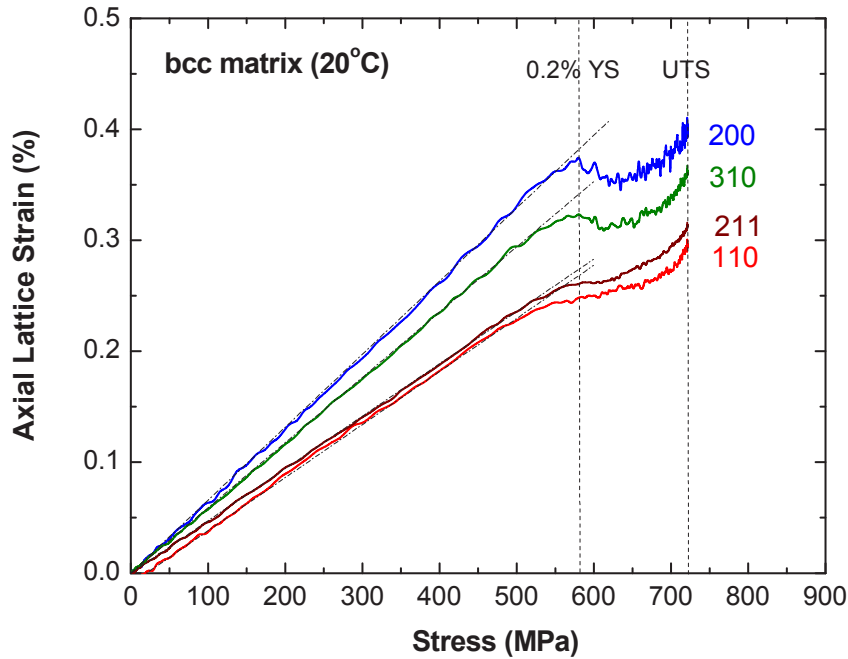
FIG. 3. *The evolution of lattice strain in the axial direction as a function of the applied stress for mod.9Cr-1Mo steel in situ tensile tested at 20°C.*

To extend this valuable in situ experimental capability to irradiated materials, a capability which is currently unavailable at any synchrotron radiation source, an in situ high energy X ray probe is being developed for the characterization of activated materials at the APS. This probe will allow simultaneous wide angle X ray scattering (WAXS) and small angle X ray scattering (SAXS) and full-field imaging to observe the evolution of lattice strain, texture and load sharing between phases and characterization of nanoscale voids, bubbles and second phase particles and to allow the detection of microsize cracks and porosity.

4. SUMMARY

This paper presents the applications of transmission electron microscopy with in situ ion irradiation and high energy X ray diffraction with simultaneous thermal-mechanical loading in the study of nuclear energy materials.

Examples are given including a novel experiment of TEM with in situ ion irradiation of Mo thin films designed to improve and validate a rate theory based cluster dynamic model. High energy X ray diffraction measurements during thermal-mechanical loading of ferritic steels allowed simultaneous characterization of microstructural evolution and corresponding deformation and failure processes, enabling the development of a microstructure property predictive model. Currently, an in situ high energy X ray probe is being developed at Argonne National Laboratory that will allow the characterization of irradiated materials by high energy X rays during thermal-mechanical loading. These in situ capabilities allow an integrated approach of computer modelling with well controlled in situ real time experiments, which in turn allows rapid progress in model development for quantitative predictions of the material response and the science based design and development of innovative materials with superior radiation tolerance and high mechanical performance.

ACKNOWLEDGEMENTS

REFERENCES

[1]   BIRTCHER, R., KIRK, M.A., In situ transmission electron microscopy investigation of radiation effects, J. Mater. Res. **20** (2005) 1654.

[2]   KIRK, M.A., et al., In situ transmission electron microscopy and ion irradiation of ferritic materials, Microsc. Res. & Tech. **72** (2009) 182–186.

[3]   HINKS, J.A., A review of transmission electron microscopes with in situ ion irradiation, Nucl. Instr. Meth. Phy. Res. B **267** (2009) 3652–3662.

[4]   EHRHART, P., Investigation of radiation damage by X-ray diffraction, J. Nucl. Mater. **216** (1994) 170–198.

[5]   FROIDEVAL, A., et al., Application of synchrotron radiation techniques for model validation of advanced structural materials, Adv. Eng. Mater. **11** (2009) 459–463.

[6]   ODETTE, G.R., WIRTH, B.D., BACON, D.J., GHONIEM, N.M., Multiscale-multiphysics modeling of radiation-damaged materials: embrittlement of pressure-vessel steels, MRS Bulletin **26** (2001) 176–181.

[7]   WIRTH, B.D., et al., Multiscale modeling of radiation damage in Fe-based alloys in the fusion environment, J. Nucl. Mater. **329-333** (2004) 103–111.

[8]   ARSENLIS, A., WIRTH, B.D., RHEE, M., Dislocation density-based constitutive model for the mechanical behaviour of irradiated Cu, Phil. Mag. **84** (2004) 3617–3635.

[9]   LI, M., KIRK, M.A., BALDO, P.M., XU, D., WIRTH, B.D., Study of defect evolution by TEM with in situ ion irradiation and coordinated modeling, Phil. Mag. **92** (2012) 2048–2078.

[10]   LI, M., et al., "In situ synchrotron radiation study and computer modelling of advanced nuclear structural alloys" (Proc. TMS Ann. Mtg, 2010, Seattle, WA, USA) (2010).

[11]   LI, M., et al., Report on Thermal Aging Effects on Tensile Properties of Ferritic-Martensitic Steels, Report No. ANL-ARC-188, Argonne National Laboratory, Argonne, IL (2011).

THE ADVANCED PHOTON SOURCE: USING SYNCHROTRON RADIATION TO STUDY ACTINIDE CONTAINING SAMPLES RELEVANT TO NUCLEAR ENERGY SYSTEMS

L. SODERHOLM, S. SKANTHAKUMAR
Argonne National Laboratory,
Argonne, Illinois,
United States of America
Email: ls@anl.gov

Abstract

The realization of advanced nuclear reactors as a national source of reliable energy awaits materials research on fuels, reactor components under extreme environments and options for waste treatment and storage. The third generation synchrotrons such as the Advanced Photon Source (APS) provide a high flux of coherent, variable energy X rays that can be used to probe in situ a wide range of chemical, physical and materials problems of relevance to nuclear energy production. Synchrotron radiation from such a source is particularly suited to the study of radioactive samples because of its tunability, penetration and intensity. Together, these features provide the opportunity to work with small, encapsulated samples, a necessary requirement because of the inherently hazardous heavy metal, highly radioactive materials. Complicating the practical advantages of synchrotron radiation to the study of nuclear energy systems is the need for risk mitigation when bringing such materials into a user facility. The APS has used a risk based approach to the problem. As part of Argonne National Laboratory, which has a long history in nuclear energy, the APS has taken advantage of the broader Laboratory infrastructure to reach out and accommodate experiments on radioactive samples and the broad nuclear energy community.

1. INTRODUCTION

Synchrotron sources provide high intensity X rays, tuneable over a wide energy range, making them available in specialized experiments capable of providing a wealth of new information about materials and their properties. The opportunities afforded by these sources are being seized upon by a broad scientific community, including physicists, materials scientist, chemists, geologists and biologists to address issues currently at the forefront of research and engineering. Among the communities that have been slower to take advantage of the wide range of experiments available are those involved with studying radioactive materials in programmes associated with nuclear energy systems. Possible reasons for the apparent reticence include the added difficulty associated with conducting experiments on radioactive samples at a user facility, where administrative assurances of experimenter safety and added technical constraints designed to minimize risk of radioactive contamination can appear overwhelming.

Once these hurdles can be overcome, there is a wealth of opportunity that awaits the experimenter. Synchrotron radiation is particularly well suited for studying radioactive samples, particularly the actinides. Because X rays scatter from electrons, their interactions with matter increase monotonically with increasing atomic number (Z). Their complementarity to neutrons, which scatter off nuclei and therefore have a complex dependence on the scattering element and its isotope, can be used to advantage. The intense, well focused synchrotron X ray beam allows experiments to be carried out on small amounts of material, usually milligram quantities or less. This feature can be particularly important for experiments involving the transplutonium elements, where often only milligram or smaller amounts are available. Highly radioactive substances, such as spent fuel, for which the radiation field from the material itself can compete with the source for flux on detector, also require small sizes. Finally, the penetrating power of higher energy X rays (>5 keV) allows flexibility in containment design, thus providing access to a wide range of experimental capabilities by enabling sample encapsulation during their entire residence at the synchrotron facility.

Located on the campus of Argonne National Laboratory (ANL), the Advanced Photon Source (APS) has built on the site's longstanding history for work with nuclear energy systems. Upon construction, the infrastructure was already in place for radioactive work, including the technical and scientific staff with extensive experience in handling such materials and the regulatory system to transport, receive and work with them. Since the delivery of first light in March 1995, more than 1000 experiments have been conducted on radiological samples at 21 APS Sectors. Included amongst these experiments are those involving the actinides Th, U, [237]Np, [239]Pu, [242]Pu, [243]Am, [248]Cm, [249]Bk and [253]Es.

Because of ANL's history and expertise, the APS chose to adopt a philosophy that allows experiments with radioactive materials at any of the beamlines in their user programme. They impose two restrictions to this approach for dealing with radioactive samples: (1) the APS follows DOE guidelines on the total amount of radioactivity permitted in the facility at any given time. These guidelines can restrict the quantity of material permitted for an experiment but has little impact in most cases, and (2) the samples must arrive in pre-approved containment and must remain so encapsulated for their residence time at the facility. The samples must be shipped to the APS just prior to the experiment and then immediately return upon completion of the beamtime. The facility can neither work with unencapsulated samples nor store them between runs. This restriction can be problematic, particularly if a difficulty arises during the course of an experiment that could be alleviated simply by gaining access to the sample, but is ameliorated by the Actinide Facility.

1.1. Actinide Facility

The Actinide Facility is not a beamline but instead an administrative and technical construct to aid APS users in performing experiments with radioactive materials. Together with the APS Radiation Safety Committee, the Actinide Facility provides to users help and guidance with transportation, safety protocols and encapsulation, and sample repackaging if necessary. With radiological hot laboratories located on the same site as the APS, the Actinide Facility affords users the opportunity to perform simple chemistry procedures, sample loading and repackaging or radioactive materials, including α emitters. The hot laboratories are purpose built for working with macroscopic amounts of radioactivity and are thus equipped with HEPA filtered glove boxes and hoods as well as ancillary monitors for user protection. Fully trained research staff and health physics technicians are available to assist the experimenter. Although used primarily for packaging, staging or repackaging hot samples, these laboratories are also available, with mutual prior consent from Actinide Facility personnel, for more demanding procedures such as sample preparation and/or characterization. Special purpose cells have been designed, tested and deemed suitable by the APS for running experiments with radioactive samples. These cells, or their design specifications, are made available to the APS user. Of particular note are cells designed for in situ XAFS spectroelectrochemistry and surface scattering studies [1, 2].

2.   STANDARD SYNCHROTRON EXPERIMENTS

As noted above, the APS makes available, through their general user programme, most of their beamlines for use with radioactive samples. These experimental capabilities are broadly divided into three main types: (1) spectroscopy, (2) scattering and (3) imaging. Untapped opportunities to study nuclear energy problems exist in all three areas.

2.1. Spectroscopy

Within the nuclear energy community studying actinide samples, spectroscopy has been a widely used technique [3]. Typically, it can be used to simultaneously measure the chemical state of atoms in a solid, liquid or gas, and the local atomic structure around the absorbing atom. The workhorse of these techniques, X ray absorption spectroscopy (XAS), sometime referred to as X ray absorption fine structure (XAFS) [4], can be used to reveal the average speciation of a targeted (absorbing) element, even at low concentrations (ppm).

As depicted in Fig. 1, XAS is often subdivided into two techniques based on data analysis methodologies: (1) X ray absorption near edge structure (XANES), which is used primarily for oxidation state characterization, and (2) extended X ray absorption fine structure (EXAFS), which upon Fourier transform provides metrics on the coordination environment of a targeted (absorbing) atom in a solid, liquid or gaseous matrix. XAS is used either as a stand-alone technique [5, 6], as demonstrated in Fig. 2 [6, 7], or in combination with other scattering or imaging techniques, as demonstrated in Fig. 3, on complex materials, including spent fuels, radiation damaged claddings and reactor components. The influence of temperature, stress and local compositions on the variation of local chemical environments can be measured in situ. However, technical issues such as core hole lifetimes and data length in k space place a practical limit to the accessible energy range of about 2–40 keV. Because the technique relies on atomic X ray absorption, this range limits the technique to elements heavier than Si.
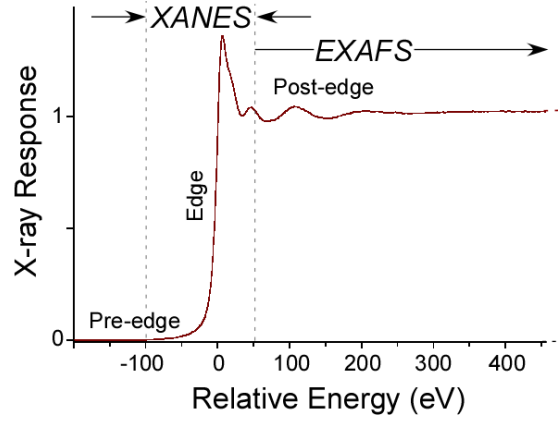
FIG. 1. *A background subtracted, normalized, XAFS spectrum indicating the XANES region, which extends from about 100 eV to about 50 eV above the absorption edge, with the higher energy component considered the EXAFS region. This distinction is somewhat arbitrary and reflects the different approach to data analysis. XANES data are considered electronic in origin, the energy of the edge jump used as an indicator of oxidation state. EXAFS can be Fourier transformed to provide metrical information about the absorber environment, including the number and identity of coordinating ligands [4].*
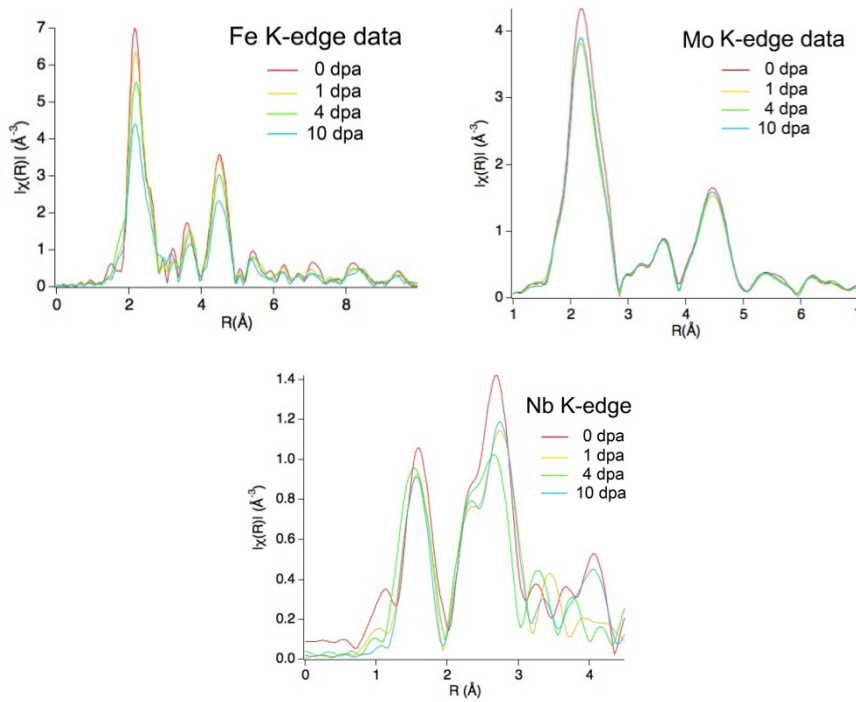
FIG. 2. *Synchrotron extended X ray absorption fine structure (EXAFS) measurements were performed to study the dose dependence and alloying effects on irradiation induced changes in local atomic environments in a mod.9Cr 1Mo F M steel irradiated up to 10 dpa at 40–70°C. The EXAFS data for Fe, Mo and Nb K edges were recorded and the local structure close to the X ray absorbing atom was determined. Irradiation caused significant reductions in peak amplitude in the Fe, Mo and Nb K edge Fourier transformed EXAFS. The fits to the EXAFS data showed a systematic decrease in coordination number of neighbouring atoms with increasing irradiation doses. The dose dependence of the coordination loss was dependent on the specific element [6] and covers the range of 16.300 keV for Th to 19.4 keV for Bk and 20.410 keV for Es [7].*
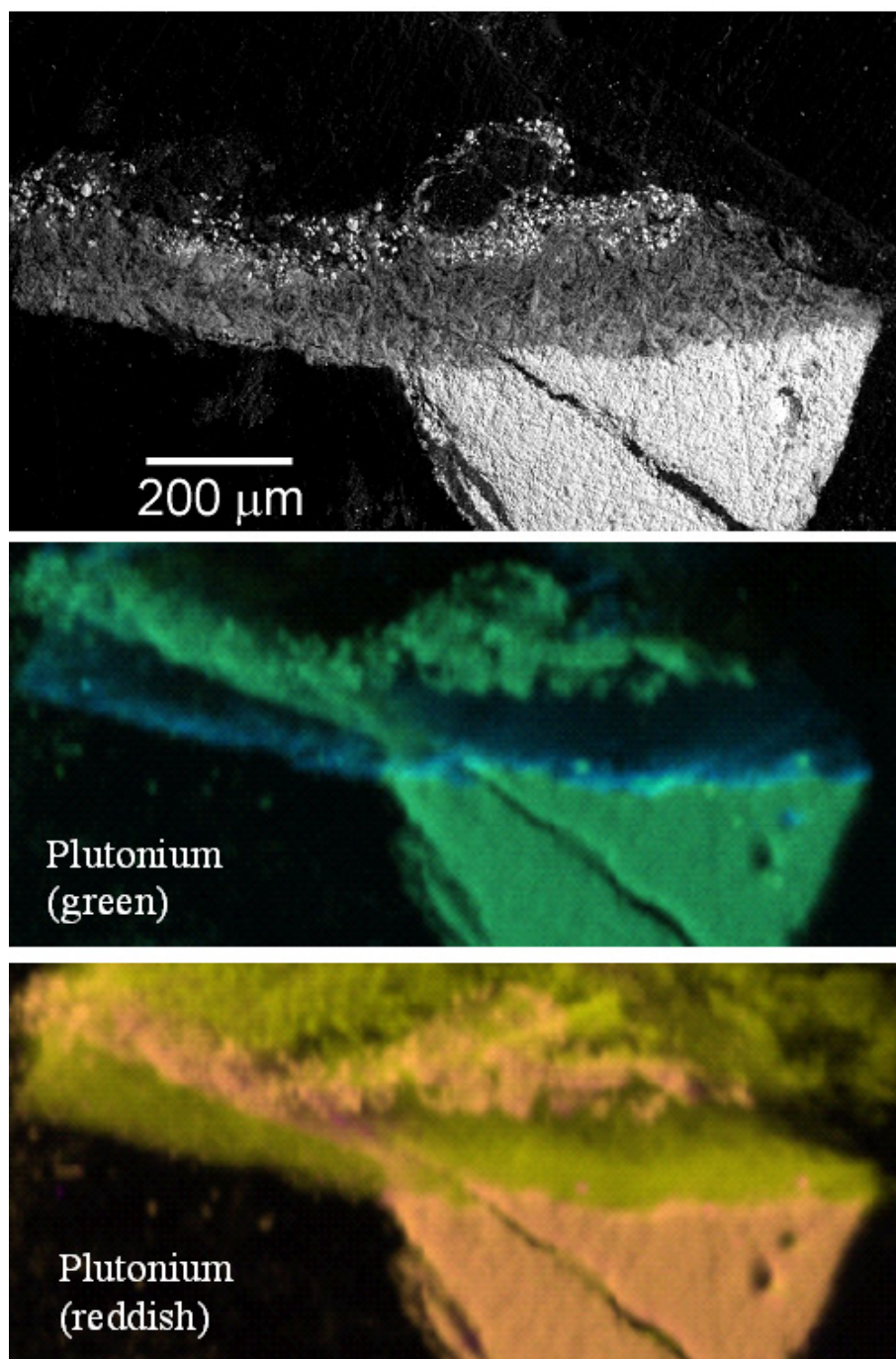
FIG. 3. A specimen of irradiated oxide nuclear fuel subjected to aqueous corrosion tests for 10 years were epoxy embedded and cross-sectioned in a hot cell for this investigation. A small core (plug) was extracted and re-embedded in epoxy to form a specimen that was small enough to handle safely. A backscatter SEM micrograph (top) reveals intact fuel (light coloured) with a 100 micrometre corrosion layer of uranyl silicate (grey). X ray fluorescence mapping and edge spectroscopy were employed to investigate the local chemical environment of key elemental components. X ray imaging of plutonium, strontium and uranium (centre and bottom) show their relative distribution near the oxidation front [9].

XAFS takes full advantage of the synchrotron X ray energy tunability. Most of the published work on actinides utilizes the L_3 absorption edges [3].

In addition to absorption spectroscopy, X ray fluorescence (XRF) spectroscopy can also be applied as an analytical technique to ascertain the elements present in the sample. By measuring the intensities of their characteristic emission lines following X ray absorption, it is possible to determine the elements present and their

relative abundances. When combined with a fine beam that is rastered across the sample, it is possible to acquire a map that provides information about the relative location of elements within the sample [8]. Figure 3 depicts the results of such an experiment on a spent fuel sample [9].

2.2. Scattering

Less utilized than absorption techniques, scattering experiments are rapidly becoming a workhorse of the nuclear energy community. A broad range of techniques has been developed for use at a synchrotron, most of which rely on beam intensity and energy tenability not available for in house sources. For ordered, crystalline systems X ray diffraction at a synchrotron has limited advantages over in house, tube based sources. Beam stability and monochromicity both can be adversely impacted owing to the manner in which X ray are generated at a synchrotron. Conversely, the ability to tune the X ray energy also has specific advantages. The low beam divergence permits a higher resolution, a particularly important characteristic when obtaining powder diffraction data from multicomponent, low symmetry samples. By tuning the energy to minimize absorption of all constituent elements, it is possible to significantly reduce the technical problems that can plague the analysis of diffraction data. Alternatively, by comparing data acquired with the energy tuned to just below to those acquired just above an element's absorption edge, it is possible to obtain direct information about that element's contribution to the overall scattering. For the actinides, these experiments would necessarily be done using an L edge.

A commonly employed scattering technique is X ray small angle scattering (SAXS), which relies on inhomogeneities in electron densities to provide contrast. The technique typically utilizes scattering in the Q range of about 0.001 to 2 Å^{-1}, probing structures on length scales of about 1 to 150 nm. It is used to determine average particle, grain and precipitate sizes and their distribution. Of particular interest in the nuclear community is information about bubble and void sizes. The contrast in electron density seen by the X rays occurs between the sample and the void, the latter of which has no electrons within its space. It is also possible to use incident X ray energies just above and below element absorption edges. By using changes in absorption for a specific element, which selectively affects the scattered intensity arising from that element, anomalous small angle X ray scattering (ASAXS) provides information on the elemental composition of the precipitates or grains. Not yet widely used in actinide systems, the application of ASAXS has been recently demonstrated on fuel cladding [10]. The development and extension of this technique to higher energies is expected to provide new opportunities to the nuclear community interested in studied defect aggregation and void formation.

X ray scattering can also be applied to disordered or amorphous solids or liquids, although the results are more limited because symmetry cannot be used to simplify and enhance information retrieval. Nevertheless, there are two general approaches to data treatment that yield information about shorter range atomic correlations. If the sample of interest is predominantly crystalline, an analysis of the diffuse scattering surrounding the Bragg reflections can provide information about structural defects [11]. For samples that are predominantly amorphous, including liquids and solutions, the scattering data, obtained as a powder pattern, can be Fourier transformed (FT) to yield pair distribution functions (PDFs). This approach requires higher energy X rays, generally >40 keV, for optimal PDF resolution, which is dependent on the Q range covered by the experiment [12–14]. The PDF approach to the analysis of high energy scattering data can reveal the presence of significant atomic pair. Also included is the FT of data obtained from a standard uranyl silicate mineral phase soddyite, $(UO_2)2SiO_4(H_2O)_2$ sample for direct comparison with the corresponding pattern obtained from the pH 5.1 precipitate. The pH dependent samples are the same ones used to obtain the XRD patterns obtained on a standard in-house machine equipped with a Cu target (7.9 keV X rays). The broadly oscillating background found for the higher pH samples, combined with the absence of any Bragg peaks, is consistent with the amorphous precipitates generated under these chemical conditions [15].

Correlations can be seen even in the absence of crystallinity, as exemplified in Fig. 3 [15]. Metrics on metal ion speciation can also be obtained solution samples using the PDF approach to gain an understanding of actinide and fission product chemistry relevant to reprocessing [16, 17], particularly when studying complicating issues such as colloid formation [18]. These new results are expected to provide experimental information supportive of theoretical modelling on mechanisms of radiation damage.
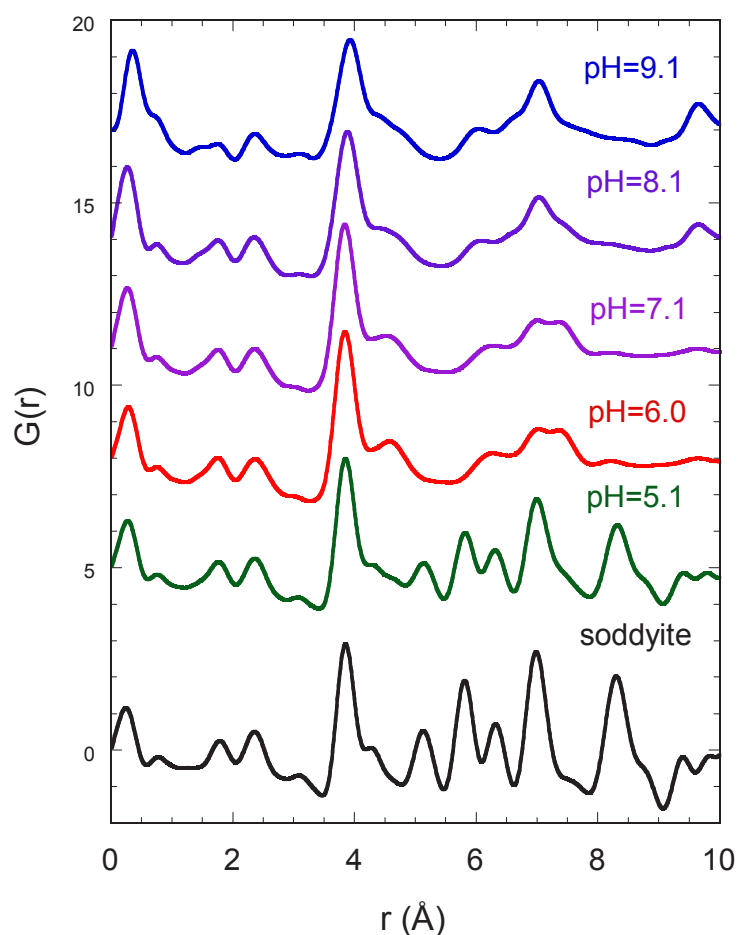
FIG. 4. Example of correlation in case of the absence of crystallinity.

Recently, X ray scattering has become an important tool for studying ion speciation at metal surfaces and interfaces [19–21]. Such experiments find relevance in several nuclear energy related areas, including contaminant geochemistry and reactor component corrosion. A variety of techniques, including X ray reflectivity (XR) and resonant anomalous X ray reflectivity (RAXR), have recently been developed to determine element specific electron density profiles perpendicular to a surface [22]. Most of the work done to date in this area at the APS has centred on radioactive contaminant behaviour in the geosphere. For example, the interaction of Pu^{3+} bearing solutions with a mineral surface has been studied using a combination of ex situ approaches, including alpha counting to determine the Pu^{3+} adsorption isotherm [20], and X ray reflectivity (XR) and resonant anomalous X ray reflectivity (RAXR) to probe the interfacial structure and Pu-specific distribution. To facilitate these studies a sample cell has been designed that permits full access to the sample surface while performing in situ flow experiments with radioactive samples [2]. Surface scattering techniques have as yet untapped potential for use in problems of relevance to the nuclear energy community.

2.3. Imaging

To date underutilized, imaging also holds the potential to provide a wealth of information otherwise not available, although it has not been employed to study nuclear energy related problems at the APS. In general, two different approaches can be taken to acquire sample images. In full field methods, an extended field of view is illuminated to image the entire area, typically in one exposure. Images are often recorded with scintillator crystals and optical cameras. Spatial resolutions down to below 1 µm can be achieved with direct imaging.

In scanning approaches, hard X rays are focused into a small spot through which the specimen is scanned and the image is built up sequentially. The achievable resolution is 100–200 nm in the hard X ray range. In addition to use of the transmitted X ray signal (absorption and phase contrast), use can be made of other contrast mechanisms
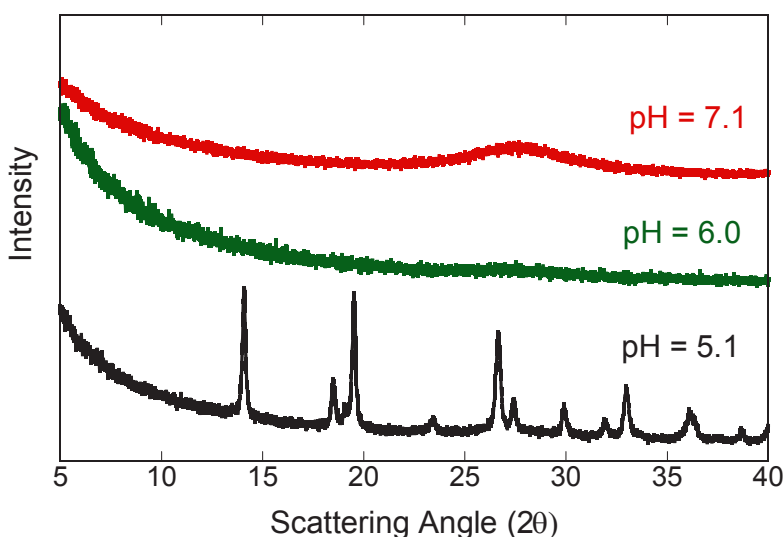
FIG. 5. *Fourier transformed (FT) X ray scattering data obtained using 90 keV synchrotron X rays on precipitates from hydrothermally treated uranyl silicate samples as a function of solution pH.*

such as X ray fluorescence for element detection, identification and location, [9] as well as X ray diffraction for reciprocal space information.

The APS X ray beam is significantly more coherent than the beams in previous generation synchrotron sources, which enables the study of surface and interface dynamics instead of the traditional time averaged states. Also, the tunablility over a wide range of X ray energy enables the study of the chemical states of most atomic elements on the surface and buried interfaces. In addition, the high brilliance enables extremely tight focusing of X ray beams from the micrometre to the nanometre scale. The micro- and nanofocused X ray beams can be used for non-destructive microscopic imaging of the structural and chemical states of the surfaces, as has been done for non-irradiated materials [23]. It would be of great interest to perform similar work on irradiated materials to verify that the oxide growth mechanisms observed in reactor irradiated samples are similar to those observed in autoclave tests. Such experiments could likely be performed in the context of existing sample containment systems.

3.   FUTURE NEEDS AND OPPORTUNITIES

Out of a recent APS sponsored workshop on the role of synchrotrons in solving scientific challenges in nuclear energy systems [24] came a clear consensus that synchrotron based studies provide an untapped potential for providing insights critical to solving problems in this area. As demonstrated by the workshop report, the community is very diverse, ranging from nuclear engineers to physicists, separations chemists and environmental geochemists. Specific concerns raised by the workshop participants for consideration by the synchrotron staff include sample size restrictions, shielding technicalities and sample handling capabilities. Critical developments in synchrotron measurements needed to facilitate the nuclear community's needs include the abilities to detect lower concentrations, to probe even smaller sample sizes independent of radioactivity level and to accurately measure reaction rates in real time. New sample cells and containment vessels must be engineered that have appropriate geometries for data acquisition. A full realization of synchrotron radiation's potential will require developments in sample shielding (for high dose samples) and its handling (weight problems). Also required are new advances in X ray detectors. Although detectors with larger dynamic ranges and higher readout speeds are a need across the synchrotron community, the problem for experiments involving radionuclides can be particularly problematic because of the added radiation generated by the sample. Experience has shown that even for relatively small samples, the detector can register 60% dead time even without beam. Interference from specific γ lines can also be of concern, pointing to the need for improved resolution.

New developments in imaging and tomography, particularly using higher energy photons, are expected to be particularly attractive to the development of materials for nuclear energy. Studies involving void formation, stress cracking, defect formation and aggregation are just three of the areas that could be revolutionized by such developments.

Overall, synchrotron radiation currently holds untapped potential to contribute to state of the art research and development in the area of nuclear energy. Very few developments are required, both on the part of the synchrotron and user communities, to begin to realize this potential.

REFERENCES

[1] ANTONIO, M.R., SODERHOLM, L., "X ray absorption spectroscopy of the actinides", Chemistry of the Actinide and Transactinide Elements (MORSS, L.R., FUGER, J., EDELSTEIN, N., Eds), Springer, Dordrecht (2006).

[2] ANTONIO, M.R., SODERHOLM, L., SONG, I., Design of spectroelectrochemical cell for in-situ X ray absorption fine structure measurements of bulk solution species, J. Appl. Electrochem. **27** (1997) 784–792.

[3] BARABASH, R.I., LEE, G.E., TURCHI, P.E.A., Diffuse Scattering and the Fundamental Properties of Materials, Momentum Press, New York (2009).

[4] BEARDEN, J.A., BURR, A.F., Reevaluation of X ray atomic energy levels, Rev. Mod. Phys. **39** (1967) 125–142.

[5] CATALANO, J.G., TRAINOR, T.P., ENG, P.J., WAYCHUNAS, G.A., BROWN, G.E.J., CTR diffraction and grazing-incidence EXAFS study of U(VI) adsorption onto α-Al$_2$O$_3$ and α-Fe$_2$O$_3$ (1102) surfaces, Geochim. Cosmochim. Acta **69** (2005) 3555–3572.

[6] EGAMI, T., BILLINGE, S.J.L., Underneath the Bragg Peaks: Structural Analysis of Complex Materials, Pergammon, Amsterdam (2003).

[7] FENTER, P., et al., Interaction of muscovite (001) with Pu^{3+} bearing solutions at pH 3 through ex-situ observatons, Geochim. Cosmochim. Acta **74** (2010) 6984.

[8] FENTER, P., PARK, C., NAGY, K.L., STURCHIO, N.C., Resonant anomalous X ray reflectivity as a probe of ion adsorption at solid-liquid interfaces, J. Thin Solid Films **515** (2007), 5654–5659.

[9] FENTER, P.A., Mineral-water interfacial structures revealed by synchrotron X ray scattering, Prog. Surf. Sci. **77/5–8** (2005) 171–258.

[10] FORTNER, J., et al., Crystal chemistry of uranium(V) and plutonium(IV) in a titanate ceramic for disposition of surplus fissile material, J. Nucl. Mater. **304** (2002) 56–62.

[11] KROPF, A., et al., Bent silicon crystal in Laue geometry to resolve X ray fluorescence for X ray absorption spectroscopy, Rev. Sci. Instr. **74** (2003) 4696–4702.

[12] LI, M., et al., Study of irradiated mod.9Cr-1Mo steel by synchrotron EXAFS, J. Nucl. Mater. **441** 1–3 (2013) 674–680.

[13] MOTTA, A.T., et al., Microstructural characterization of oxides formed on model Zr alloys using synchrotron radiation, J ASTM Inter. **5** (2008).

[14] SCHMIDT, M., ENG, P.J., STUBBS, J.E., FENTER, P., SODERHOLM, L., A new X ray interface and surface scattering environmental cell design for *in situ* studies of radioactive and atmosphere-sensitive samples, Rev. Sci. Instr. **82** (2011) 075105/1–10.

[15] SINGER, D.M., ZACHARA, J.M., BROWN, G.E.J., Uranium speciation as a function of depth in contaminated Hanford sediments — A micro-XRF, micro-XRD, and micro- and bulk-XAFS study, Environ. Sci. Technol. **43** (2009) 630–636.

[16] SKANTHAKUMAR, S., ANTONIO, M.R., WILSON, R.E., SODERHOLM, L., The curium aqua ion, Inorg. Chem. **46** (2007) 3485–3491.

[17] SKANTHAKUMAR, S., SODERHOLM, L., Studying actinide correlations in solution using high energy X ray scattering, Mater. Res. Soc. Symp. Proc. **893** (2006) 411–416.

[18] SODERHOLM, L., Report on the Workshop on the Role of Synchrotron Radiation in Solving Scientific Challenges in Advanced Nuclear Energy Systems (2010),
www.aps.anl.gov/News/Conferences/2010/RAD/RAD-Workshop-Report.pdf

[19] SODERHOLM, L., ALMOND, P.M., SKANTHAKUMAR, S., WILSON, R.E., BURNS, P.C., The structure of the 38-plutonium oxide nanocluster [Pu$_{38}$O$_{56}$Cl$_{54}$(H$_2$O)$_8$]$^{14-}$, Angew. Chem. Int. Ed. **47** (2008) 493–498.

[20] SODERHOLM, L., SKANTHAKUMAR, S., GORMAN-LEWIS, D., JENSEN, M.P., NAGY, K.L., Characterizing solution and solid-phase amorphous uranyl silicates, Geochim. Cosmochim. Acta **72** (2008) 140–150.

[21] SODERHOLM, L., SKANTHAKUMAR, S., NEUEFEIND, J., Determination of actinide speciation in solution using high-energy X ray scattering, Anal. Bioanal. Chem. **383** (2005) 48–55.

[22] SODERHOLM, L., SKANTHAKUMAR, S., WILSON, R.E., Structural correspondence between uranyl chloride complexes in solution and their stability constants, J. Phys. Chem. A **115** (2011) 4959–4967.

[23]   TEO, B.K., EXAFS: Basic Principles and Data Analysis, Springer, Berlin (1986).

[24]   YILMAZBAYHAN, A., et al., Structure of zirconium alloy oxides formed in pure water studied with synchrotron radiation and optical microscopy: Relation to corrosion rate, J. Nucl. Mater. **324** (2004) 6–22.

CONTRIBUTORS TO DRAFTING AND REVIEW

Avasthi, D.K.	Nuclear Science Centre, India
Becker, J.	Aarhus University, Denmark
Bras, W.	Netherlands Organisation for Scientific Research (NWO), Netherlands
Gregoratti, L.	Sincrotrone Trieste SCpA, Italy
Hussain, Z.	Advanced Light Source, Lawrence Berkeley National Laboratory, United States of America
Ionescu, M.	Australian Nuclear Science and Technology Organization, Australia
Kiyanagi, Y.	Hokkaido University, Japan
Lehmann, E.H.	Paul Scherrer Institute (PSI), Switzerland
Li, Meimei	Argonne National Laboratory, United States of America
Skuratov, V.	Flerov Laboratory of Nuclear Reaction, Joint Institute for Nuclear Research, Russian Federation
Soderholm, L.	Argonne National Laboratory, United States of America
Yu, L.	Plasma and Beam Physics, Department of Physics, Chiang Mai University, Thailand

LIST OF PARTICIPANTS

Country	Name	Institute/Organisation
AUSTRALIA	Ionescu, M.	Australian Nuclear Science and Technology Organisation, New Illawarra Rd, Lucas Heights, NSW Sydney 2234 Tel: +612 9717 3301 Email: Mihail.Ionescu@ansto.gov.au
BANGLADESH	Khan, M.A.	Institute of Nuclear Science and Technology P.O. Box: 3787 Dhaka 1000 Tel: +8802 7788245 Fax: +8802 7789620 Email: makhan.inst@gmail.com
CHINA	Xu, H.	Shanghai Institute of Applied Physics, Chinese Academy of Sciences (SINAP, CAS) Tel: +86 21 33933021 Email: xuhongjie@sinap.ac.cn
DENMARK	Becker, J.	Aarhus University, Langelandsgade 140, Aarhus C. 8000 Tel: +4520656862 Email: jbecker@chem.au.dk
IAEA	Zeman, A.	NAPC/Physics Section, International Atomic Energy Agency, Vienna, P.O. Box 100, 1400 Vienna, Austria Tel: +43 1 2600 21705 or 21754 Fax: +43 1 26007 21705 Email: A.Zeman@iaea.org
INDIA	Avasthi, D.K.	Nuclear Science Centre, Aruna Asaf Ali Road, P.O. Box: 10502, New Delhi-110067 Tel: +919818077001 Fax: +911126893666 Email: dka4444@gmail.com
ITALY	Gregoratti, L.	Sincrotrone Trieste SCpA, SS14 Km163.5 in Area Science Park, Trieste 34149 Tel: +390403758025 Fax: +390403758565 Email: luca.gregoratti@elettra.trieste.it
JAPAN	Kiyanagi, Y.	Hokkaido University, Kita-13, Nishi-8, Kita-ku, Sapporo 060 8628 Hokkaido Tel: +81 117066650 Fax: +81 117067368 Email: kiyanagi@qe.eng.hokudai.ac.jp

LIST OF PARTICIPANTS

KOREA, REPUBLIC OF	Kim, K.Y.	Korea Atomic Energy Research Institute, 1045 Daeduk Daero, Yuseong-Gu, Daejeon 305 353 Tel: +82428684974 Fax: +82428688881 Email: ky@kaeri.re.kr
MALAYSIA	Mohamed, A.A.B.	Malaysian Institute for Nuclear Technology Research Komplek PUSPATI, Bangi, Kajang 43000 Tel: +60389250510 Fax: +60389250907 Email: aziz_mohd@nuclearmalaysia.gov.my
NETHERLANDS	Bras, W.	Netherlands Organisation for Scientific Research (NWO), DUBBLE@ESRF, P.O. Box: BP 220, F38043, Grenoble Cedex, France Tel: +33476882351 Fax: +33476882412 Email: wim.bras@esrf.fr
RUSSIAN FEDERATION	Kulevoy, T.V.	Institute for Theoretical and Experimental Physics, ITEP, B.Cheremushkinskaya 25, Moscow 117218, Russian Federation Tel: +74991274650 Fax: +74991274650 Email: kulevoy@itep.ru
SWITZERLAND	Lehmann, E.H.	Paul Scherrer Institute (PSI), Villigen CH-5232 Switzerland Tel: +41563102963 Fax: +41563103131 Email: eberhard.lehmann@psi.ch
THAILAND	Yu, L.	Plasma and Beam Physics, Department of Physics, Faculty of Science, Chiang Mai University, Chiang Mai 50200, Thailand Tel: +6653943379 Fax: +6653222776 Email: yuld@fnrf.science.cmu.ac.th
UKRAINE	Borodin, O.	Kharkov Institute of Physics and Technology, 1, Akademicheskaya St., Kharkov, 61108, Ukraine Kharkov Tel: +380573386584 Email: borodin@kipt.kharkov.ua
UNITED STATES OF AMERICA	Anderson, I.	Oak Ridge National Laboratory, 1 Bethel Valley Road, P.O. Box: P. O. Box 2008, Oak Ridge 37831 6477, Tennessee, USA Tel: +865 241 1499 Fax: +865 576 3041 Email: Andersonian@ornl.gov

UNITED STATES OF AMERICA	Li, M.	Argonne National Laboratory 9700 South Cass Avenue, Argonne, IL, USA Email: mli@anl.gov
UNITED STATES OF AMERICA	Hussain, Z.	Advanced Light Source, Lawrence Berkeley National Laboratory, Berkeley, California, USA Email: ZHussain@lbl.gov
UNITED STATES OF AMERICA	Soderholm, L.	Argonne National LaboratoryArgonne, IL 60439, USA Email: ls@anl.gov
VIET NAM	Tran, T.D.	Center for Theoretical Physics, Institute of Physics, 10 St. Dao Tan, Ba Dinh, Hanoi 10000, Viet Nam Tel: +84 983201915 Fax: +84 4 37669050 Email: tdthiep@iop.vast.ac.vn

ORDERING LOCALLY

In the following countries, IAEA priced publications may be purchased from the sources listed below or from major local booksellers.

Orders for unpriced publications should be made directly to the IAEA. The contact details are given at the end of this list.

AUSTRALIA
DA Information Services
648 Whitehorse Road, Mitcham, VIC 3132, AUSTRALIA
Telephone: +61 3 9210 7777 • Fax: +61 3 9210 7788
Email: books@dadirect.com.au • Web site: http://www.dadirect.com.au

BELGIUM
Jean de Lannoy
Avenue du Roi 202, 1190 Brussels, BELGIUM
Telephone: +32 2 5384 308 • Fax: +32 2 5380 841
Email: jean.de.lannoy@euronet.be • Web site: http://www.jean-de-lannoy.be

CANADA
Renouf Publishing Co. Ltd.
5369 Canotek Road, Ottawa, ON K1J 9J3, CANADA
Telephone: +1 613 745 2665 • Fax: +1 643 745 7660
Email: order@renoufbooks.com • Web site: http://www.renoufbooks.com

Bernan Associates
4501 Forbes Blvd., Suite 200, Lanham, MD 20706-4391, USA
Telephone: +1 800 865 3457 • Fax: +1 800 865 3450
Email: orders@bernan.com • Web site: http://www.bernan.com

CZECH REPUBLIC
Suweco CZ, spol. S.r.o.
Klecakova 347, 180 21 Prague 9, CZECH REPUBLIC
Telephone: +420 242 459 202 • Fax: +420 242 459 203
Email: nakup@suweco.cz • Web site: http://www.suweco.cz

FINLAND
Akateeminen Kirjakauppa
PO Box 128 (Keskuskatu 1), 00101 Helsinki, FINLAND
Telephone: +358 9 121 41 • Fax: +358 9 121 4450
Email: akatilaus@akateeminen.com • Web site: http://www.akateeminen.com

FRANCE
Form-Edit
5 rue Janssen, PO Box 25, 75921 Paris CEDEX, FRANCE
Telephone: +33 1 42 01 49 49 • Fax: +33 1 42 01 90 90
Email: fabien.boucard@formedit.fr • Web site: http://www.formedit.fr

Lavoisier SAS
14 rue de Provigny, 94236 Cachan CEDEX, FRANCE
Telephone: +33 1 47 40 67 00 • Fax: +33 1 47 40 67 02
Email: livres@lavoisier.fr • Web site: http://www.lavoisier.fr

L'Appel du livre
99 rue de Charonne, 75011 Paris, FRANCE
Telephone: +33 1 43 07 50 80 • Fax: +33 1 43 07 50 80
Email: livres@appeldulivre.fr • Web site: http://www.appeldulivre.fr

GERMANY
Goethe Buchhandlung Teubig GmbH
Schweitzer Fachinformationen
Willstätterstrasse 15, 40549 Düsseldorf, GERMANY
Telephone: +49 (0) 211 49 8740 • Fax: +49 (0) 211 49 87428
Email: s.dehaan@schweitzer-online.de • Web site: http://www.goethebuch.de

HUNGARY
Librotrade Ltd., Book Import
PF 126, 1656 Budapest, HUNGARY
Telephone: +36 1 257 7777 • Fax: +36 1 257 7472
Email: books@librotrade.hu • Web site: http://www.librotrade.hu

INDIA

Allied Publishers
1st Floor, Dubash House, 15, J.N. Heredi Marg, Ballard Estate, Mumbai 400001, INDIA
Telephone: +91 22 2261 7926/27 • Fax: +91 22 2261 7928
Email: alliedpl@vsnl.com • Web site: http://www.alliedpublishers.com

Bookwell
3/79 Nirankari, Delhi 110009, INDIA
Telephone: +91 11 2760 1283/4536
Email: bkwell@nde.vsnl.net.in • Web site: http://www.bookwellindia.com

ITALY

Libreria Scientifica "AEIOU"
Via Vincenzo Maria Coronelli 6, 20146 Milan, ITALY
Telephone: +39 02 48 95 45 52 • Fax: +39 02 48 95 45 48
Email: info@libreriaaeiou.eu • Web site: http://www.libreriaaeiou.eu

JAPAN

Maruzen Co., Ltd.
1-9-18 Kaigan, Minato-ku, Tokyo 105-0022, JAPAN
Telephone: +81 3 6367 6047 • Fax: +81 3 6367 6160
Email: journal@maruzen.co.jp • Web site: http://maruzen.co.jp

NETHERLANDS

Martinus Nijhoff International
Koraalrood 50, Postbus 1853, 2700 CZ Zoetermeer, NETHERLANDS
Telephone: +31 793 684 400 • Fax: +31 793 615 698
Email: info@nijhoff.nl • Web site: http://www.nijhoff.nl

SLOVENIA

Cankarjeva Zalozba dd
Kopitarjeva 2, 1515 Ljubljana, SLOVENIA
Telephone: +386 1 432 31 44 • Fax: +386 1 230 14 35
Email: import.books@cankarjeva-z.si • Web site: http://www.mladinska.com/cankarjeva_zalozba

SPAIN

Diaz de Santos, S.A.
Librerias Bookshop • Departamento de pedidos
Calle Albasanz 2, esquina Hermanos Garcia Noblejas 21, 28037 Madrid, SPAIN
Telephone: +34 917 43 48 90 • Fax: +34 917 43 4023
Email: compras@diazdesantos.es • Web site: http://www.diazdesantos.es

UNITED KINGDOM

The Stationery Office Ltd. (TSO)
PO Box 29, Norwich, Norfolk, NR3 1PD, UNITED KINGDOM
Telephone: +44 870 600 5552
Email (orders): books.orders@tso.co.uk • (enquiries): book.enquiries@tso.co.uk • Web site: http://www.tso.co.uk

UNITED STATES OF AMERICA

Bernan Associates
4501 Forbes Blvd., Suite 200, Lanham, MD 20706-4391, USA
Telephone: +1 800 865 3457 • Fax: +1 800 865 3450
Email: orders@bernan.com • Web site: http://www.bernan.com

Renouf Publishing Co. Ltd.
812 Proctor Avenue, Ogdensburg, NY 13669, USA
Telephone: +1 888 551 7470 • Fax: +1 888 551 7471
Email: orders@renoufbooks.com • Web site: http://www.renoufbooks.com

United Nations
300 East 42nd Street, IN-919J, New York, NY 1001, USA
Telephone: +1 212 963 8302 • Fax: 1 212 963 3489
Email: publications@un.org • Web site: http://www.unp.un.org

Orders for both priced and unpriced publications may be addressed directly to:

IAEA Publishing Section, Marketing and Sales Unit, International Atomic Energy Agency
Vienna International Centre, PO Box 100, 1400 Vienna, Austria
Telephone: +43 1 2600 22529 or 22488 • Fax: +43 1 2600 29302
Email: sales.publications@iaea.org • Web site: http://www.iaea.org/books

The papers contained in this publication were presented at the IAEA Technical Meeting on the Utilization of Accelerator Based Real Time Methods in Investigation of Materials with High Technological Importance, which had the objective of presenting the state of the art in the development and application of various accelerator based real time techniques, of identifying research trends and scientific challenges and of highlighting the need for and benefits of increased interdisciplinary and international collaborations. The meeting discussed specific techniques and research areas that can benefit from real time material characterizations using synchrotron radiation, neutron, ion and electron beams, and simultaneous combinations of different techniques.